The Dissertation Committee for Aubrey Koch Converse Certifies that this is the approved version of the following Dissertation:

Functions and signaling mechanisms of the membrane androgen receptor ZIP9 in Atlantic croaker (*Micropogonias undulatus*) and zebrafish (*Danio rerio*) ovaries

Committee:

Peter Thomas, Supervisor

Deana Erdner

Andrew Esbaugh

John Richburg

Functions and signaling mechanisms of the membrane androgen receptor ZIP9 in Atlantic croaker (*Micropogonias undulatus*) and zebrafish (*Danio rerio*) ovaries

by

Aubrey Koch Converse

Dissertation

Presented to the Faculty of the Graduate School of

The University of Texas at Austin

in Partial Fulfillment

of the Requirements

for the Degree of

Doctor of Philosophy

The University of Texas at Austin

December 2018

Dedication

I dedicate this work to my father Jeff Koch and daughter Chloe Converse, I love you both with all my heart.

Acknowledgements

First and foremost, I need to thank my advisor Peter Thomas, who has provided immeasurable support in the completion of this work. My research and writing skills have considerably improved under his guidance. Thank you to my committee, Deana Erdner, Andrew Esbaugh, and John Richburg, for their guidance and feedback on this work over the years. To my lab members, Yefei Pang, Jing Dong, and Md. Saydur Rahman, thank you for your patience in teaching me the protocols and skills that were essential in to research. To my dear friend Susan Lawson, I could not have completed this work without your dedicated care to our wet lab and fish, and I would not have stayed sane without your company and friendship. To past labmates and visitors, Wenxian Tan, Kathryn Ondricek, Joseph Aizen, Hakan Berg, Maria Camilletti, Amanda Fitzgerald, Luca Castelnovo, and Chenan Zhang, thank you all in your support in this undertaking. Thank you Bob Dickey and all of the staff at UTMSI, everyone's dedication to the institute after Hurricane Harvey allowed for our research to continue. To my family, thank you for your support and patience over the many years, I'm am so sincerely appreciative. And finally, thank you to everyone I have met at UTMSI for truly enriching my life.

Abstract

Functions and signaling mechanisms of the membrane androgen receptor ZIP9 in Atlantic croaker (*Micropogonias undulatus*) and zebrafish (*Danio rerio*) ovaries

Aubrey Koch Converse, Ph.D.

The University of Texas at Austin, 2018

Supervisor: Peter Thomas

The overall goal of this research was to further characterize and verify the role of ZIP9 in mediating androgen-induced apoptosis of teleost granulosa/theca (G/T) cell co-culture. In addition, a global ZIP9 knockout zebrafish model was used to infer other roles of the receptor in the ovary, *in vivo*. While ZIP9 was first identified and found to mediate apoptosis of croaker G/T cells, little was known on the signaling mechanism mediated by the receptor. Therefore, stimulatory G protein alpha subunit-mediated signaling, MAP kinase (MAPK) activity, and the role of extracellular zinc were investigated in ZIP9-mediated apoptosis of croaker G/T cells. Additionally, the role of ZIP9 in mediation of testosterone-induced anti-apoptotic response observed in croaker G/T cells from fish outside of the reproductive peak was examined. To determine if ZIP9 mediates androgen-induced apoptosis in G/T cells of other teleosts, a zebrafish primary G/T culture system was used to examine androgen-mediated events. Finally, a global ZIP9 knockout zebrafish

strain was developed to examine the effects of global ZIP9 knockout on female reproduction.

The ZIP9-mediated apoptotic pathway in croaker G/T cells was found to require stimulatory G protein signaling and MAPK activity. Additionally, extracellular zinc is essential for the induction of ZIP9-mediated apoptosis in this model, and downstream responses to these signaling cascades include increased mRNA expression of pro-apoptotic protein members and caspase 3 activity. Pro- and anti-apoptotic effects of testosterone on croaker G/T cells was confirmed, and both responses were found to be mediated by ZIP9 in an ovarian follicle stage-dependent manner. ZIP9 activation of stimulatory and inhibitory G proteins elicits the pro- and anti-apoptotic responses, respectively. In pooled zebrafish G/T cells, testosterone treatment results in an increased incidence of apoptosis, caspase 3 activity, upregulation of pro-apoptotic protein member mRNA, and a rapid rise in intracellular free zinc. This testosterone-mediated response was attributed to ZIP9 activity, thus, ZIP9 mediates apoptosis through a similar mechanism in zebrafish G/T cells as observed in croaker. Finally, examination of ZIP9 global knockout zebrafish demonstrated that ZIP9 mutation results in reduced fecundity and abnormal egg phenotypes, even though no abnormalities in ovarian morphology were apparent through histological examination.

Table of Contents

List of Tables

List of Figures

Chapter 1: Introduction

Cellular apoptosis

Cell death typically occurs through two mechanisms. Apoptosis is a cell-mediated, energy-dependent form of cell death, while necrosis is a passive, energy-independent process that results in an inflammatory response (1). Apoptosis is genetically programmed to allow for the elimination of cells at different periods of development and is essential for the maintenance of homeostasis. Apoptosis can also be triggered by external and internal cellular stressors, which differ between cell type and stimuli. There are two primary mechanisms of apoptosis, the intrinsic and extrinsic pathways. The intrinsic pathway of apoptosis is characterized by the formation of a permeability pore in the mitochondrial outer membrane, which leads to the release of cytochrome C and the subsequent activation of caspases, or apoptotic specific proteases. The extrinsic apoptotic pathway involves ligand binding to a transmembrane receptor which results in the recruitment of adaptor proteins and procaspase-8 to form a death inducing signaling complex (DISC) that results in the activation of various caspases.

The intrinsic pathway can be initiated by various stressors, such as oxidative or metabolic stress (2,3), DNA damage (4), heat shock (5), toxicants (6,7), and by the absence or presence of growth factors (8,9). Cellular stress leads to the activation of pro-apoptotic members of the Bcl-2 protein family (10,11). The Bcl-2 family also contains pro-survival proteins that act to prevent apoptosis in healthy cells. Activation of pro-apoptotic or pro-survival members of the Bcl-2 family can shift a cell's fate towards apoptosis or survival, respectively. Once activated, pro-apoptotic Bcl-2 proteins form permeability pores in the mitochondrial outer membrane, resulting in the release of cytochrome C to the cytoplasmic

compartment (11). Cytochrome C release results in the development of apoptosomes, which consist of cytochrome C, deoxyadenosine triphosphate (dATP), apoptotic protease activating factor 1 (Apaf-1), and caspase 9 (10). Once an apoptosome is assembled, caspase 9 is activated which in turn leads to the activation of other caspases, including caspase 3 (10). Caspase 3 is considered an execution caspase (10) that when activated directs DNA and protein degradation (12), resulting in cell death. While numerous factors can influence cell apoptosis, steroid hormones are known to play a role in the regulation of apoptosis in both reproductive (13–15), and non-reproductive tissues (13).

Classical vs. nonclassical steroid action

Steroid hormones can act through both classical and nonclassical (nongenomic) modes of action. Classical steroid action involves the diffusion of the steroid through the plasma membrane of the target cell, binding to a nuclear receptor in the cytosol, and subsequent dimerization of bound receptors that allows for the complex to translocate to the nucleus where it acts as a transcription factor to alter expression of target genes (16). These changes in gene expression result in the observable physiological responses that are associated with the steroid hormone's action in target tissues. This classical mode of steroid action is relatively slow due to the time required to complete transcription and protein translation.

Nonclassical steroid actions are characterized by the rapid activation of intracellular signal transduction pathways, which occur too rapidly to be associated with classical genomic mechanisms (17). Some of these rapid responses include an increase in intracellular calcium (18–20), adenylyl cyclase activation and inhibition (21–26), and activation/inhibition of the protein kinases (21,24,26–31). These responses can occur on a timescale of seconds to minutes and are often initiated by activation of G proteins by receptors on the cell surface. This results in signaling cascades similar to those mediated

by peptide hormone activation of members of the G protein-coupled receptor (GPCR) superfamily. In addition to acting directly to mediate physiological changes, rapid signaling members can act to mediate events that ultimately result in altered gene transcription, or in a pregenomic fashion.

Nonclassical androgen actions

Nonclassical steroid actions have been reported for all major groups of steroid hormones, and the field of membrane-mediated steroid action has rapidly progressed in the last two decades. Membrane progestin and estrogen receptors were first cloned and characterized in 2003 and 2005 respectively (32–34). These receptors were found to mediate various nonclassical actions in an array of vertebrate cells and tissues. Nonclassical androgen actions have also been observed in a broad number of cell and tissue types, but the underlying mechanism and receptor mediating many of these responses are elusive. Nonclassical membrane-initiated androgen actions have been reported in the brain (27,35–37), Sertoli cells (38–40), granulosa cells (41), T cells and macrophages (42,43), oocytes (44–46), and a number of cancer cell lines including prostate (39,47–51), colon (52), and breast (53). While several of these responses were found to require expression of the nuclear androgen receptor (AR) (40,45), a number of these models are AR-negative (PC-3 and DU145 prostate cancer cell lines (28,39), and IC-21 macrophages (43)). Thus, while some nonclassical androgen actions can be regulated by the AR acting in a nonclassical fashion, there must be additional ways in which androgens can mediate nonclassical actions.

Interestingly, a number of responses mediated by nonclassical androgen actions are shared between various tissue and cell types. Androgen regulation of rapid intracellular calcium fluxes has been observed in pituitary cells (36), Sertoli cells (38,39), granulosa cells (41), T cells and macrophages (42,43), and in prostate cancer cell lines (39,48).

Likewise, androgen-induced apoptosis has also been observed in a number of models including LNCaP and DU145 prostate cancer cells (28,50), Caco2 and HCT116 colon cancer cell lines (29), T47D breast cancer cells (53), cortical astrocytes (37), and C6 glial cells (27). These analogous responses mediated through androgens acting on the cell surface suggest that there may be a common underlying mechanism that can mediate nonclassical androgen actions in vertebrates.

Androgens action in the ovary

Androgens have been found to be involved in various processes within the ovary including follicle growth (54–57), follicle cell proliferation (55,58), the transition of follicles to more advanced stages (56,57,59), cell survival (55), and in apoptosis and atresia (60–65). These differential effects of androgens between studies may be due to differences in experimental design, the model organism used, and the follicle stages in which the functions were examined. In addition, androgen effects in the ovary are typically attributed to AR action due to the limited evidence and understanding of actions mediated through membrane androgen receptors distinct from the nuclear receptor. Thus, in many studies, androgen effects were never directly linked to AR action through loss of function verification methods. The most informative studies on potential mechanisms include those performed in nuclear androgen receptor knockout (ARKO) models. Murine global ARKO models have been used to investigate the role of the AR in female reproduction in a number of studies (66–70). ARKO results in reproduction impairments including longer estrous cycles (68), increase in atretic or unhealthy follicles (68,70), reductions in follicle numbers (66,69), corpora lutea (68,70), and litter size (67–70), and premature ovarian failure with age progression (66,69). However, complete female infertility was not observed in any ARKO model, indicating that the AR plays a significant role in female fecundity, but is not essential for female reproduction. Recent studies using granulosa cell-specific ARKO

models have reported similar effects to global ARKO models such as increases in apoptosis/atresia (71–73) and decreased litter size (71,72), but again animals were only subfertile. These studies provide evidence for the role of the nuclear AR in normal folliculogenesis and suggest that androgens may be anti-apoptotic when acting through the AR, and thus may account for many of the actions of androgens reported in non-knockout models. However, AR knockout models do not account for the apoptotic actions of androgens in the ovary that have been reported in murine and porcine models (60–65).

Discovery and characterization of the novel membrane androgen receptor ZIP9

In 2004, Braun and Thomas (74) reported testosterone binding to the membrane fraction of Atlantic croaker ovary fragments, which was later the basis for characterization of a putative membrane androgen receptor in croaker ovarian tissues. The putative receptor was found to be homologous with the zinc transport protein ZIP9, which is the lone member of the SLC39A9 subfamily I (25). ZIP9 was the first, and still the only membrane androgen receptor identified to date that shows a high affinity, limited capacity, single binding site specific to androgens (25). Interestingly, ZIP9 was found to mediate androgen-induced apoptosis of primary croaker granulosa/theca (G/T) cell co-culture, as well as in a SKBR-3 breast cancer cell line expressing recombinant croaker ZIP9 (ZIP9-SKBR-3) (25,75). Subsequently, human recombinant ZIP9 was characterized and found to mediate androgen-induced apoptosis in ZIP9 transfected PC-3 (ZIP9-PC-3) prostate cancer cells and MDA-MB-231 breast cancer cells. Similarly, endogenous human ZIP9 was examined in LNCaP prostate cancer cells and the MDA-MB-468 (468) breast cancer cells (26). With the exception of the LNCaP prostate cancer cell line, all of the human cell lines used for ZIP9 characterization are AR-negative.

ZIP9 was found to be coupled to an inhibitory G protein (G_i) in the cancer cell line models, but to a stimulatory G protein (G_s) in the croaker ZIP9-SKBR-3 model (25,26). It

is unknown whether this difference is due to the difference in species (croaker vs. human), or a difference in cell type (reproductive vs. malignant). In both models, ZIP9 is activated by testosterone and induces an apoptotic response. This response involves a rapid increase in free intracellular zinc (25,26), which when chelated, abrogates the apoptotic response. In the croaker model, ZIP9 activation of a G_s leads to increased adenylyl cyclase activity and increased cyclic AMP (cAMP) levels (25). In the cancer cell models, ZIP9 activation of a G_i inhibits adenylyl cyclase activity and results in decreased cAMP levels (26). It is not clear if G protein α-subunit signaling is significant in the croaker G/T cell or human cancer cell line models since ZIP9 activates different G proteins between these models. In addition, the apoptotic pathway in the human cells involves Erk activation (468 cells), the upregulation of pro-apoptotic members p53 and Bax, and caspase 3 activation (26). However, these signaling members have not been examined in the croaker ZIP9 model to date.

Of interest, while ZIP9 has been found to mediate androgen-induced apoptosis in croaker G/T cells, preliminary research (Zhang thesis (75)) has indicated that testosterone mediates different survival responses of G/T cells depending on the reproductive stage of the fish (75). G/T cells from fish at the peak of their reproductive cycle, typically show the apoptotic response to testosterone, which was confirmed to be mediated by ZIP9 by Berg et al. 2014 (25). In contrast, in G/T cells from fish outside the peak of the reproductive season, testosterone is protective against cell death (75). However, the role of ZIP9 in this anti-apoptotic effect has not been examined.

This dissertation seeks to further characterize the ZIP9-mediated apoptotic pathway in croaker G/T cells. The anti-apoptotic response exhibited by G/T cells from fish outside of the peak of the reproductive season will also be examined to determine if opposing effects of androgens can be attributed to different stages of follicle development.

Furthermore, the role of ZIP9 and the AR will be examined in the anti-apoptotic response. To date, the role of ZIP9 has only been examined in the ovary of croaker. To determine if ZIP9-mediates G/T cell apoptosis in the ovary of other teleosts, a G/T cell culture system will be utilized to examine the role of ZIP9 in zebrafish ovaries. Additionally, because zebrafish are a genetic model organism, a CRISPR-cas9 system will be used to establish a ZIP9 knockout mutant strain. ZIP9 knockout fish will be assessed for morphological and reproductive phenotypes that can be attributed to ZIP9 knockout.

Overall Goals

The overall goal of this research is to test the hypotheses that ZIP9 plays an important physiological role in the teleost ovary, and that the signaling mechanisms and functions of the receptor are conserved in teleosts. Five objectives were developed to examine these hypotheses.

1. To further characterize ZIP9-mediated apoptosis and the role of pro-apoptotic proteins Bax, p53, and JNK.
2. To characterize the role of MAPK (Erk) and the $G_s\alpha$-subunit-mediated pathway in ZIP9-mediated apoptosis of croaker G/T cells.
3. To determine the role of extracellular zinc in the induction of apoptosis by ZIP9 in croaker G/T cells.
4. To determine if ZIP9 mediates the anti-apoptotic response observed in croaker G/T cells from fish outside the peak of the reproductive season.
5. To investigate the role of ZIP9 in zebrafish G/T cells and overall ovarian physiology by comparison of ZIP9 knockout zebrafish with a wild-type model

Chapter 2: Membrane androgen receptor ZIP9 induces croaker ovarian cell apoptosis via stimulatory G protein alpha subunit and MAP kinase signaling[1]

ABSTRACT

Recent studies show that androgen-induced apoptosis in Atlantic croaker primary granulosa/theca (G/T) cells and in human breast and prostate cancer cell lines is mediated by the novel membrane androgen receptor ZIP9 which belongs to the SLC39A zinc transporter family. However, the apoptotic signaling pathways remain unclear because ZIP9 activates an inhibitory G protein in human cancer cells, whereas recombinant croaker ZIP9 activates a stimulatory G protein (G_s) in transfected cancer cells. Here we investigated androgen-dependent apoptotic pathways in order to identify the signaling pathways regulated through wild-type croaker ZIP9 in ovarian follicle cells. We show that the ZIP9-mediated apoptotic signaling pathway in croaker G/T cells shares several pro-apoptotic members with those in human cancer cells, but is activated through a $G_s\alpha$ subunit-dependent pathway. Testosterone treatment of croaker G/T cells increased intracellular zinc levels, Erk activity, caspase 3 activity, mRNA levels of pro-apoptotic members Bax, p53, and JNK, and the incidence of apoptosis, similar to findings in mammalian cancer cells, but also increased cAMP concentrations. Transfection with small interfering RNA targeting croaker ZIP9 blocked the testosterone-induced increase in *bax*, *p53*, and *jnk* expression. Testosterone-induced apoptosis and caspase 3 activation were dependent on the presence of extracellular zinc and were effectively blocked with co-treatment of

[1] Chapter 2 has previously been published (with slight modification) as: Converse A, Zhang C, Thomas P. Membrane androgen receptor ZIP9 induces croaker ovarian cell apoptosis via stimulatory G protein alpha subunit and MAP kinase signaling. Endocrinology. 2017;158(9):3015–3029. The dissertator's contributions included design and performing of experiments, data analysis, and writing of the manuscript.

inhibitors of the $G_s\alpha$ subunit, adenylyl cyclase, PKA, and Erk activation. These results indicate that ZIP9-mediated testosterone signaling in croaker G/T cells involves multiple pathways, some of which differ from those activated through ZIP9 in human cancer cells even though a similar apoptotic response is observed.

INTRODUCTION

Androgens regulate important ovarian processes in vertebrates including folliculogenesis, proliferation, and apoptosis (54,55,59,61,64,76), but the mechanisms controlling these functions are often unclear. Many actions of androgens are genomic and are regulated by the nuclear androgen receptor (AR), a ligand-activated transcription factor belonging to the nuclear receptor superfamily (77,78). Nuclear androgen receptor knockout (ARKO) models show increases in atretic and unhealthy ovarian follicles, and reductions in the number of corpora lutea and litter size (68,70), thus demonstrating that the AR plays an important role in ovarian physiology. In contrast, nongenomic androgen actions and the receptors that mediate them in vertebrate ovaries have received much less attention and remain poorly understood. Nevertheless, rapid, nongenomic androgen actions have been described in human and Atlantic croaker ovaries (41,79), and androgen binding moieties have been identified on croaker ovarian plasma membranes with binding characteristics different from those of ARs (74,80). More recent evidence indicated that androgens induce apoptosis in croaker granulosa and theca (G/T) cells by a cell surface-initiated mechanism that is not mimicked by the AR agonist, mibolerone, which suggests this androgen action is mediated by a novel membrane androgen receptor, although its identity remained unknown (75).

The croaker ovarian membrane androgen receptor was subsequently cloned and identified as ZIP9, the sole member of the ZIP zinc transporter (SLC39A) subfamily I (25).

Experiments using small interfering RNA (siRNA) targeting this protein confirmed that ZIP9 is a membrane androgen receptor and the intermediary in testosterone-induced apoptosis in croaker G/T cells (25). ZIP9 is the first membrane androgen receptor to be identified in vertebrates and is widely expressed in croaker and human tissues (25,26). Human ZIP9 mediates androgen-induced apoptosis in a variety of breast and prostate cancer cell lines (26), which indicates that ZIP9 initiates a common response to testosterone in both croaker G/T primary cells and human cancer cells. Apoptosis is thought to be the primary mechanism regulating ovarian follicle atresia in mammals and also has been observed in late stage atretic follicles of teleosts (81–83). Apoptosis also plays an important role in the regression of the corpus luteum in mammals and post-ovulatory follicles in teleosts (81–85). ZIP9's high expression in croaker ovaries and its stimulation of apoptosis (25) suggest that the receptor may have an important role in ovarian remodeling by regulating follicle cell apoptosis during the breakdown of atretic and postovulatory follicles.

Although ZIP9 was first discovered in the croaker primary G/T cells, further characterization of the receptor was conducted with recombinant croaker ZIP9-in transfected SKBR3 (SKBR3-ZIP9) AR-null breast cancer cells (25), and with wild-type and overexpressed human ZIP9 in several AR-null breast and prostate cancer cell lines (26). Human ZIP9-dependent apoptosis has been well characterized in MDA-MB-468 breast cancer cells and in PC-3 prostate cancer cells overexpressing ZIP9 (PC3-ZIP9) where it shows a dose-dependent, specific response to testosterone that is accompanied by increases in intracellular free zinc (26). The finding that testosterone treatment increases caspase 3 activity and mRNA levels of the pro-apoptotic regulators p53, Bax, and JNK as well as increased protein levels of caspase 3, Bax, and mitochondrial cytochrome C in these cells, indicates a plausible intrinsic apoptotic pathway through which testosterone induces

apoptosis and cell death in these cancer cells. Although testosterone also induces apoptosis and increases intracellular free zinc in croaker G/T cells, it is not known if it involves the same apoptotic regulators as those identified in the human cancer cell models. Information on testosterone regulation of pro-apoptotic regulators in croaker G/T cells would indicate if ZIP9 mediates apoptosis through a common mechanism in different cell types.

The apoptosis mechanisms in croaker G/T cells and human cancer cells potentially could differ because recombinant croaker ZIP9 and human ZIP9 have been shown to activate different G proteins (25,26). In SKBR3-ZIP9 cells, croaker ZIP9 activates a stimulatory G protein (Gs) resulting in increased cyclic adenosine monophosphate (cAMP) levels (25), whereas in MDA-MB-468 and PC-3-ZIP9 cell lines human ZIP9 activates an inhibitory G protein (Gi) (26). The consequences of these differences in G protein activation in these models on their ZIP9 signaling are unknown since the pathway initiated by croaker ZIP9 is still obscure. In MDA-MB-468 cells, testosterone treatment increased Erk activation, and co-treatment with an Erk inhibitor (PD98059) effectively blocked testosterone-induced upregulation of pro-apoptotic genes. On the other hand, a rapid progestin-induced increase in Erk activity associated with a reduction in the incidence of apoptosis mediated by the membrane progestin receptor mPRα was observed in croaker primary G/T cells (24). Erk activity has not been examined in relation to ZIP9 signaling in G/T cells so it is not known whether Erk is primarily associated with cell survival in these cells, or if it may also be involved in the apoptotic response initiated by ZIP9, as observed with activation of mammalian ZIP9 in cancer cells.

Interestingly, ZIP9 is the only steroid receptor identified so far that is also a zinc transporter. Zinc is an essential trace element that has a critical role in numerous physiological functions including transcriptional regulation of many genes, as a cofactor for hundreds of enzymes, signal transduction and rapid calcium signaling (86,87), and

apoptosis (88,89). Zinc homeostasis is essential for maintaining these physiological functions. While zinc deficiency causes cell death (90–92), a rise in intracellular free zinc may increase apoptosis (93,94). Intracellular free zinc levels are controlled by zinc transporters belonging to the ZnT and ZIP families. The ZIP zinc transporter (SLC39A) family transport zinc across membranes from extracellular and subcellular compartments into the cytosol (95). Androgen activation of ZIP9 causes a rise in intracellular free zinc in all the cell models in which it has been examined to date (25,26). This increase in free zinc levels was found to be androgen specific in the human cancer lines (26). Moreover, co-treatment with the membrane permeable zinc-chelator N,N,N',N'-Tetrakis(2-pyridylmethyl)ethylenediamine (TPEN) inhibits testosterone-induced apoptosis in both SKBR3-ZIP9 and MDA-MB-468 cells (25,26). These results indicate that the increase in intracellular zinc is a critical component of the ZIP9-induced signaling pathway mediating apoptosis. However, the source of this increased intracellular free zinc and the role of extracellular zinc on ZIP9's apoptotic functions have not been examined to date in any of the cell models.

Therefore, the goal of the current study was to characterize androgen-induced apoptosis and its signaling pathways through wild-type croaker ZIP9 in primary G/T cells. The testosterone specificity of the apoptotic and zinc responses were examined and compared to those of the specific AR agonist mibolerone, since the AR is also expressed in croaker G/T cells. The testosterone regulation of pro-apoptotic members, Bax, p53, and JNK, through ZIP9 in croaker G/T cells was assessed for comparison with the previous results with human ZIP9 in cancer cells. In addition, the involvement of multiple signaling pathways and caspase 3 were examined in order to compare the ZIP9-mediated responses between the croaker G/T and human cancer cell models. A research emphasis was placed on the potential role of signaling induced through activation of the G protein α ($G_s\alpha$)

subunit in ZIP9-mediated apoptosis, since this pathway is absent in the previously characterized human cancer cell models. Finally, the role of extracellular zinc in the induction of apoptosis through ZIP9 was investigated.

MATERIALS AND METHODS

Chemicals and materials

Chemicals were purchased from Sigma-Aldrich (St. Louis, MO) unless otherwise stated. Testosterone, 17,20β,21-trihydroxy-4-pregnen-3-one (20β-S), estradiol-17β, and cortisol were purchased from Steraloids (Newport, RI). Mibolerone was a gift from the Upjohn Laboratories (Kalamazoo, MI). Bovine serum albumin-conjugated steroids were dialyzed to remove any free steroid by incubation with 5 mg/mL charcoal and 0.5 mg/mL dextran at 55°C with gentle rotation for 30 min followed by removal of charcoal by two centrifugation cycles at 4600 x g for 20 min each.

Animal care and tissue collection

Atlantic croaker were purchased from local bait shops near Port Aransas, Texas, and transferred to fish holding facilities at the University of Texas Marine Science Institute. Fish were maintained in recirculating saltwater tanks (salinity 30-32 ppt), and fed commercial pellets. Photoperiod was adjusted to replicate the local summer and fall conditions (13 hr light, 11 dark at 26°C in August; 11 hr light, 13 dark at 22-23°C in December) during gonadal recrudescence. Fish were acclimated to laboratory conditions for a minimum of 2 months before being used for G/T cell isolation. Female fish at the peak of the reproductive period (gonadosomatic index > 12) with oocytes averaging greater than 440 μm in diameter were considered reproductively mature and used for experimentation. Fish were deeply anesthetized by immersion in a bath containing 20 mg/L MS-222 and humanely euthanized by rapid decapitation in accordance with procedures

approved by the University of Texas Animal Care and Use Committee. Ovarian tissue was excised and placed in CMF buffer (138 mM NaCl, 8.6 mM KCl, 1.62 mM Na_2HPO_4, 5 mM D-glucose, 15.8 mM HEPES, 1 mM EDTA, 100 mg/L streptomycin, 60 mg/L penicillin, pH 7.4) for G/T cell isolation.

Primary granulosa/theca cell culture

Unlike for mammalian ovaries, reliable methods for the separation of pure G (granulosa) and T (theca) cell populations from fish ovaries have not been developed; consequently, a co-culture system was employed. Croaker G/T cells were isolated from ovarian fragments by enzymatic digestion with collagenase as previously described (96). G/T cells were resuspended in DMEM supplemented with 3% bovine calf serum. In order to prevent the possible conversion of testosterone and endogenous steroid production by G/T cells, 100 μM of the P450 side chain cleavage and aromatase inhibitor DL-Aminoglutethimide (Alfa Aesar, Ward Hill, MA) was added to all the culture media. In co-culture conditions, granulosa cells predominate (approximately 60-90%) after 3 to 4 days of culturing when experiments are typically performed. For ZIP9 knockdown experiments, cells were switched to antibiotic-free media and transfected with either a mixture of ZIP9-targeting siRNA primers or scrambled primers (Dharmacon, Lafayette, CO) twice at 0 and 16 hr using Lipofectamine 2000 (Invitrogen, Carlsbad, CA). Treatments were administered 24 hr after the second transfection for apoptosis and RNA expression experiments, and 3 days after the second transfection for cAMP assay.

Membrane protein preparation

G/T cells were harvested by adding cold (4°C) HAED buffer (25 mM HEPES, 10 mM NaCl, 1 mM EDTA, 1 mM DTT, pH 7.6) containing protease inhibitor (1μL/mL) to plates followed by scraping. All following steps were carried out at 4°C. Cells were rinsed 2-3 times and the buffer removed by centrifugation at 1,000 x g. Cell pellets were then

resuspended and cells lysed by sonication for 4 s. The sample was centrifuged at 1,000 x g for 7 min to pellet the nuclear fractions. The supernatant containing membrane protein fraction was removed, placed into clean tubes, and centrifuged at 20,000 x g for 20 min to pellet the membrane protein fraction. The resulting pellet was resuspended in HAED buffer and 4X reducing sample buffer was added before boiling for 10 min, and subsequent storage at -80°C until protein detection by Western blot analysis.

Western blot analysis

Electrophoresis was performed on membrane or whole cell lysate protein samples loaded on a 10% SDS-PAGE gel. Protein samples were transferred to a nitrocellulose membrane and blocked with 5% nonfat milk for 1 hr. After blocking, the membrane was incubated with the first antibody (ZIP9 1:5000 (AB_2651045); actin 1:2000 (AB_11232819); p-Erk1/2 1:1000 (AB_331768); t-Erk1/2 1:1000 (AB_330744)) overnight at 4°C. The croaker ZIP9 primary polyclonal antibody was generated in mice against a partially-purified ovarian membrane fraction with androgen receptor activity and validated for measurement in this species as described previously (25). After incubation, the membranes were washed 3 times followed by incubation with the secondary antibody (HRP-linked mouse or rabbit 1:2000; LI-COR mouse 1:5000) for 1 hr. Protein bands were visualized using Odyssey infrared imaging system (LI-COR, Lincoln, NE) or using SuperSignal chemiluminescent substrate (Thermo Scientific, Grand Island, NY).

Hoechst apoptosis analysis

G/T cells were grown for 1-2 days on round 15 mm glass coverslips placed in 12-well culture plates, serum-starved for 16-24 hr, and then incubated with the experimental treatments in serum-free DMEM (zinc: 1.5 µM) for 16 hr. At the end of the incubation, cells were fixed with 4% paraformaldehyde for 20 min. Cells were stained with 1µg/µL Hoechst 33342 for 1-5 min, rinsed with PBS (NaCl 137 mM, KCl, 2.7 mM, Na_2HPO_4

10mM, KH_2PO_4 1.8 mM), and mounted face down on microscope slides. Apoptotic cells were identified based on the morphology of chromatin under epifluorescent microscopy. Apoptotic nuclei in 400 cells from 2-3 replicates of each treatment were counted and expressed as the percent apoptotic cells. Zinc-free DMEM base (Sigma-Aldrich) media alone or with added zinc sulfate (1.5 μM) was used to investigate the effects of external zinc on the apoptosis response. Cells were washed once and incubated in the base media for 3 hr prior to the beginning of the experiment. Each experiment was repeated at least three times.

Intracellular zinc assay

G/T cells were grown in 96-well plates for 1-2 days until confluent. Cells were serum starved for 30 min followed by treatment with various steroids for 30 min. Cells were then fixed with 4% paraformaldehyde for 25 min at 4°C, stained with 10 μM zinquin ethyl esther (Enzo Life Sciences, Inc., Farmingdale, NY) for 30 min, washed, and immediately analyzed with fluorescence plate reader (excitation 368 nm, emission 490 nm). Results are expressed as the relative intensity of the zinc signals compared to the vehicle controls. Each treatment was replicated in 8-16 wells and repeated with cells from at least 3 fish.

Inhibitor treatments

Cells were pretreated with inhibitors of caspase 3 (10 μM, Z-DEVD-FMK), caspase 8 (10 μM, ZIETD-FMC), and Bax (50 μM, peptide V5) for 1 hr prior to co-treatment with testosterone. Likewise, specific inhibitors of the $G_s\alpha$ subunit (NF449, Cayman Chemicals, Ann Arbor, MI), adenylyl cyclase (2', 5'-dideoxyadenosine (dd-Ado)), Protein kinase A (KT5720, Biomol, Plymouth, MA), and Erk (PD98059, Biomol) were used to pretreat cells for 1 hr prior to co-treatment with testosterone.

Cyclic AMP assay

Cyclic AMP was measured in cell lysates using a cAMP EIA kit (Cayman Chemicals). After isolation, G/T cells were cultured overnight, followed by serum starvation for 48-72 hr. Cells were treated for 10 min with vehicle or testosterone, washed twice with ice-cold PBS, and lysed by 20 min incubation with 100 µL 0.1 M HCl (12-well plate) on ice followed by scraping and repeated pipetting (20x) to homogenize the suspension. The suspension was centrifuged at 1,000 x g for 10 min and the supernatant was diluted 2-3x and either assayed immediately or stored at -80°C. Data was normalized and presented as relative cAMP concentration

Caspase 3 activity

Cells were treated as in the Hoechst apoptosis assay, harvested, and caspase 3 activity was determined using a Caspase-Glo 3/7 Assay kit (Promega, Madison, WI) according to the manufacturer's instructions. Briefly, after treatment cells were scraped, lysed by sonication, and the supernatant was added to a 1:1 volume of Caspase-Glo reagent. The luminescence of each sample was immediately analyzed by a plate reader, and subsequent readings were taken every 3 min. The highest luminescence value obtained for each sample was used and expressed relative to vehicle control values. Each experiment was repeated at least 3 times.

Erk activation assay

G/T cells grown in 12-well plates were serum starved for 48-72 hr prior to a 15-min treatment with testosterone, EGF (100 nM) (positive control), or vehicle. Cells were harvested on ice using RIPA buffer (EMD Millipore, Billerica, MA) containing phosphatase and protease inhibitors, and the lysates were centrifuged at 15,000 x g for 5 min to remove insoluble material. Reducing sample buffer was added, the samples were boiled for 10 min, and then stored at -80°C until used for Western blot analysis. Total Erk and phosphorylated Erk were detected by primary antibodies directed at total p42/44 and

phospho-p42/44 (Cell Signaling Technology Inc.). Horseradish peroxidase-conjugated-secondary antibodies were detected with SuperSignal chemiluminescent substrate.

Quantitative real-time RT-PCR analysis

G/T cells were starved for 16-24 hr prior to treatment with ethanol vehicle or testosterone for the indicated time (4-48 hr), followed by RNA isolation and analysis. Quantitative real-time PCR (qPCR) primers were designed against cloned sequences of *bax*, *p53*, and *jnk* (Table 2.1). qPCR was performed using Verso 1-step RT-qPCR SYBR Green Low ROX kit (Thermo Scientific), 15 µL reaction volume with 100 ng of RNA per reaction, following the manufacturer's protocol. The qPCR program was set to 50°C for 15 min, 95°C 15 min, and 40 cycles of 95°C for 15 s, 55°C for 30 s, 72°C for 30 s. Amplification was followed by the melting curve program, 95°C for 15 s, 60°C for 15 s and a gradual increase to 95°C over 20 min. Samples were run in duplicates and expression of target genes was normalized to the housekeeping gene 18S.

Statistical Analysis

All experiments were repeated at least three times with G/T cells from different fish. Statistical significance was determined by Student's t-test or one- or two-way ANOVA with a post hoc Bonferroni multiple comparison test. The one-way ANOVA was used to analyze experimental results with multiple steroid treatments and concentrations. The two-way ANOVA was used to analyze data from the experiments in which inhibitors, different siRNA transfections, or multiple zinc concentrations were used. All data is expressed as the mean ± SEM using GraphPad Prism 5 software (GraphPad Software, San Diego, CA).

RESULTS

Characterization of the testosterone-induced apoptotic response

Testosterone treatment increased G/T cell apoptosis in a concentration-dependent manner, with concentrations of 10 nM and higher resulting in significant increases compared to the vehicle control (Figure 2.1A). Treatment of G/T cells with 100 nM estradiol (E_2), cortisol, and the maturation-inducing steroid in croaker 17, 20β, 21-trihydroxy-4-pregnen-3-one (20β-S) (97) for 16 hr had no effect on apoptosis, which suggests the apoptotic response is specific to androgens (Figure 2.1B). Apoptosis was not increased by treatment with the AR agonist, mibolerone (100 nM), which suggests the pro-apoptotic action of testosterone is not mediated through the AR (Figure 2.1C). The male androgen, 11-ketotestosterone also had no effect of G/T cell apoptosis (Figure 2.1C). Treatment with the 5-alpha reductase inhibitor finasteride (50 μM) did not affect testosterone-induced apoptosis (Supplemental Figure 2.1A), which suggests that the apoptotic response is specific to testosterone and not a result of the conversion of testosterone to DHT. Treatment with 100 nM testosterone conjugated to bovine serum albumin (T-BSA) also resulted in a significant increase in G/T cell apoptosis compared to vehicle control, while treatment with E2-BSA had no effect, similar to that seen with E2 (Supplemental Figure 2.1B/C).

Characterization of the intracellular free zinc

Testosterone treatment for 30 min caused a significant increase in intracellular free zinc over the concentration range of 10 to 50 nM, but the response was not concentration-dependent (Figure 2.2A). Intracellular free zinc levels in G/T cells were unaltered compared to vehicle controls after 30 min treatment with 100 nM mibolerone and non-androgen steroids, whereas they were significantly increased after treatment with 100 nM testosterone, indicating the steroid specificity of the effect (Figure 2.2B). T-BSA treatment also resulted in an increase in intracellular free zinc concentrations, indicating that this response is mediated at the cell surface (Figure 2.2C).

Role of caspases in testosterone-induced apoptosis

Cells were treated with selective inhibitors of caspase 3 (10 μM, Z-DEVD-FMK) and caspase 8 (10 μM, ZIETD-FMC) to identify which caspases may be involved in the testosterone-induced apoptotic pathway in G/T cells. Co-treatment with the caspase 3 inhibitor, but not the caspase 8 inhibitor, abolished testosterone-induced apoptosis (Figure 2.3A,B). Furthermore, testosterone (100 nM) treatment for 16 hr caused a significant increase in caspase 3 activity (Figure 2.3C).

Role of a $G_s\alpha$ subunit pathway in testosterone-induced apoptosis

Treatment of G/T cells with either testosterone or T-BSA (50 nM) for 10 min resulted in a significant increase in intracellular cAMP levels (Figure 2.4A), indicating that testosterone induces a rise in cAMP levels through a cell surface-mediated mechanism. The role of downstream members of the $G_s\alpha$ subunit-mediated pathway in testosterone-induced apoptosis and caspase 3 activity was investigated using specific inhibitors of activation of the $G_s\alpha$ subunit (10 μM, NF449), adenylyl cyclase (50 μM, dd-Ado), and PKA (1 μM , KT5720). Co-treatment with the inhibitors blocked the testosterone-induced apoptosis and increase in caspase 3 activity, whereas treatment with the inhibitors alone did not alter apoptosis and caspase 3 activity (Figure 2.4B,C).

Role of Erk signaling in testosterone-induced apoptosis

Phosphorylation of Erk was increased after incubation of G/T cells with testosterone (100 nM) for 15 min (Figure 2.5A). The Erk inhibitor PD98056 did not alter apoptosis or caspase 3 activity of G/T cells when administered alone, but co-treatment of the inhibitor and testosterone effectively inhibited testosterone induction of apoptosis and caspase 3 activity (Figure 2.5B,C).

Role of pro-apoptotic members

The role of Bax in the testosterone-induction of apoptosis was investigated using a selective inhibitor of the protein (50 μM, peptide V5). Co-treatment with the Bax inhibitor abolished testosterone-induced apoptosis (Figure 2.6A). The effect of testosterone treatment on the regulation of pro-apoptotic members Bax, p53, and JNK was determined by qPCR. A 24 hr treatment with 50 nM testosterone resulted in upregulation of expression of *bax*, *p53*, and *jnk* transcripts (Figure 2.6B). A time-course experiment showed that *bax* expression is upregulated after 16 hr treatment with 100 nM testosterone (Supplemental Figure 2.2).

Role of ZIP9 in testosterone-induced pro-apoptotic gene expression, apoptosis, and cAMP response

siRNA was used to knockdown the expression of ZIP9 to determine whether the upregulation of the pro-apoptotic genes, apoptosis, and the testosterone-induced cAMP responses are mediated by ZIP9. ZIP9 knockdown completely abrogated the effect of 24 hr testosterone treatment on *bax*, *p53*, and *jnk* mRNA expression while scrambled primers did not abolish the testosterone effect (Figure 2.7A-C). ZIP9 siRNA treatment also blocked the apoptotic response to testosterone as measured by Hoechst assay (Figure 2.7D). Transfection with ZIP9 siRNA also abolished the testosterone-induced increase in cAMP levels whereas scrambled primers were ineffective (Figure 2.7E). ZIP9 siRNA transfection resulted in a decrease in ZIP9 protein expression while transfection with scrambled primers did not affect ZIP9 levels (Figure 2.7F).

Requirement of zinc in the culture media for testosterone-induced apoptosis

The absence of added zinc in the zinc-free culture media resulted in an abrogation of the typical testosterone response, resulting in no significant difference between control and testosterone treatment in apoptosis as determined by the Hoechst assay (Figure 2.8A). The absence of supplemented extracellular zinc also resulted in the inhibition of the

testosterone-induced increase in *bax* expression (Figure 2.8B) and caspase 3 activity (Figure 2.8C).

DISCUSSION

This study provides an in-depth investigation of ZIP9's actions in primary G/T cells from the croaker model in which the receptor was first cloned. Here we demonstrate that in Atlantic croaker G/T cells, ZIP9 elicits testosterone induction of apoptosis through a mechanism involving a $G_s\alpha$ subunit-dependent signaling pathway, Erk signaling, and the pro-apoptotic members caspase 3, Bax, p53, and JNK. The finding that testosterone treatment increases caspase 3 activity, but not caspase 8 activity, is consistent with ZIP9 induction of apoptosis through an intrinsic pathway. Recombinant croaker ZIP9 has previously been shown to be coupled to a stimulatory G protein and mediate a testosterone-induced increase in cAMP levels in transfected SKBR3 cells (25). However, the current data provides the first evidence for a role of a $G_s\alpha$ subunit-dependent pathway in ZIP9-mediated apoptosis. Interestingly, ZIP9-induced apoptosis involves activation of an Erk signaling pathway, as well as upregulation of the same pro-apoptotic members in G/T cells as observed in human breast and prostate cancer cell lines where ZIP9 induces apoptosis through activation of a G_i protein (26). These findings suggest that the ZIP9-induced apoptosis in vertebrate cells can be regulated through different signal transduction pathways. Finally, the observation that the absence of supplemented zinc in the culture media blocked downstream testosterone-induced apoptotic events indicates that both the $G_s\alpha$ signaling and zinc transport functions of ZIP9 are required for testosterone-induced apoptosis in G/T cells. The discovery that the ZIP9-mediated response requires the presence of supplemented extracellular zinc supports the role of ZIP9 concurrently acting as a membrane steroid receptor and as a zinc transporter.

Although it is perhaps surprising that a similar downstream apoptotic mechanism is induced by ZIP9 in diverse cell types through activation of different G proteins, the ability of ZIP9 to activate multiple G proteins is not unusual and has been reported with other hormone receptors (17,98). For example, membrane progesterone receptor alpha induces the resumption of meiosis through activation of an inhibitory G protein in croaker oocytes whereas it causes sperm hypermotility in this species through activation of a stimulatory G protein (17). ZIP9 has also been shown to interact directly with the G protein Gnα11, which is a member of the Gqα protein family, in the murine spermatogenic GC-2 cell line (99), which further supports the notion that ZIP9 can couple to a variety of different G proteins, and therefore, activate different signaling pathways to modulate cell functions. It remains unknown if these differences in ZIP9 activation of a particular G protein are a reflection of the different cell models examined, or species differences, or a combination of both. Further studies on G protein coupling of ZIP9 in multiple cell types within a species and the same cell types in different species would clarify the basis for ZIP9 coupling to different G proteins.

The results show that the testosterone-induced increases in caspase 3 activity and apoptosis in croaker G/T cells are regulated by multiple signaling pathway components, involving activation of the Gαs protein subunit, membrane adenylyl cyclase, protein kinase A, and MAP kinase (MAPK). Whereas it is well accepted that activation of the membrane adenylyl cyclase/cAMP/protein kinase A pathway is mediated through the Gα subunit of the G_s protein, the signal transduction mechanism resulting in increased MAPK/Erk activity remains unclear. Simultaneous activation of multiple signaling pathways through both the G protein α and βγ subunits is commonly observed with G protein-coupled receptors (100). Signaling through the βγ subunit of the G protein is a potential mechanism of Erk activation in G/T cells since Erk can be activated through the βγ subunits of both

G_i- and G_s-proteins (101). A common mechanism of Erk activation through the G protein βγ subunits would provide a plausible explanation of how Erk is activated through ZIP9 in both G/T cells and human cancer cells. Alternatively, Erk can be activated downstream of PKA (102), and thus the G_sα-subunit could be primarily involved in activation of both signaling pathways in croaker G/T cells.

The involvement of cAMP in G/T cell apoptosis in croaker has previously been documented in granulosa cells isolated from rat preovulatory follicles (103,104), human ovum (105), and in immortalized human granulosa cells (106), which suggests that the induction of granulosa cell apoptosis through cAMP-dependent signaling is a common mechanism in vertebrate ovaries. There are no reports, to our knowledge, that testosterone treatment elevates cAMP concentrations in granulosa cells. However, androgens have been shown to increase cAMP levels in other tissues, although apoptosis was not examined in these studies (107,108). Many of the cAMP-related apoptotic responses in mammalian granulosa cells involve activation of the same pro-apoptotic members as those observed in the ZIP9-mediated G/T and cancer cell models, including p53 (104,106,109) and Bax (104). The fact that ZIP9 has been detected in human ovaries and an immortalized rat granulosa cell line (26), suggests it also has a physiological function in mammalian granulosa cells. A major question that is currently under investigation is whether the same pathway activated by the ZIP9-coupled G_sα subunit in androgen-induction of apoptosis of croaker G/T cells is activated by ZIP9 in mammalian ovarian follicle cells.

Members of the ZIP family of zinc transporters transport zinc into the cytoplasmic compartment, either from the extracellular region or intracellular compartments (95,110). ZIP9 is no exception as demonstrated in earlier siRNA experiments in croaker G/T cells and MDA-MB-468 cells and in ZIP9-transfected SKBR3 and PC-3 cells, in which ZIP9 expression was required for the increase in intracellular free zinc levels in response to

testosterone treatments (25,26). However, the ZIP9 zinc response differs from those reported to date for all the other members of the ZIP family in that is induced by a steroid hormone, testosterone. The present results show the highly specific zinc response to testosterone in G/T cells is very similar to that reported for human ZIP9 in MDA-MB-468 cells (26). The finding that the induction of apoptosis in the G/T cells shows the same steroid specificity is consistent with the hypothesis that the rise in intracellular free zinc is required for the testosterone-mediated apoptotic response. Previous results showing that chelation of internal zinc with TPEN in croaker ZIP9-transfected SKBR3 cells blocked testosterone-induced apoptosis further support this proposed role of zinc (25). Although it is unclear how free intracellular zinc mediates apoptosis in this mode, zinc signaling has been shown to mediate cellular responses through multiple mechanisms. Zinc acts a cofactors to numerous enzymes and metelloproteins, but has also been shown to inhibit phosphotases and can stimulate calcium release (111). The present results provide the first evidence that extracellular zinc is required for testosterone upregulation of pro-apoptotic members and the completion of the apoptotic response through ZIP9. The testosterone-induced increase in apoptosis, intracellular free zinc concentrations, and cAMP levels in croaker G/T cells is mimicked by T-BSA which cannot enter the cells and activate intracellular androgen receptors. These actions of testosterone initiated at the cell surface further suggest the transport of extracellular zinc across the plasma membrane into the cell is the primary mechanism through which testosterone causes increases in intracellular free zinc concentrations. ZIP9 is primarily localized on the cell membranes of croaker G/T cells and SKBR3-ZIP9 cells but is found in multiple cellular fractions including the mitochondrial, membrane, and nuclear fractions of MDA-MB-468 and ZIP9-transfected PC-3 cells (26), and was reported to be confined to the *trans*-Golgi network in the chicken pre-B cell line DT40 (112). Therefore, it cannot be inferred from the current experiments

that the testosterone-induced increase in intracellular free zinc is solely a result of ZIP9 importing extracellular zinc into the cell. Additional research on the movement of zinc between cellular compartments will be required to clarify the actions of zinc in ZIP9-mediated apoptosis.

Mibolerone was used as a negative control in the current studies to differentiate androgen actions mediated through ZIP9, which does not bind mibolerone (25), from those regulated by the AR which is expressed in croaker ovaries and displays a high binding affinity for this AR agonist (80). The finding that mibolerone does not cause increases in intracellular free zinc and apoptosis is consistent with previous results with AR siRNA indicating a lack of involvement of this receptor in androgen-induced G/T cell apoptosis (25). Androgens have been reported to stimulate follicle growth, granulosa cell proliferation and inhibit apoptosis in some studies (54,55,59), while others have shown a pro-apoptotic effect of androgen treatment on porcine and rat granulosa cells (61,64,65). Murine nuclear androgen receptor knockout models exhibit decreased follicle growth and increases in apoptosis and atresia within the ovary (68,70,73). This suggests that the nuclear receptor likely plays an important role in murine folliculogenesis but not in the mediation of testosterone-induced apoptotic events. Differential activation of nuclear and membrane androgen receptors present in granulosa cells under different physiological conditions could partially explain the disparate effects of testosterone in the ovary, especially since different effects of androgens acting through intracellular and membrane androgen receptors have been reported in C6 glial cells (27).

ZIP9 regulation of ovarian follicle cell apoptosis may be particularly important for maintenance of ovarian physiology in teleost fishes such as croaker, which release thousands of eggs during each spawn and require extensive gonadal reconstruction following oocyte release. After teleosts spawn, apoptosis is required for follicular atresia

and in the breakdown of the numerous post-ovulatory follicles (82–85). In contrast, apoptosis occurs during follicle attrition in the prenatal period and in atresia throughout life in mammals, but only a relatively small number of ovarian follicles undergo this process at any given time which may explain, at least partially, the relatively low expression of ZIP9 in human ovaries (26). Information on the expression of ZIP9 and its promotion of apoptosis in granulosa cells at different stages of follicular development in both teleosts and mammals will be required for a better understanding of ZIP9's role in teleost and mammalian ovarian physiology.

Based on the results presented here and prior findings (25), we propose a model for ZIP9 mediation of testosterone-induced apoptosis in croaker G/T cells through an intrinsic apoptotic pathway (Figure 2.9). In this model, testosterone binds to ZIP9 on the cell surface to elicit an apoptotic pathway involving increased mRNA expression of pro-apoptotic genes, increased caspase 3 activity, and a higher incidence of apoptosis. ZIP9 mediates these responses by activating a stimulatory G protein which results in increased levels of cAMP and MAPK activity. Both MAPK and members of the $G_s\alpha$/adenylyl cyclase/cAMP/PKA pathway are required for testosterone-mediated caspase 3 activation and apoptosis. In addition, supplemented extracellular zinc is required for testosterone-mediated increases in pro-apoptotic gene expression, caspase 3 activity, and apoptosis. Moreover, chelation of intracellular free zinc inhibits testosterone-induced apoptosis. This apoptotic response involves increased expression of JNK and P53, both of which are known to regulate expression of Bcl-2 family members such as Bax. Additionally, JNK and Bax can modulate mitochondrial membrane permeability leading to subsequent cytochrome c release (1,113). To date, we have shown that ZIP9 knockdown results in abrogation of testosterone-mediated rapid signaling events such as increases in intracellular

free zinc and cAMP levels, as well as downstream changes in pro-apoptotic gene expression, activation of caspase 3, and apoptosis.

In summary, the present results show that testosterone activation of the novel membrane receptor ZIP9 results in G/T cell apoptosis through a mechanism involving $G_s\alpha$ subunit signaling and activation of the Erk signaling pathway. The activation of multiple pathways in the croaker G/T cell model suggests that ZIP9-mediated apoptosis is tightly controlled, and inhibition of any one of the numerous members of the pathway may control the shift between cell survival and cell death. The mechanism of action of ZIP9 through a G_s protein in croaker G/T cells differs from that previously examined in human cancer cell lines (26). The requirement of extracellular zinc for the completion of androgen-induced apoptotic events suggests that in addition to acting as a membrane steroid receptor, ZIP9 also maintains zinc-transporter functions which are critical for its apoptotic functions. While ZIP9's functions in ovarian physiology are not fully understood, the finding that it induces G/T cell apoptosis suggests it likely has a role in follicular cell apoptosis during atresia and postovulatory follicle breakdown. The present study further characterizes a recently discovered mechanism by which steroid hormones can directly influence zinc homeostasis through a single protein, ZIP9. This novel mechanism coordinates androgen-induced G protein signaling pathways with zinc signaling to induce an essential cellular function, apoptosis, in vertebrate cells.

FIGURES

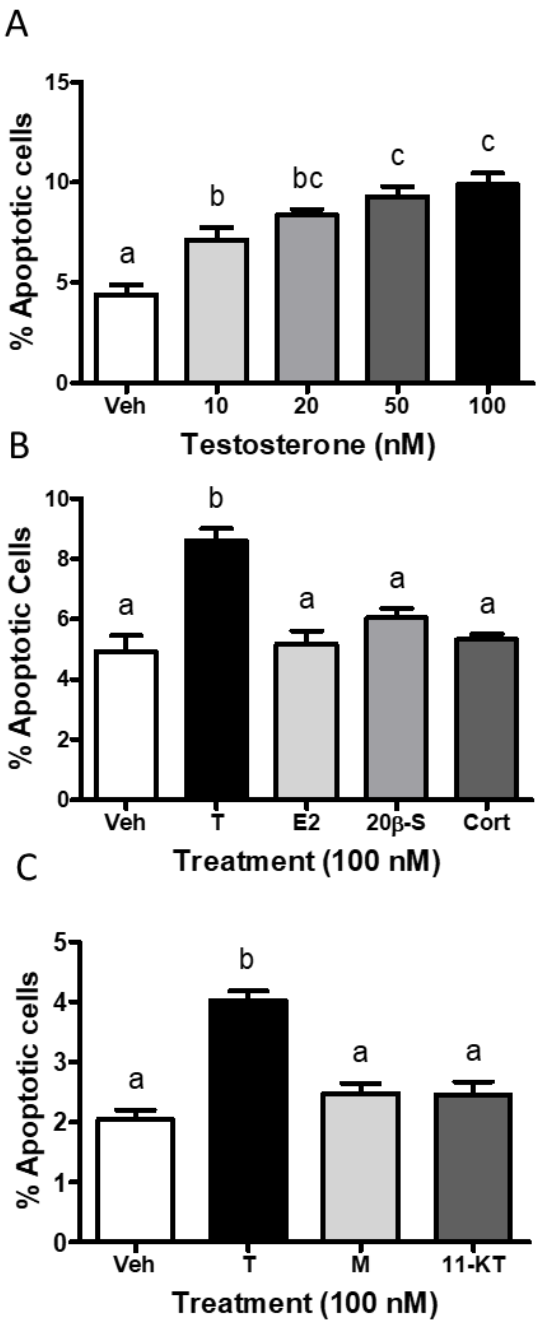

Figure 2.1: Testosterone induction of apoptosis in croaker G/T cells. A, Effects of various concentrations of testosterone on % apoptotic nuclei. B, Effects of testosterone and other steroid treatments on % apoptotic nuclei. C, Effects of androgen treatments on % apoptotic nuclei. All data represents means ± SEM. Significance was determined by one-way ANOVA with Bonferroni multiple comparison post-test. Different letters indicate significant differences between the treatment groups in the *post hoc* test at $p < 0.05$. Experiments were repeated with three fish and each treatment conducted in triplicate with similar results obtained for each. Veh, ethanol control; T, testosterone; E2, estradiol-17β; Cort, cortisol; 20β-S, 17,20β,21-trihydroxy-4-pregnen-3-one; M, mibolerone; 11-KT, 11-ketotestosterone.

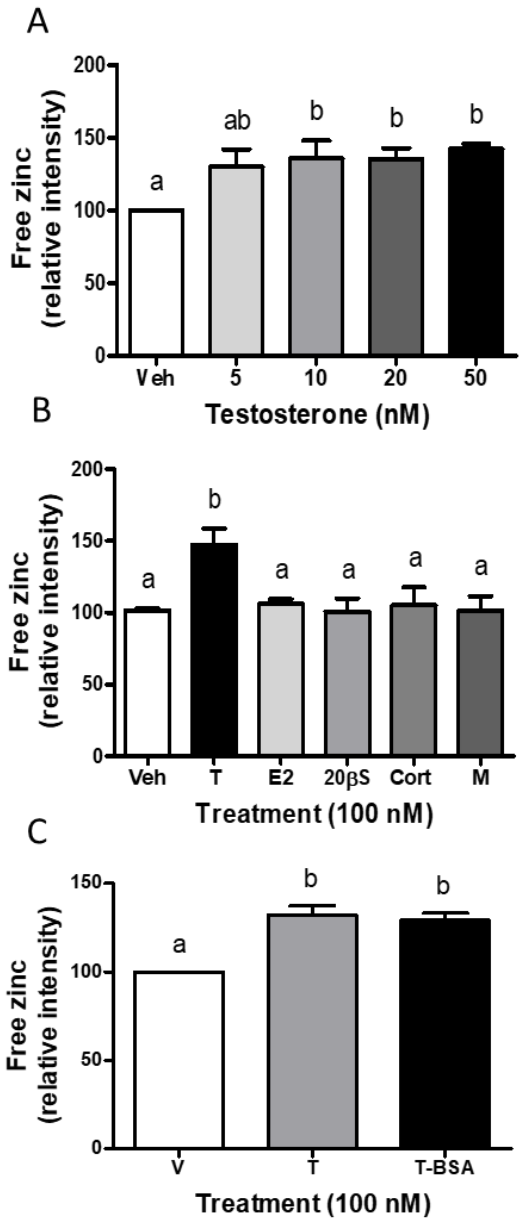

Figure 2.2: Testosterone modulation of intracellular free zinc levels in G/T cells. A, Effects of various concentrations of testosterone on intracellular free zinc levels. B, Effects of testosterone and other steroid treatments on intracellular free zinc levels. C, Effects of T-BSA on free intracellular zinc levels. All data represents means ± SEM. Significance was determined by one-way ANOVA with Bonferroni multiple comparison post-test. Different letters indicate significant differences between different treatment groups in the *post hoc* test at $p < 0.05$. Each treatment was conducted in 8-16 wells of a 96-well plate and averaged. The experiments were conducted with G/T cells from 3-6 fish and the average values of each treatment were used to determine significance. T-BSA; testosterone conjugated to bovine serum albumin.

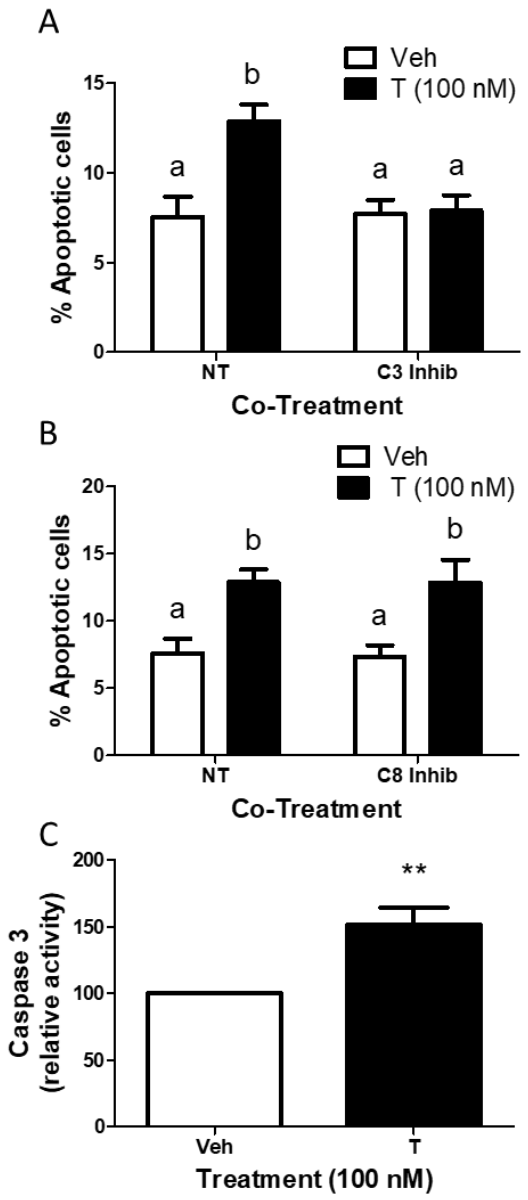

Figure 2.3: Role of caspases in testosterone-induced apoptosis. A, Effect of co-treatment with 10 μM caspase 3 inhibitor (Z-DEVD-FMK) on testosterone-induced apoptosis in G/T cells. Significant interactive effects of testosterone in the presence of the inhibitor on G/T cell apoptosis was detected by two-way ANOVA, which was predicted because the inhibitor blocked this androgen-induced response. B, Effect of co-treatment with 10 μM caspase 8 inhibitor (ZIETD-FMC). No significant interactive effects of testosterone treatment in the presence of the inhibitor on G/T cell apoptosis was detected by two-way ANOVA, which was predicted because the inhibitor had no effect on the androgen-induced response. ANOVAs for (A) and (B) were followed by Bonferroni multiple comparison test. Different letters indicate significant differences between different treatment groups in the post hoc test at $p < 0.05$. C, Relative caspase 3 activity after 16-hr testosterone treatment. Results for (C) were analyzed with Student's t-test. **, $p<0.01$. All data represent means ± SEM. Apoptosis experiments were repeated with 3 fish and each treatment conducted in duplicate with similar results obtained for each. Caspase 3 activity was assessed for 5 fish. NT, no inhibitor treatment; C3 Inhib, Z-DEVD-FMK; C8 Inhib, ZIETD-FMC.

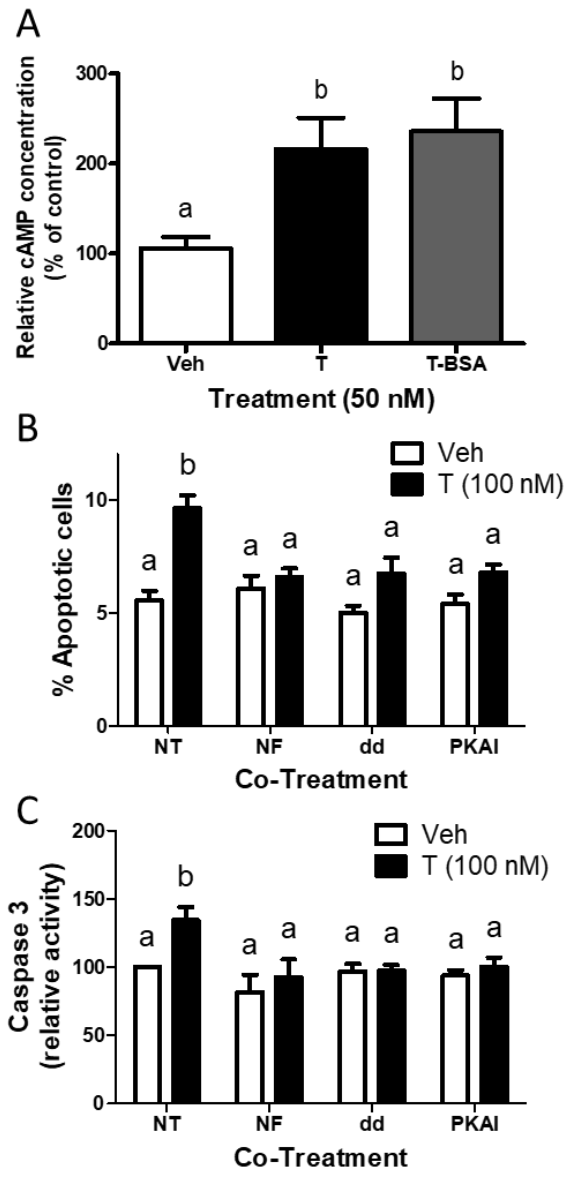

Figure 2.4: Involvement of members of a $G_s\alpha$ subunit signaling pathway in testosterone-mediated apoptosis and caspase 3 activity. A, Relative cAMP concentrations in G/T cells treated for 10 min with vehicle, testosterone, or T-BSA. Significance was determined by one-way ANOVA with Bonferroni multiple comparison post-test. Different letters indicate significant differences between different treatment groups in the post hoc test at $p < 0.05$. B, Effects of co-treatment with inhibitors of the $G_s\alpha$ subunit, adenylyl cyclase, and PKA on testosterone-mediated apoptosis. C, Effects of co-treatment with inhibitors on testosterone-mediated activation of caspase 3. In experiments (B) and (C) significant interactive effects of testosterone treatment in the presence of each inhibitor on G/T cell apoptosis and caspase 3 activity was detected by two-way ANOVA, which was predicted because the inhibitors blocked these androgen-induced responses. Different letters indicate significant differences between different treatment groups in the Bonferroni multiple comparison post-test test at $p < 0.05$. All data represent means ± SEM. All experiments were repeated with 3-6 fish and each treatment was conducted in duplicate or triplicate with similar results obtained for each. NT, no inhibitor treatment; NF, NF449 (10 μM); dd, dd-Ado (50 μM); PKAI, KT5720 (1 μM).

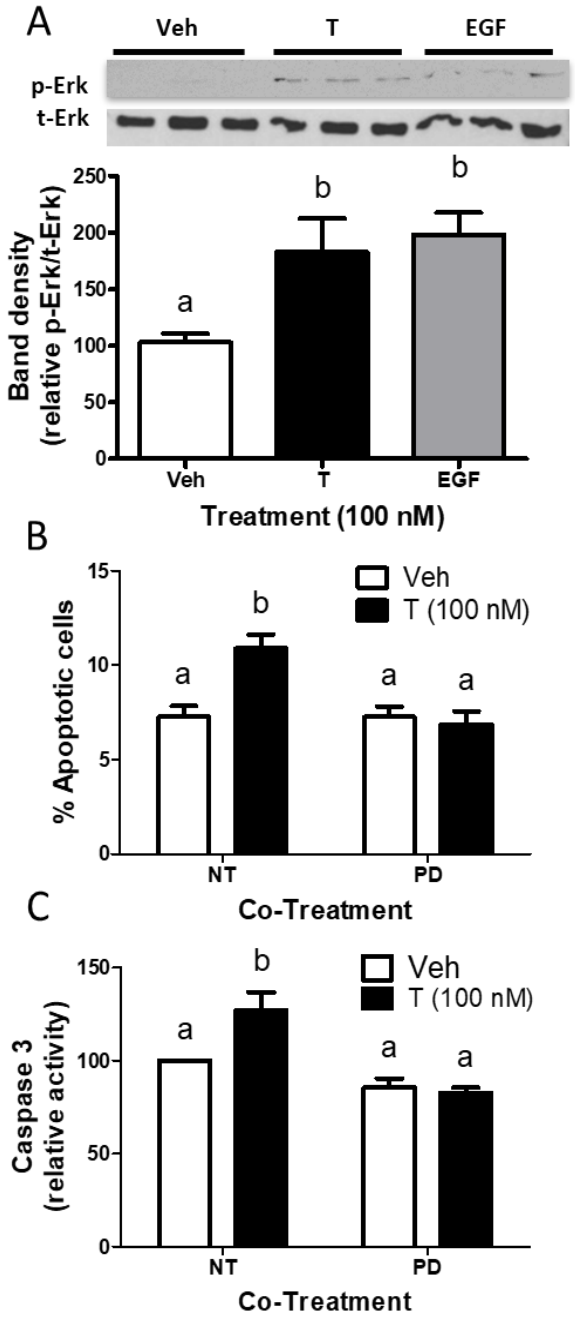

Figure 2.5: Involvement of MAPK signaling in the testosterone-mediated apoptotic pathway. A, Relative phospho-Erk normalized to total-Erk in G/T cells treated with vehicle, 100 nM testosterone, or 100 nM EGF. B, Effects of co-treatment with an Erk inhibitor (PD98059) on testosterone-mediated apoptosis. C, Effects of co-treatment with the Erk inhibitor on testosterone-mediated caspase 3 activation. Significance was determined by one- or two-way ANOVA with Bonferroni multiple comparison post-test. Different letters indicate significant differences between different treatment groups in the post hoc test at $p < 0.05$. In experiments (B) and (C) significant interactive effects of testosterone treatment in the presence of the inhibitor on G/T cell apoptosis and caspase 3 activity was detected by the two-way ANOVA, which was predicted because the inhibitor blocked these androgen-induced responses. All data represent means ± SEM. All experiments were repeated with 3-5 fish and each treatment conducted in duplicate or triplicate with similar results obtained for each. NT, no inhibitor treatment; PD, PD98059 (10 μM).

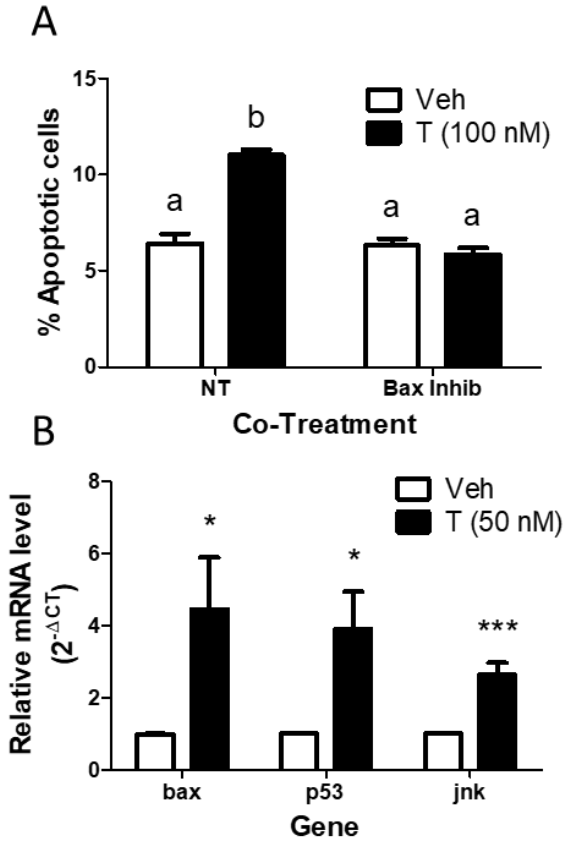

Figure 2.6: Role of pro-apoptotic members in testosterone-mediated apoptosis. A, Effect of co-treatment with 50 μM Bax inhibitor (peptide V5) on testosterone-induced apoptosis in G/T cells. Significant interactive effects of testosterone treatment in the presence of the inhibitor on G/T cell apoptosis was detected by two-way ANOVA, which was predicted because the inhibitor blocked the androgen-induced response. In experiment (A), each treatment was conducted in duplicate or triplicate and repeated with 3 fish with similar results obtained for each. C, Expression of bax, p53, and jnk mRNA after 24 hrs of 50 nM testosterone treatment. In experiment (C) treatments were conducted in duplicate and repeated with 8 fish with similar results obtained for each. All qPCR data was normalized to the housekeeping gene 18S. All data represent means ± SEM. Significance was determined by one- or two-way ANOVA with Bonferroni multiple comparison post-test or Student's t-test. Different letters indicate significant differences between different treatment groups in the post hoc test at $p < 0.05$. *, $p < 0.05$; ***, $p < 0.001$ compared to control in Student's t-test. NT, no inhibitor treatment; Bax Inhib, peptide V5.

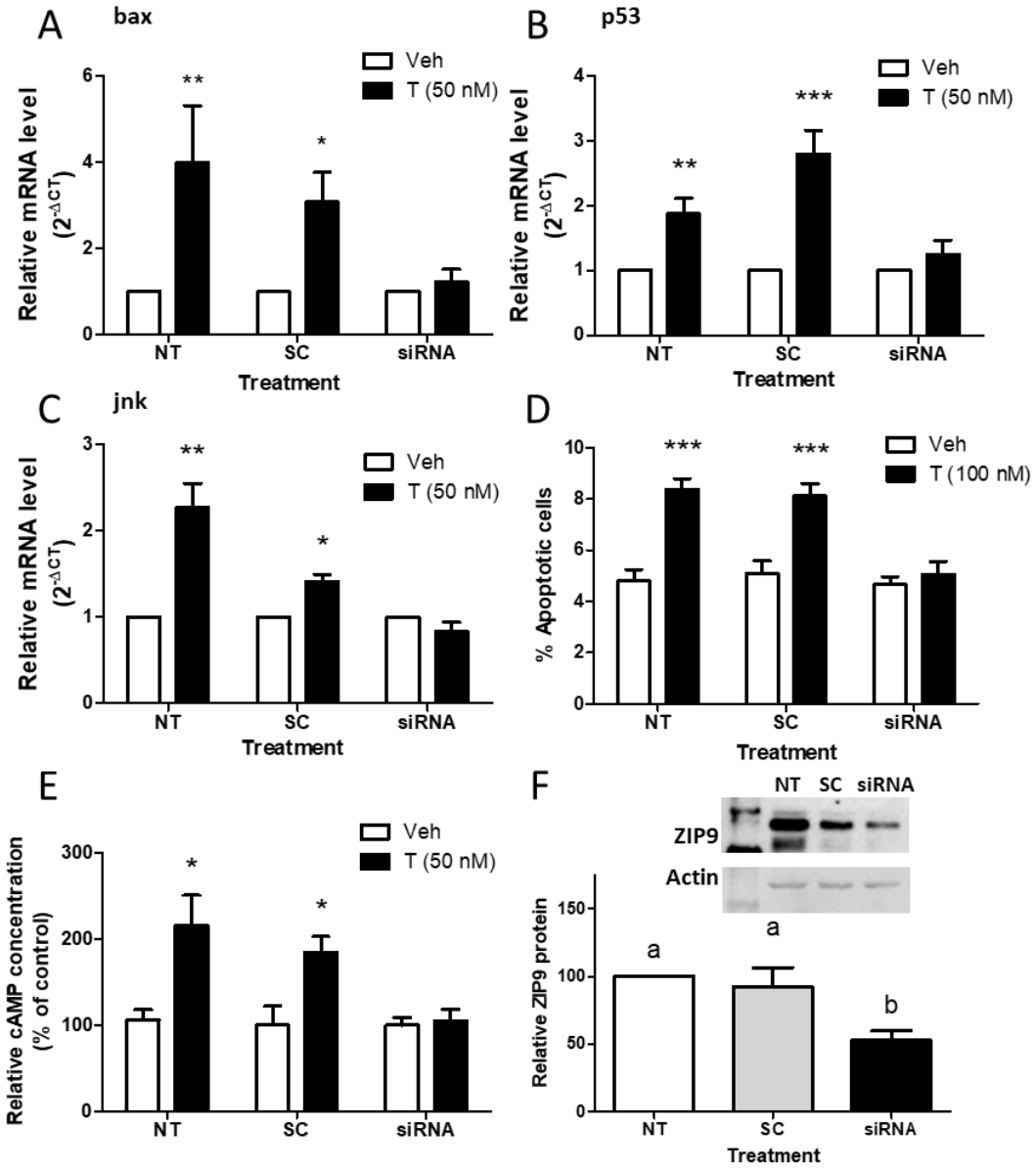

Figure 2.7: Effect of ZIP9-targeting siRNA on mRNA expression of pro-apoptotic members, apoptosis, and cAMP levels.

Figure 2.7 (continued): Effect of ZIP9-targeting siRNA on mRNA expression of pro-apoptotic members, apoptosis, and cAMP levels. A-F, Effects of ZIP9-targeting siRNA on the testosterone-induced increase in bax (A), p53 (B), and jnk (C) expression, apoptosis (D), cAMP levels (E), and on relative ZIP9 protein expression (F). All qPCR data was normalized to housekeeping gene 18S. In experiments (A-E) significant interactive effects of each steroid treatment (Veh & T) and the transfection treatments on pro-apoptotic member mRNA expression, G/T cell apoptosis, and cAMP was detected by the two-way ANOVA, which was predicted because ZIP9-targeting siRNA blocked the androgen-induced responses. *, $p < 0.05$; **, $p < 0.01$; ***, $p < 0.001$ compared to control in Student's t-test. In experiment (F) significance was determined by one-way ANOVA followed by with Bonferroni multiple comparison post-test. Different letters indicate significant differences between different treatment groups in post hoc test at $p < 0.05$. All data represent means ± SEM. For gene expression and apoptosis experiments, steroid treatments were conducted in duplicate and repeated with 5 fish with similar results obtained for each. For cAMP experiment steroid treatments were conducted in triplicate with 3 fish with similar results obtained for each. NT, no transfection; SC, scramble siRNA control; siRNA, small interfering RNA targeted at croaker ZIP9; actin, actin loading control.

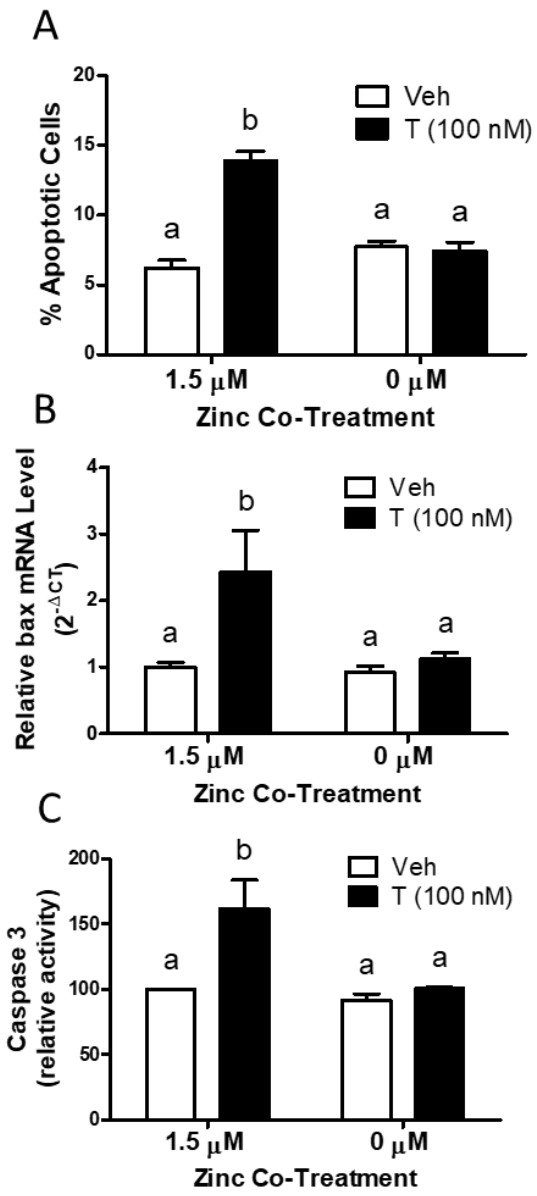

Figure 2.8: Effect of extracellular zinc in testosterone-mediated apoptotic events. Testosterone-induction of apoptosis (A), bax expression upregulation (B), and caspase 3 activity (C) when the testosterone treatment was administered in media supplemented with 1.5 µM or 0 µM zinc. Significant interactive effects of testosterone at different zinc concentrations on G/T cell apoptosis, bax expression, and caspase 3 activity was detected by two-way ANOVA, which was predicted because the low zinc concentrations blocked these androgen-induced responses. All data represents means ± SEM. Different letters indicate significant differences between different treatment groups in the Bonferroni multiple comparison post-test at $p < 0.05$. All Experiments were repeated with 3 fish and each treatment was conducted in duplicate or triplicate with similar results obtained for each.

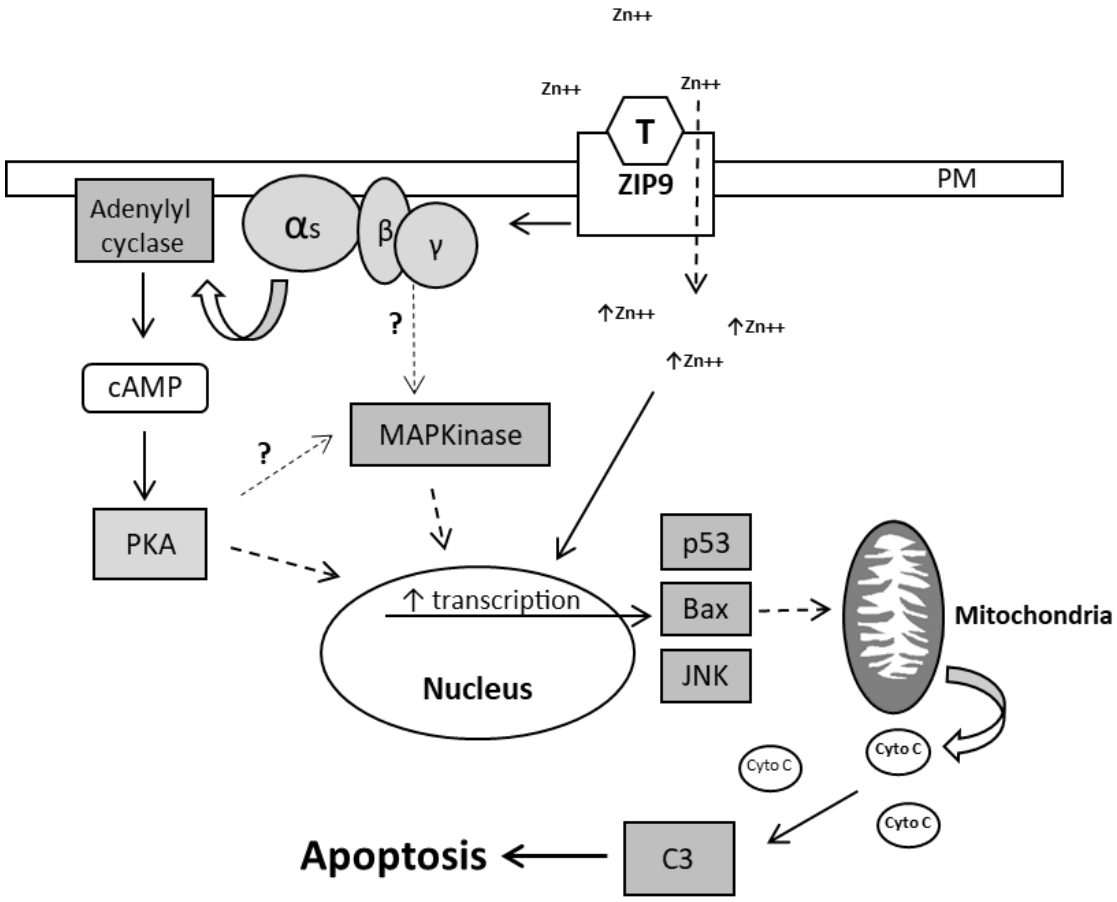

Figure 2.9: Proposed model of testosterone acting through ZIP9 to mediated croaker G/T cell apoptosis. ZIP9 is coupled to a stimulatory G protein which leads to increased cAMP levels and MAPK activity, which along with intracellular free zinc, are required for the induction of apoptosis. Further details of the model are described in the discussion. T, testosterone; PM, plasma membrane; αs, stimulatory G protein α-subunit; βγ, G protein βγ-subunit; PKA, protein kinase A; Cyto C, cytochrome c; C3, caspase 3.

SUPPLEMENTAL DATA

Peptide/protein target	Antigen sequence (if known)	Name of Antibody	Manufacturer, catalog #, and/or name of individual providing the antibody	Antibody RRID	Species raised in; monoclonal or polyclonal	Dilution used
Atlantic croaker membrane androgen receptor	Purified Atlantic membrane androgen receptor protein	Atlantic croaker mAR	custom, Charles D. Rice/Peter Thomas	AB_2651045	Mouse, polyclonal	1:5000
Phosporylated-Erk1/2	Phosphorylation at Thr202 and Tyr204 of Erk1 and Thr185 and Tyr187 of Erk2	Phospho-p44/42 MAPK (Erk1/2)	Cell Signaling, 9106	AB_331768	Mouse, monoclonal	1:1000
Total-Erk1/2	Near the C-terminus of p 44/42 MAPK	p44/42 MAPK (Erk1/2)	Cell Signaling, 9102	AB_330744	Rabbit, polyclonal	1:1000
Actin-beta	The C-terminal region of zebrafish actin-beta protein	Anti-Actin-beta (NT), Z-Fish	AnaSpec, 55338s	AB_11232819	Rabbit, polyclonal	1:1000

Table 2.1: List of antibodies used in Chapter 2.

Primer	Forward	Reverse
Bax	TGTCGACTCGTCATCAAAGC	GCCAAAGTGGGAACGAATAC
P53	CAGGGTGGAGGGCAGCCAGA	GGGTCTGCGGTTCATGCCCC
JNK	TTCTCAAGCGCTACCAGCAA	GGACTTCTGAGGCGTGAACA
18S	AGAAACGGCTACCACATCCA	TCCCGAGATCCAACTACGAG

Table 2.2: Sequence of primers (5'-3') used for qPCR experiments (Chapter 2).

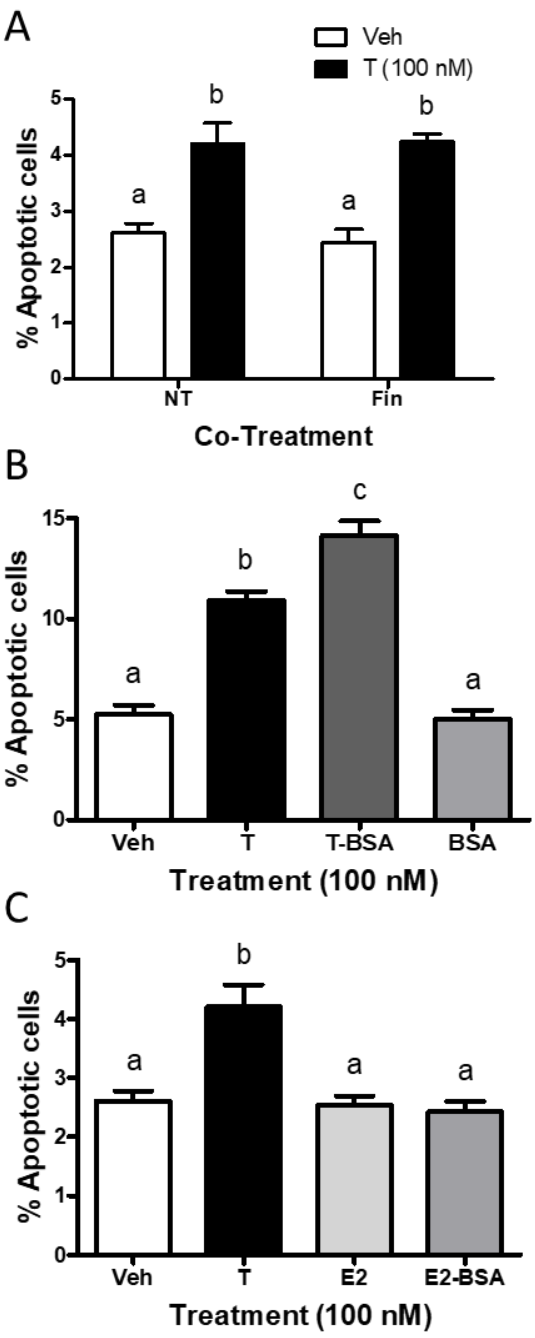

Figure 2.10: Further characterization of androgen-induced G/T cell apoptosis. A, effect of 5-alpha reductase inhibitor (finasteride 50 µM) on testosterone-mediated apoptosis. No significant interactive effects of testosterone treatment in the presence of the inhibitor on G/T cell apoptosis was detected by two-way ANOVA, which was predicted because the inhibitor had no effect on the androgen-induced response. B/C, effects of BSA conjugated testosterone and estradiol on G/T cell apoptosis. Significance was determined by one-way ANOVA with Bonferroni multiple comparison post-test. Different letters indicate significant differences between different treatment groups in the post hoc test at $p < 0.05$. All data represents means ± SEM. Experiments were repeated with 3 fish and each treatment conducted in triplicate with similar results obtained for each. Fin, finasteride (50 µM); T-BSA, testosterone conjugated to bovine serum albumin; E2-BSA, estradiol conjugated to bovine serum albumin.

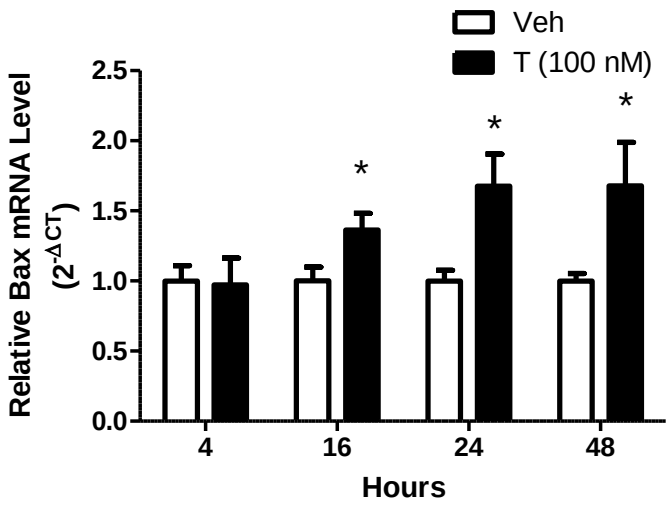

Figure 2.11: Time course of testosterone's effect on relative Bax mRNA levels. All data represents means ± SEM. Significance was determined by Student's t-test. *, $p < 0.05$. Experiments were repeated with six fish and each treatment conducted in duplicate with similar results obtained for each.

Chapter 3: The membrane androgen receptor ZIP9-mediates pro- and anti-apoptotic responses in Atlantic croaker ovarian follicle cells by activating G_i and G_s in a follicle stage-dependent manner

ABSTRACT

ZIP9 was previously found to mediate androgen-induced apoptosis of Atlantic croaker granulosa/theca (G/T) cells isolated from reproductively mature ovaries. This apoptotic response involves stimulatory G protein activation, increased cAMP and free intracellular zinc levels, and upregulation of pro-apoptotic member mRNA. Interestingly, preliminary evidence was obtained indicating that testosterone acts in an anti-apoptotic fashion in G/T cells from ovaries not at the reproductive peak. Here we show that testosterone-mediates both pro- and anti-apoptotic responses in a follicle stage-dependent manner. G/T cells from early stage follicles (diameter <300μm) exhibited the anti-apoptotic response while G/T cells from late stage follicles (diameter >400μm) showed the apoptotic response. siRNA targeting ZIP9, but not the nuclear androgen receptor, blocked the anti-apoptotic response, indicating ZIP9 mediates both pro- and anti-apoptotic responses. Testosterone treatment of early stage G/T cells resulted in opposite trends in signaling from the ZIP9-mediated apoptotic response, with decreased cAMP and intracellular free zinc levels, and downregulation of pro-apoptotic member mRNA expression. Furthermore, activators of stimulatory G protein signaling antagonized the anti-apoptotic response. Proximity ligation and G protein activation assays were employed to determine if ZIP9 mediates these differential responses by activating different G proteins. In G/T cells from early stage follicles ZIP9 was in close proximity and activated an inhibitory G protein, while in G/T cells from late stage follicles ZIP9 was in close proximity and activated a stimulatory G protein. This indicates that ZIP9 mediates opposite

survival responses of croaker G/T cells by activating different G proteins in a follicle stage-dependent manner.

INTRODUCTION

In the mammalian ovary, androgens are involved in a number of physiological processes such as follicle growth, proliferation, apoptosis, and atresia. These processes are typically exhibited at specific stages of folliculogenesis with androgens promoting growth, proliferation, and survival in early stage follicles, and apoptosis and atresia at later stages of development (54,55,58–64,114). While these processes have been better characterized in mammalian models, a limited number of studies have shown that androgens promote follicle growth of previtellogenic follicles in a number of teleosts including short-finned eel, Atlantic cod, and coho salmon (57,115,116). Together these studies suggest that androgen promotion of early follicle growth may be a shared response in mammals and teleosts (116). Androgens have also been reported to promote apoptosis and atresia in a number of mammalian models, although there are discrepancies in the follicle stages that exhibit these responses (60–64,114). Early *in vivo* studies demonstrated androgens promote apoptosis and follicle atresia in both preantral (60–62) and antral (61–63) murine follicles. However, more recent *in vitro* studies have indicated that the androgen-induced apoptotic response is primarily exhibited by antral follicle cells in porcine and murine models (64,114). Recently, testosterone was found to induce apoptosis of co-cultured granulosa/theca (G/T) cells from reproductively mature Atlantic croaker ovaries with a high proportion of late stage vitellogenic follicles (25,117). This suggests that androgen-induced apoptosis in late stage follicles may also be a shared response between teleosts and mammals.

While androgens have been observed to promote a number of physiological responses in mammalian and teleost ovaries, a direct role of the nuclear androgen receptor (AR) in many of these responses remains unclear. The physiological relevance of androgen actions in the ovary that are mediated by the AR has been demonstrated in a number of murine AR knockout (ARKO) models. ARKOs are subfertile, showing reduced litter sizes, defective cumulus-oocyte complex formation, decreased oocyte viability, and increased numbers of atretic and apoptotic follicles (68,70–72). However, ARKO models have not been used to verify the loss of function of many androgen responses previously reported in *in vitro* and *in vivo* study systems. The ARKO models support a role of the AR in mediating growth and proliferative effects of androgens previously observed in wild-type models, but further work is required to confirm the role of the receptor in specific responses. An additional confounding factor in determining androgen mechanisms of action in the ovary lies in the recent discovery of the novel membrane androgen receptor ZIP9, and the finding that it mediates the androgen-induced apoptotic response observed in Atlantic croaker G/T cells (25). The zinc transport protein ZIP9 (SLC39A9) was recently cloned and characterized in Atlantic croaker ovaries and found to mediate apoptosis of croaker G/T cells independently of the AR (25). ZIP9 possesses characteristics of a membrane androgen receptor distinct from the nuclear receptor including the presence of a high-affinity and limited capacity binding site specific for androgen hormones but not for synthetic AR agonist and antagonists. ZIP9 expression is regulated by steroid hormones, and the receptor activates rapid secondary messenger cascades to induce physiological responses (25). ZIP9 is expressed in both reproductive and non-reproductive tissues in mammals and fish, but information is currently lacking on the receptor's role in mediating androgen actions in the majority of these tissues. To date, ZIP9 has been found to be involved in androgen-induced

apoptosis in a number of human cancer cell lines and croaker G/T cells, tight junction formation in murine Sertoli cells, and migration in glioblastoma cell lines (26,118,119).

ZIP9 is the only known zinc transporter belonging to the ZIP (SLC39A) family that also functions as a steroid receptor. Interestingly, the zinc transport and androgen receptor characteristics of ZIP9 appear to be tightly associated in that androgens mediate intracellular free zinc concentrations though ZIP9 activation (25,26). In addition, the ZIP9-mediated increase in intracellular free zinc is essential for the apoptotic response in both croaker G/T cells and human cancer cell lines, the regulation of which is known to involve G protein activation in PC-3 prostate cancer cells overexpressing ZIP9 (25,120). While ZIP9-mediated apoptosis involves intracellular zinc regulation, the role of ZIP9's zinc transporter activity in other physiological responses the receptor mediates remains unclear.

Membrane receptors specific for progestins and estrogens have been extensively studied over the last 15 years since the discovery of the membrane progestin receptor α (mPRα) and G protein-coupled estrogen receptor 1 (GPER), formerly known as GPR30, in 2003 and 2005, respectively (32,34,121). It has been well established that these receptors mediate physiological responses by coupling to and activating G proteins, similar to that observed with receptors for peptide hormones in the G protein-coupled receptor (GPCR) superfamily. The membrane estrogen receptor GPER couples to stimulatory G proteins (G_s) in most models (21,121,122), although a number of studies have demonstrated that GPER can mediate pertussis toxin-sensitive events (123,124), suggesting that the receptor may also activate inhibitory G proteins (G_i). mPR's are primarily known to couple to inhibitory G proteins (24,32,125,126), although coupling of mPRα to an olfactory G (G_{olf}) protein has been reported in teleost sperm (127). ZIP9 has been found to activate different G proteins in diverse cell models, including a G_s in croaker G/T cells, a G_i in human breast and prostate cancer cell lines, and a G_q in the spermatogenic cell line GC-2 (25,26,99). To

date, ZIP9 has been found to couple to different G proteins in every cell model that ZIP9-G protein interactions have been examined. It remains unclear if the differential coupling of ZIP9 to G proteins is determined by species or cell type differences, or by another mechanism.

We previously reported that ZIP9 mediates androgen-induced apoptosis in G/T cells from reproductively mature Atlantic croaker through a nonclassical signaling pathway (25,117). This apoptotic response is independent of the AR and specific to testosterone. Of interest, preliminary data has indicated that testosterone inhibits apoptosis in G/T cells from fish collected outside the peak of the reproductive season whose ovaries are not fully grown as shown by a moderate gonado-somatic index (GSI) (75). This anti-apoptotic effect was not mimicked by the AR agonist mibolerone, suggesting that this response may be mediated by an alternative androgen receptor such as ZIP9. We hypothesize that the pro- and anti-apoptotic androgen-induced responses in croaker G/T cells can be attributed to differential effects of androgens in early and late stage follicles. This may be why G/T cells from fish with lower GSI's respond differently to testosterone than G/T cells from fish with high GSI's and a corresponding higher proportion of late stage vitellogenic follicles. Therefore, the goal of the current study was to characterize androgen actions in croaker G/T cells from early and late stage ovarian follicles, <300 μm and >400 μm in diameter, respectively. These two size classes are typical of early stage follicles that are pre- or early vitellogenic, and late stage follicles that have completed vitellogenesis and are competent to undergo final oocyte maturation. We confirmed that testosterone induces and inhibits apoptosis in a follicle-stage dependent manner, and further investigated the role of ZIP9 in both responses. Relative expression of ZIP9, as well as membrane androgen binding, was examined in G/T cells from early and late follicle stages. Next, we investigated the role of members of the known ZIP9-mediated apoptotic pathway (117) in the anti-apoptotic

response. Finally, we examined potential mechanisms of ZIP9 action between the apoptotic and anti-apoptotic models by exploring the interactions of ZIP9 with inhibitory and stimulatory G proteins as well as testosterone activation of these G proteins.

MATERIALS AND METHODS

Chemicals and materials

Chemicals were purchased from Sigma-Aldrich (St. Louis, MO) unless otherwise stated. Testosterone and 4-estren-7α, 17α-dimethyl-17β-ol-3-one (Mibolerone) were purchased from Steraloids (Newport, RI). [1,2,6,7-^{3}H]Testosterone ([^{3}H]T) (100 Ci/mmol) was purchased from American Radiolabeled Chemicals (St. Louise, MO), and guanosine 5'-(γ-thio)triphosphate-[^{35}S] ([^{35}S]GTPγS) (1250 Ci/mmol) was purchased from PerkinElmer (Waltham, MA). 8-bromoadenosine 3′,5′-cyclic monophosphate (8-Br-cAMP) was purchased from Selleck Chemicals (Houston, TX). Forskolin was purchased from MP Biomedicals (Santa Ana, CA). N,N,N',N'-tetrakis(2-pyridylmethyl)-1 ,2-ethylenediamine (TPEN) was purchased from Cayman Chemicals (Ann Arbor, MI). GTPyS was purchased from Calbiochem (Burlington, MA). Bovine serum albumin-conjugated testosterone (TBSA) was dialyzed to remove free testosterone by incubation with 5 mg/mL charcoal and 0.5 mg/mL dextran at 55°C under gentle rotation for 30 min followed by removal of charcoal by two centrifugation cycles at 4600 x g for 20 min each.

Animal care and tissue collection

Atlantic croaker were purchased from bait shops near Port Aransas, Texas, and transferred to holding facilities at the University of Texas Marine Science Institute. Fish were maintained in recirculating water tanks (salinity 30-32 ppt) and fed a diet composed of commercial pellets and shrimp. Photoperiod was adjusted to replicate local summer and fall conditions (13 hr light, 11 dark at 26°C in August; 11 hr light, 13 dark at 22-23°C in

December) to induce gonadal recrudescence. Fish were acclimated to laboratory conditions for a minimum of 2 months before being used for experimentation. All experiments were conducted with ovaries from reproductively mature females (GSI >12). Fish were deeply anesthetized by immersion in a bath containing 20 mg/L MS-222 and humanely euthanized by rapid decapitation in accordance with procedures approved by the University of Texas Animal Care and Use Committee. Excised ovarian tissue was placed in Ca/Mg-free buffer (138 mM NaCl, 8.6 mM KCl, 1.62 mM Na_2HPO_4, 5 mM D-glucose, 15.8 mM HEPES, 1 mM EDTA, 100 mg/L streptomycin, 60 mg/L penicillin, pH 7.4) for follicle separation and G/T cell isolation.

Primary granulosa/theca cell culture

Croaker ovarian follicles were separated by repeated pipetting and divided into two size classes, <300 μm and >400 μm, using sieves. After the follicles had been separated by size class, G/T cells were isolated by enzymatic digestion with collagenase as previously described (96). G/T cells were resuspended in Dulbecco's Modified Eagle's medium supplemented with 3% charcoal-stripped bovine calf serum. In order to prevent G/T cells from producing endogenous steroids and converting testosterone, 100 μM of the P450 side chain cleavage and aromatase inhibitor DL-Aminoglutethimide (Alfa Aesar, Ward Hill, MA) was added to all culture media. For gene silence experiments, G/T cells were transfected with either a mixture of ZIP9 or AR targeting siRNA primers or non-targeting control primers (Dharmacon, Lafayette, CO) twice, first during plating and again after 16 hours, using Lipofectamine 2000 (Invitrogen, Carlsbad, CA). Treatments were administered 72 hr after the initial transfection.

Follicle size and stage determination

A small subset of follicles from the early and late stage pools were examined and imaged under bright field microscopy (4X). Images were used to characterize 120-200

follicles from each size subset as perinuclear stage (PNS, <100 µm), early vitellogenic (EV, 100-300 µm), or late vitellogenic (LV, >300 µm). Characterization was performed on follicles from 3 individual separations.

Membrane protein preparation

All steps were carried out at 4°C. Ovarian tissue or G/T cells were homogenized in ice-cold HAED buffer (25 mM HEPES, 10 mM NaCl, 1 mM EDTA, 1 mM DTT, pH 7.6) containing protease inhibitor (1µL/mL), followed by centrifugation at 1000 x g for 7 min to pellet the nuclear fraction. The supernatant containing the membrane protein fraction was removed and centrifuged at 20000 x g for 20 min to pellet membrane proteins. For Western blot analyses the resulting pellet was resuspended in HAED, followed by the addition of 5X reducing sample buffer (Thermo Fisher Scientific, Waltham, MA), boiling for 10 min, and subsequent storage at -80°C. For the androgen receptor binding assay, the pellet was resuspended in HAED buffer with protease inhibitor. For GTPγS binding and precipitation assays the membrane protein pellet was resuspended in GTPγS binding buffer (100mM NaCl, 5 mM $MgCl_2$, 1 mM $CaCl_2$, 0.6 mM EDTA, 0.1% BSA, 50 mM Tris-HCl, pH 7.6) with protease inhibitor.

Quantitative real-time PCR analysis

Total mRNA was isolated using Tri-reagent (Sigma-Aldrich) following the manufacturer's protocol. For expression of ZIP9 in G/T cells from different stage follicles, G/T cells were lysed in Tri-reagent immediately after isolation. For examining the effects of testosterone on the expression of the pro-apoptotic genes, G/T cells were starved for 16-24 hr prior to a 24 hr testosterone treatment, after which mRNA isolation and analysis were performed. Quantitative real-time PCR (qPCR) primers were designed against the mRNA sequences of *zip9, bax,* and *p53* (Table 3.1). qPCR was performed using Verso 1-step RT-qPCR SYBR Green Low ROX kit (Thermo Scientific), with 100 ng of mRNA per 15 µL

reaction, following the manufacturer's protocol. The qPCR program was set to 50°C for 15 min, 95°C for 15 min, and 40 cycles of 95°C for 15 s, 55°C for 30 s, 72°C for 30 s. Amplification was followed by the melting curve program, 95°C for 15 s, 60°C for 15 s and a gradual increase to 95°C over 20 min. Samples were run in duplicate and expression of target genes was normalized to the housekeeping gene 18S.

Western blot analysis

Electrophoresis was performed on membrane protein samples loaded on a 10% SDS-PAGE gel. Protein samples were transferred to a nitrocellulose membrane and blocked with 5% nonfat milk for 1 hr. After blocking, the membrane was incubated with primary antibodies for ZIP9 1:5000, actin 1:2000 (AnaSpec, Fremont CA), G_s (Proteintech, Rosemont, IL), or $G_{i(1/2)}$ (Abcam, Cambridge, MA)) overnight at 4°C. The croaker ZIP9 primary antibody was generated in mice against a partially-purified ovarian membrane fraction with androgen receptor activity and validated for measurement in this species as previously described (25). After incubation, the membranes were washed 3 times with PBS (NaCl 137 mM, KCl, 2.7 mM, Na_2HPO_4 10mM, KH_2PO_4 1.8 mM) followed by incubation with secondary antibodies (1:15000) for 1 hr at room temperature. Protein bands were visualized using Odyssey infrared imaging system (LI-COR, Lincoln, NE).

Androgen receptor binding competition assay

The ability of steroid competitors to displace [^{3}H]T binding to the membrane fractions of ovarian follicles in single-point competitive binding assays was assessed using methods described previously (74). Membrane protein (0.5-1.25 mg/ml final) was added to 3 nM (final) [^{3}H]T in the presence of vehicle, or 100 nM unlabeled testosterone or mibolerone. Nonspecific binding was determined in the presence of 1000x unlabeled testosterone (3 μM) and subtracted from total binding to determine specific [^{3}H]T binding. Reactions were conducted in triplicate, and the results expressed as % of specific binding.

Apoptosis analyses

Croaker G/T cells grown on round glass coverslips were serum-starved for 16-24 hr prior to the addition of steroid and/or drug treatment for 24 hours. All treatments were performed in duplicate or triplicate. For Hoechst staining, once treatment was complete the cells were fixed in 4% paraformaldehyde for 20 min at room temperature, stained with 1µg/ml Hoechst 33342 for 2-3 min, rinsed with PBS, and mounted face down on microscope slides. Apoptotic nuclei were identified based on the morphology of chromatin under epifluorescent microscopy, and % apoptotic cells was determined by examination of 400 cells from each slide. For TUNEL staining, cells were fixed and stained following the manufacturer's protocol (*In Situ* Cell Death Detection Kit; Roche, Indianapolis, IN). Apoptosis was assessed as fluorescent staining of the nuclei, and % apoptotic cells was determined by examination of 800-1200 cells total from a minimum of 4 frames of view (10x) for each slide.

Intracellular zinc assay

G/T cells were grown in 96-well plates for 1-2 days until confluent. Cells were serum starved for 30 min followed by steroid treatment (20 nM) for 30 min. Cells were fixed with 4% paraformaldehyde for 25 min at 4°C, stained with 10 µM zinquin ethyl esther (Enzo Life Sciences, Inc., Farmingdale, NY) for 30 min, washed, and immediately analyzed with a fluorescence plate reader (excitation 368 nm, emission 490 nm). Results are expressed as the relative intensity of the zinc signals between treatments. Each treatment was replicated in 8-16 wells/experiment, with the average being used to calculate statistical differences between experiments.

Cyclic AMP assay

Cyclic AMP was measured in cell lysates using a cAMP EIA kit (Cayman Chemicals). After isolation, G/T cells were cultured overnight, followed by serum

starvation for 72 hr. Cells were treated for 10 min with vehicle, testosterone, mibolerone, or TBSA, washed twice with ice-cold PBS, lysed by 20 min incubation with 100 µL 0.1 M HCl on ice, then scraped and repeatedly pipetted (20x) to homogenize the suspension. The suspension was centrifuged at 1000 x g for 10 min, and the supernatant was diluted 2x and assayed immediately. Treatments were conducted in triplicate and data is expressed as relative cAMP concentrations.

Proximity ligation assay

Interaction of ZIP9 with inhibitory and stimulatory G proteins was assessed *in situ* using a proximity ligation assay (PLA) following the manufacturer's protocol (Duolink; Sigma Aldrich). G/T cells grown on coverslips for 1-2 days were fixed, blocked, and incubated with primary antibodies for ZIP9 (mouse 1:200), and G_s (rabbit 1:100) or G_i (rabbit 1:100) overnight at 4°C, before continuing the manufacturer's ligation protocol. For co-staining apoptotic cells, G/T cells were treated, fixed, and stained as in the TUNEL assay prior to blocking and incubation with primary antibodies for the PLA assay. Stained cells were imaged under oil-immersion fluorescence microscopy (100x). Representative images were chosen for the presentation of results.

G protein activation assays

G protein activation was assessed by measuring [^{35}S]GTPγS binding to G/T cell plasma membranes after incubation with 100 nM testosterone or the same volume of vehicle (1 µl/100 µl) for 20 minutes at room temperature, using excess GTP to stop the reaction, as described previously (121). Membrane-bound [^{35}S]GTPγS was immunoprecipitated with specific antibodies for inhibitory (1:100, $G\alpha_i$ 1/2) and stimulatory (1:100, $G\alpha_s$) G proteins or rabbit IgG (1:100; R&D Systems, Minneapolis, MN) using protein A/G Plus-agarose beads (Santa Cruz Biotechnology, Inc., Dallas, TX).

Statistical Analysis

All experiments were repeated with G/T cells from a minimum of 3 fish. In experiments that examined both early and late stage G/T cells, the two subsets were isolated from the same fish. Statistical significance was determined by Student's *t*-test or one- or two-way ANOVA with a post hoc Bonferroni multiple comparison test. The one-way ANOVA was used to analyze experimental results with multiple steroid treatments and concentrations. The two-way ANOVA was used to analyze data from the experiments in which cells were co-treated with pharmacological drugs and testosterone, underwent different siRNA transfections, or when both early and late stage G/T cells were used. All data is expressed as the mean ± SEM using GraphPad Prism 5 software (GraphPad Software, San Diego, CA).

RESULTS

Characterization of ZIP9 in different size follicles

The actual composition of the early and late stage follicle pools was determined by characterizing a subset of follicles from each pool. The early stage size class was primarily made up of PNS (75%) and EV follicles (15%), with approximately 10% LV follicles (Fig 3.1A). The late stage size class consisted of primarily LV follicles (74%), with EV and PNS follicles making up 7% and 19%, respectively. ZIP9 mRNA (Fig 3.1B) and protein (Fig 3.1C) expression were significantly higher in G/T cells from the early stage follicles compared to late stage follicles. The binding of various androgens to the plasma membrane fractions of early and late stage follicles was assessed by a single point competitive androgen binding assay. In membrane fractions from both stages, [^{3}H]T binding was displaceable by unlabeled testosterone but not by mibolerone, a nuclear androgen receptor agonist (Fig 3.1D-E). This indicates that an androgen binding site is present on the plasma membranes in both follicle stages and that androgen binding is not to the AR.

Characterization of testosterone's effect on survival of G/T cells from early and late stage follicles

To determine the effect of testosterone on survival of G/T cells from early and late stage follicles, the incidence of apoptosis, as well as mRNA expression of the pro-apoptotic genes bax and p53, was examined. Testosterone significantly decreased the incidence of apoptosis compared to vehicle controls in early stage G/T cells but induced apoptosis in late stage G/T cells, as determined by TUNEL labeling (Fig 3.2A). The incidence of apoptosis was also examined by Hoechst staining (Fig 3.2B), which showed similar trends to that of the TUNEL assay, confirming the validity of the Hoechst assay for use in apoptosis analysis in subsequent experiments. The testosterone dose-response relationship and the androgen specificity of the anti-apoptotic response were examined in early stage G/T cells. The anti-apoptotic response showed an inverse dose-dependent relationship with 10 and 20 nM doses being more potent than 50 and 100 nM at inhibiting apoptosis (Fig 3.2C). The response was testosterone-dependent, with significantly reduced apoptosis in cells treated with free or BSA-conjugated testosterone (TBSA), but not with the nuclear androgen receptor agonist mibolerone (Fig 3.2D). The dose and specificity of the apoptotic response were not assessed in this study because these measures have previously been examined in croaker G/T cells that exhibit testosterone-induced apoptosis (117). The mRNA expression of the pro-apoptotic members Bax and p53 was differentially regulated by testosterone in G/T cells from early and late stage follicles, with late stage follicles showing a significant increase in expression and early stage showing significantly decreased expression of both Bax and p53 mRNA (Fig 3.2E-F).

Role of ZIP9 in the testosterone-mediated anti-apoptotic response

To determine which androgen receptor mediates the anti-apoptotic response of early stage G/T cells, the cells were transfected with siRNA targeting ZIP9 or the AR. The

testosterone-mediated anti-apoptotic response was lost after transfection with siRNA targeting ZIP9 but not with transfection of AR targeting siRNA (Fig 3.3C-D). Western blot analysis of ZIP9 expression in plasma membrane samples verified a significant decrease in the targeting siRNA treatment, while the non-targeting control siRNA showed no decrease compared to non-transfected control (Fig 3.3A). A similar decrease in expression of AR after transfection with AR-targeting siRNA but not non-targeting siRNA was confirmed by qPCR (Fig 3.3B).

Testosterone modulation of intracellular free zinc and Gα signaling

Previous work has demonstrated that ZIP9 mediates testosterone-induced apoptosis by increasing intracellular free zinc levels and by activating a G_s in croaker G/T cells from mature ovaries (25,117). Therefore, androgen regulation of intracellular zinc and members of the G_s signaling pathway were examined in the ZIP9-mediated anti-apoptotic response. Testosterone and TBSA treatment significantly reduced intracellular free zinc levels of early stage G/T cells, while mibolerone had no effect (Fig 3.4A). Treatment with the zinc chelator TPEN significantly reduced apoptosis compared to no treatment vehicle controls, similar to that of testosterone treatment (Fig 3.4B). This indicates that low intracellular zinc levels are anti-apoptotic in G/T cells. In early stage G/T cells the $G_s\alpha$-subunit inhibitor NF499 had no effect on the testosterone-mediated anti-apoptotic response (Fig 3.4C), indicating the response does not require $G_s\alpha$ activity. Co-treatment of testosterone with either the adenylyl cyclase activator forskolin or the cAMP analog 8-Bromoadenosine 3′,5′-cyclic monophosphate (8-Br-cAMP) abolished the testosterone-mediated anti-apoptotic response (Fig 3.4D), indicating that G_s-meditated signaling actively antagonizes the anti-apoptotic response. Early stage G/T cells treated with testosterone or TBSA showed a significant decrease in cAMP levels compared to vehicle, while mibolerone had

no effect (Fig 3.4E). This suggests that testosterone may activate an inhibitory G protein in early stage G/T cells.

ZIP9-G protein interactions in early and late stage G/T cells

A proximity ligation assay (PLA) was used to examine if different G proteins may be able to interact with ZIP9 in G/T cells from early and late stage follicles. ZIP9-G_i and ZIP9-G_s interactions (>40 nm) were evident in both G/T cell populations, but the intensity of the ZIP9-G_i signal was enhanced in early follicle stage G/T cells while in late stage G/T cells the ZIP9-G_s signal was more prevalent (Fig 3.5A). Additionally, in testosterone-treated late stage G/T cells that were TUNEL stained prior to PLA probing, apoptotic nuclei were found to co-localize with the ZIP9-G_s interaction (Fig 3.5B). Expression of G_i and G_s on the plasma membranes of G/T cells from early and late stage follicles was confirmed by Western blot analysis. Both G_i and G_s are expressed in early and late stage follicles, with G_i expression significantly higher in early stage G/T cells, and no difference in expression of G_s between stages (Fig 3.5C). Next, the activation of G_i and G_s by testosterone was examined. Binding of the radiolabeled, non-hydrolyzable, GTP analog GTPγS ([^{35}S]GTPγS) to the plasma membrane of G/T cells from both early and late stage follicles was significantly increased by testosterone treatment, indicating that testosterone activates a G protein in G/T cells from each subclass (Fig 3.6A). Membrane-bound [^{35}S]GTPγS from G/T cell membranes pre-treated with testosterone was immunoprecipitated with a G_i antibody in early stage G/T cells and a G_s antibody in G/T cells from late stage follicles, but not with rabbit IgG in either G/T cell subset, demonstrating that testosterone activates a G_i in early stage and a G_s in late stage G/T cells (Fig 3.6B-C).

DISCUSSION

This study demonstrates that the zinc transporter ZIP9 acts as a membrane androgen receptor to mediate differential survival responses in Atlantic croaker G/T cells in a follicle stage-dependent manner. While ZIP9 has previously been reported to elicit apoptosis of croaker G/T cells, here we demonstrate that this response can be attributed to G/T cells from late stage vitellogenic follicles. In G/T cells from perinuclear and early vitellogenic follicles ZIP9-mediates an anti-apoptotic response. We have provided evidence that indicates ZIP9 mediates these opposing responses by activating either a stimulatory or inhibitory G protein, dependent upon the stage of the ovarian follicle development. Although it has been shown that ZIP9 can activate various G proteins in different models, this is the first evidence indicating ZIP9 can activate multiple G proteins within a single cell model, (25,26,118). Furthermore, the current work highlights that testosterone regulates opposite intracellular free zinc responses between early and late stage G/T cells, which corresponds to the opposite survival responses mediated by ZIP9 in early and late stage G/T cells. The finding that ZIP9 can mediate both survival and apoptotic responses in croaker G/T cells depending on the stage of follicular development indicates that the receptor may play a critical role in multiple physiological processes essential for folliculogenesis and maintaining homeostasis in the ovary of Atlantic croaker.

Previously, a ZIP9-mediated apoptotic pathway was characterized using G/T cells pooled from total follicles present in ovaries of reproductively mature fish (GSI>12). This apoptotic pathway was found to involve the activation of a G_s and upregulation of pro-apoptotic members (25,117), similar to as seen in late stage G/T cells in the current study. Atlantic croaker are indeterminate asynchronous spawners that maintain ovarian follicles at all stages of development throughout the reproductive season (128), but the majority of the volume of reproductively mature ovaries is made up of late vitellogenic follicles (author

observation). Thus, in G/T cells pooled from mature ovaries, the larger proportion of late stage G/T cells would likely mask any differential phenotypes of the early stage G/T cells. It is concluded that the ZIP9-mediated apoptotic response is attributed to the late stage follicle G/T cells, and therefore it is assumed that the apoptotic response of these cells involves signaling pathways and pro-apoptotic members characterized previously (117). Thus, in the current study, the emphasis was placed on the examination of the testosterone-mediated effects exhibited by the early stage follicle cells.

Arguably the most important finding of this study is that ZIP9-mediates testosterone-induced pro- and anti-apoptotic responses through activation of different G proteins and subsequent differential signaling cascades. Previously, the ZIP9-mediated apoptotic pathway was characterized as involving G_s-mediated signaling, MAPK activity, and a rise in intracellular free zinc (25,117). These signaling events are upstream of increases in caspase 3 activity, increased mRNA expression of pro-apoptotic members, and cell death by apoptosis. In the current study, the anti-apoptotic response is characterized by G_i activation, subsequent decreased cAMP levels, and decreased mRNA expression of pro-apoptotic members and apoptosis. Furthermore, the anti-apoptotic response downstream of G_i-mediated signaling is antagonized by G_s-mediated signaling as demonstrated by the inhibitory effect of an adenylyl cyclase activator or cAMP analog on the anti-apoptotic response. In croaker G/T cells, mPRα also mediates an anti-apoptotic response through activation of a G_i (24), suggesting that different receptors may be able to elicit similar survival or death responses by activation of a G_i or G_s in this model.

Interestingly, it was found that the effect of testosterone on intracellular free zinc levels also differs between early and late stage G/T cells. While the ZIP9-mediated apoptotic pathway involves an increase in free intracellular zinc (25), an opposite trend was found in early stage G/T cells that exhibit the anti-apoptotic response in the present

study. Previously, the rise in intracellular free zinc associated with androgen-induced apoptosis in croaker G/T cells was attributed to ZIP9 activity and found to be essential for the induction of androgen-induced apoptosis (25). In human breast and prostate cancer cell lines, ZIP9-mediated apoptosis also involves an increase in intracellular free zinc that is ZIP9-dependent and required for the apoptotic response. Of interest, in the cancer cell lines ZIP9 mediates apoptosis by activating a G_i (26). In PC-3 prostate cancer cells overexpressing ZIP9 (PC3-ZIP9), the ZIP9-mediated increase in free zinc is pertussis toxin-sensitive and can be blocked by the addition of the non-hydrolyzable GTP analog GTPγS, indicating that the zinc response is downstream of G_i activation (120). To our knowledge, ZIP9 is the only ZIP family member that regulates zinc by G protein activation, but its ability to do so has not been examined in the croaker G/T cell model. It is also of interest to further examine the testosterone-induced decrease in free intracellular zinc exhibited by early stage G/T cells and the role of ZIP9. ZIP family members regulate the transport of zinc into the cytoplasmic compartment (95), thus, it is unclear how ZIP9 may mediate a reduction in free zinc. One possibility is that the decrease in free zinc is mediated by an androgen-dependent inhibition of the zinc transport activity of ZIP9, resulting in reduced zinc transport into the cytoplasm from extracellular and subcellular compartments.

While differential ZIP9-G protein coupling occurs in croaker G/T cells, G_i coupling in early stage follicles followed by G_s coupling in late stage follicles, the mechanism driving this switch in coupling is unclear. Whereas most G protein-coupled receptors are associated with a single class of G proteins, a number of receptors are known to have the ability to couple to different classes of G proteins even within a single model. This was first documented for the β_2-adrenergic receptor (β_2-AR) (98) but has further been established for other G protein-coupled receptors including the β_1-adrenergic, the prostacyclin, and vasoactive intestinal peptide receptors (129–131). Similar to the current

study, the β_2-AR can mediate both pro- and anti-apoptotic responses through activation of a G_s and G_i, respectively, in cardiac myocytes (132). The G protein coupling switch observed in the β_2-AR and prostacyclin receptor models has been attributed to the receptors initially coupling to a G_s to promote PKA activity followed by PKA phosphorylation of the receptor which reduces G_s and heightens G_i coupling affinities. Thus, in these models the G_i coupling is dependent on the G_s-mediated pathway. In the croaker G/T cells, the anti-apoptotic effect is unaffected by co-treatment with the $G_s\alpha$-subunit inhibitor, NF449. While this may indicate that the differential coupling of ZIP9 may be through a different mechanism to that of the β_2-AR and the prostacyclin receptor, it is important to note that the studies on the β_2-AR and the prostacyclin receptor were done in transfected cell models, whereas the differential coupling of ZIP9 in the current model was examined in a primary culture system. Thus, desensitization of one G protein may occur *in vivo* and remain fixed through isolation, culturing, and experimentation. Furthermore, early and late stage follicle G/T cells have different expression profiles of ZIP9 and the G_i, which may also play a role in the regulation of ZIP9-G protein coupling. While the current study does not address the mechanism behind this shift in ZIP9-G protein coupling, the fact that ZIP9 can couple to multiple G proteins in the current model as well as different G proteins between models indicate that ZIP9-G protein interactions should be further examined to determine if the receptor can switch G protein coupling in other models.

Androgens have been found to promote survival and growth as well as death in various mammalian and fish ovarian models (54,55,57–64,114–116). These studies demonstrate a general trend that androgens promote growth and survival during earlier stages of follicle development (54,55,57–59,115,116) and promote apoptosis and atresia in both preantral and antral follicles in mammals (60–65,114). It is important to note that in many of these studies the role of a specific androgen receptor in mediation of the response

was not confirmed. Recently, Lim et al. 2017 demonstrated that the androgen dihydrotestosterone (DHT) promotes apoptosis in granulosa cells from rat antral follicles, but is protective and promotes proliferation of granulosa cells from preantral follicles. Further examination of the anti-apoptotic/proliferative effect attributed it to AR-mediated expression of soluble Kit ligand (114). The role of the AR in early stage ovarian follicle growth and development is further supported by the AR knockout models which show detrimental phenotypes including decreased ovarian follicle growth and increases in atretic and apoptotic follicles (68,70–72). In the current study, we found no evidence for a role of the AR in the anti-apoptotic response exhibited by early stage croaker G/T cells. The nuclear androgen receptor agonist mibolerone, which does not interact with ZIP9 (25), did not mimic the effect of testosterone on G/T cell survival. Additionally, siRNA knockdown of ZIP9, but not the AR, effectively abrogated the testosterone-mediated anti-apoptotic effect. While this may indicate that the mechanism behind the androgen-mediated anti-apoptotic response differs between rat and croaker models, ZIP9's role has not been examined in androgen-mediated survival of early stage ovarian follicles in any mammalian model to date, so its significance in these models remains unclear. In addition, the receptor mediating androgen-induced apoptosis in murine (114) and porcine (64,65) antral ovarian granulosa cells has not been investigated. We have demonstrated that ZIP9 plays a role in androgen-mediated apoptosis of late stage croaker G/T cells that respond to androgens in a similar manner to mammalian antral stage granulosa cells (114), but it remains unknown if a ZIP9-mediated mechanism is involved in the mammalian models. Overall, the discovery of a novel membrane androgen receptor, ZIP9, highlights the need to re-examine the receptor mediating androgen-mediated responses that were previously attributed to the AR without loss of function verification in the ovary and other tissues that are androgen receptive.

The ability of ZIP9 to mediate both survival and death responses in an ovarian follicle stage-dependent manner may be a means of regulating the fate of individual follicles within the ovary. Androgens have been shown to be present in the plasma throughout the reproductive season of a number of teleosts, including members of the Sciaenidae family of which Atlantic croaker is a member (133). Thus, it may be of benefit for a stimulus that is present throughout folliculogenesis, to have the ability to induce differential responses depending on the developmental stage of the ovarian follicle. This may be especially important in an asynchronous spawning teleost such as the Atlantic croaker, which can have follicles of all developmental stages present in the ovary throughout the reproductive season (128). In this way, testosterone may act as a protective factor in follicles undergoing early growth and vitellogenesis, and an apoptotic factor in follicles at later stages of development. The physiological relevance of androgen-induced apoptosis in late stage ovarian follicles is unclear. However, apoptosis is involved in the removal of atretic follicles in both teleosts and mammalian ovaries, as well in the regression of mammalian corpus luteum and post-ovulatory follicle in teleost (81,83–85). Of interest, upregulation of ZIP9 and members of the ZIP9-mediated apoptotic pathway were associated with impaired oogenesis and increased ovarian apoptosis and atresia in Atlantic croaker exposed to the environmental stressor hypoxia (134). Thus, ZIP9-mediation of survival and death responses may also allow for the adjustment of the recruited ovarian follicle reserve in response to environmental stressors and stimuli. However, further work investigating the mechanism mediating the switch in ZIP9-G protein coupling is required to determine this.

In conclusion, the present study demonstrates that the novel membrane androgen receptor ZIP9 can mediate opposite survival responses in Atlantic croaker G/T cells by differentially activating a G_i and G_s. ZIP9-G protein interaction is follicle stage-dependent,

with ZIP9 activating a G_i to elicit a survival response in early stage follicle G/T cells, while ZIP9 activation of a G_s mediates apoptosis of late stage G/T cells. This is the first evidence that ZIP9 can mediate different physiological responses by activating multiple G proteins in a single model. Although the physiological relevance of the pro- and anti-apoptotic responses was not investigated in the current study, the ability of a single receptor to elicit opposing responses at different developmental stages may be a mechanism that allows for more precise control of folliculogenesis in the dynamic ovarian environment. ZIP9 is expressed in the majority of croaker and human tissues examined, but knowledge on ZIP9's role in meditation of androgen-induced responses in vertebrates is greatly lacking. Additional studies on the role of ZIP9 in the ovary of teleosts as well as higher vertebrates will provide insight into the role of the receptor in ovarian physiology. Our current findings indicate that ZIP9 possesses unique characteristics that warrant further investigation in a wide range of vertebrate models.

FIGURES

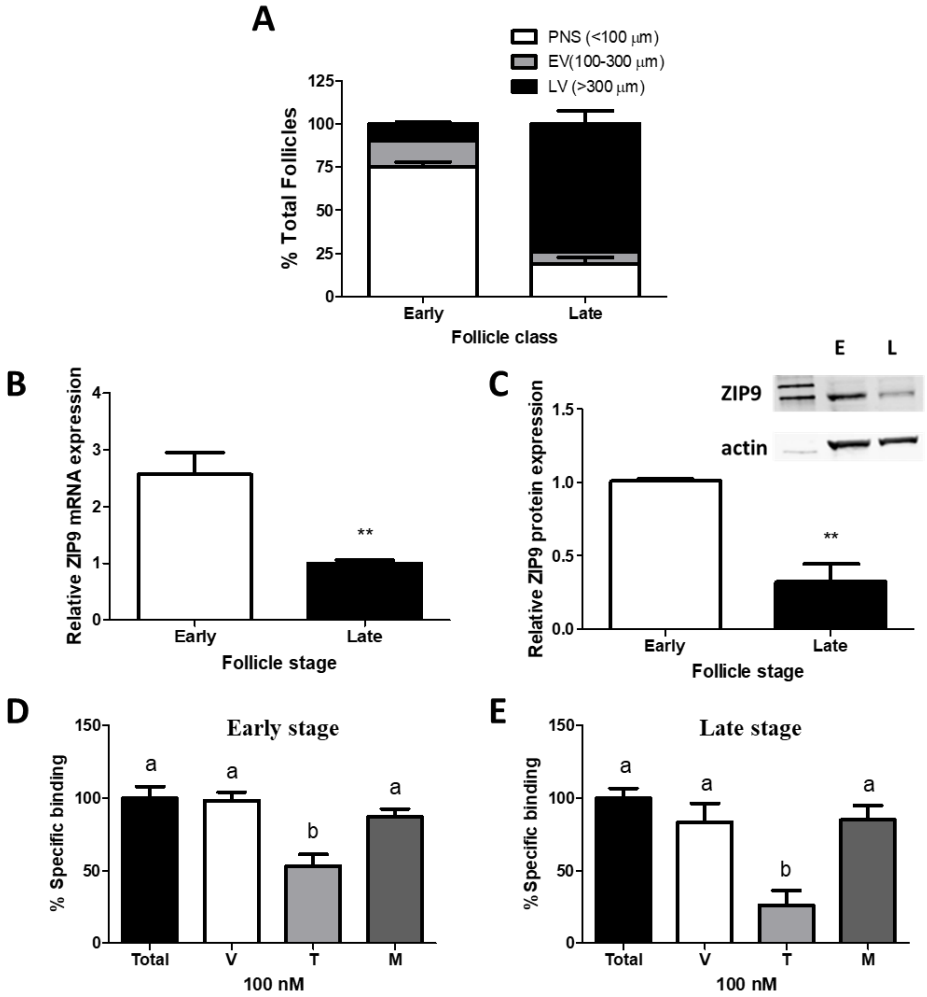

Figure 3.1: Characterization of follicle classes and ZIP9 in early and late stage ovarian follicles. A, Relative composition of early and late stage follicle classes. B-C, mRNA (B) and membrane protein (C) expression of ZIP9 in G/T cells from early and late stage follicles. D-E, Displacement of membrane-bound [3H]T by various androgen in early (D) and late (E) stage follicles, expressed as percentage of maximal [3H]T binding. All data represents means ± SEM, n=3-4 (A-C), n=9 (D, E). Significance was determined by Student's t-test (B, C; **, $p<0.01$) or one-way ANOVA with Bonferroni multiple comparison post-test (D, E). Different letters indicate significant differences between the treatment groups in the post hoc test at $p < 0.05$. Follicle class distribution and ZIP9 expression analyses were conducted with 3-4 fish. For binding experiments, each treatment was conducted in triplicate with similar results obtained for each, and the experiments were repeated with 3 fish. PNS, perinuclear stage; EV, early vitellogenic stage; LV, late vitellogenic stage; E, early stage; L, late stage; V, ethanol control; T, testosterone; M, mibolerone.

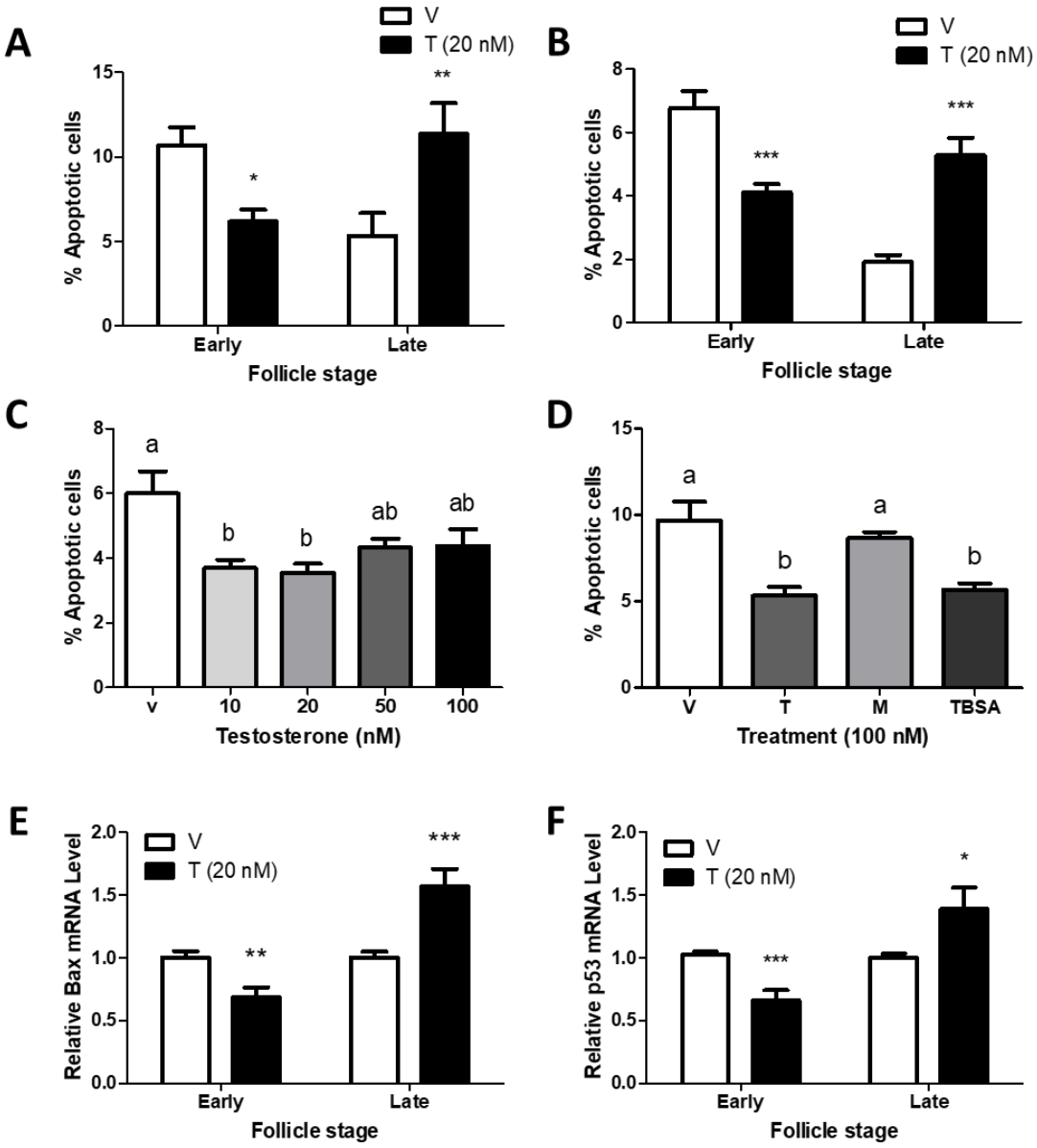

Figure 3.2: Effect of testosterone on apoptosis and expression of pro-apoptotic members in early and late stage G/T cells.

Figure 3.2 (continued): Effect of testosterone on apoptosis and expression of pro-apoptotic members in early and late stage G/T cells. A-B, Effect of testosterone on apoptosis of G/T cells from early and late stage follicles as determined by TUNEL staining (A) and Hoechst staining (B). C, Effect of various concentrations of testosterone on % apoptotic nuclei as determined by Hoechst staining. D, Effects of androgen treatments on % apoptotic nuclei as determined by Hoechst staining. E-F, Expression of *bax* (E) and *p53* (F) mRNA after 24 hr testosterone treatment of late and early stage G/T cells. All data represents means ± SEM, n=6-9 (A-D), n=12 (E, F). Significance was determined by one- (C-D) or two-way (A-B) ANOVA followed by Bonferroni multiple comparison post-test, or by Student's *t*-test (E-F). Different letters indicate significant differences between the treatment groups in the one-way ANOVA *post hoc* test at $p < 0.05$. Level of significance between vehicle and testosterone treatments as determined by Student's *t*-test or the two-way ANOVA *post hoc* are indicated as *, $p<0.05$; **, $p<0.01$; ***, $p<0.001$. In experiments A-B, significant interactive effects of testosterone treatment on G/T cell survival between early and late stage cells was detected by the two-way ANOVA, which was predicted because early and late stage G/T cells show differential responses to testosterone. Incidence of apoptosis experiments (A-D) were repeated with three fish and each treatment conducted in duplicate or triplicate with similar results obtained for each. Pro-apoptotic member mRNA expression analyses (E-F) were repeated with 6 fish and each treatment conducted in duplicate. M, mibolerone; TBSA, testosterone-BSA.

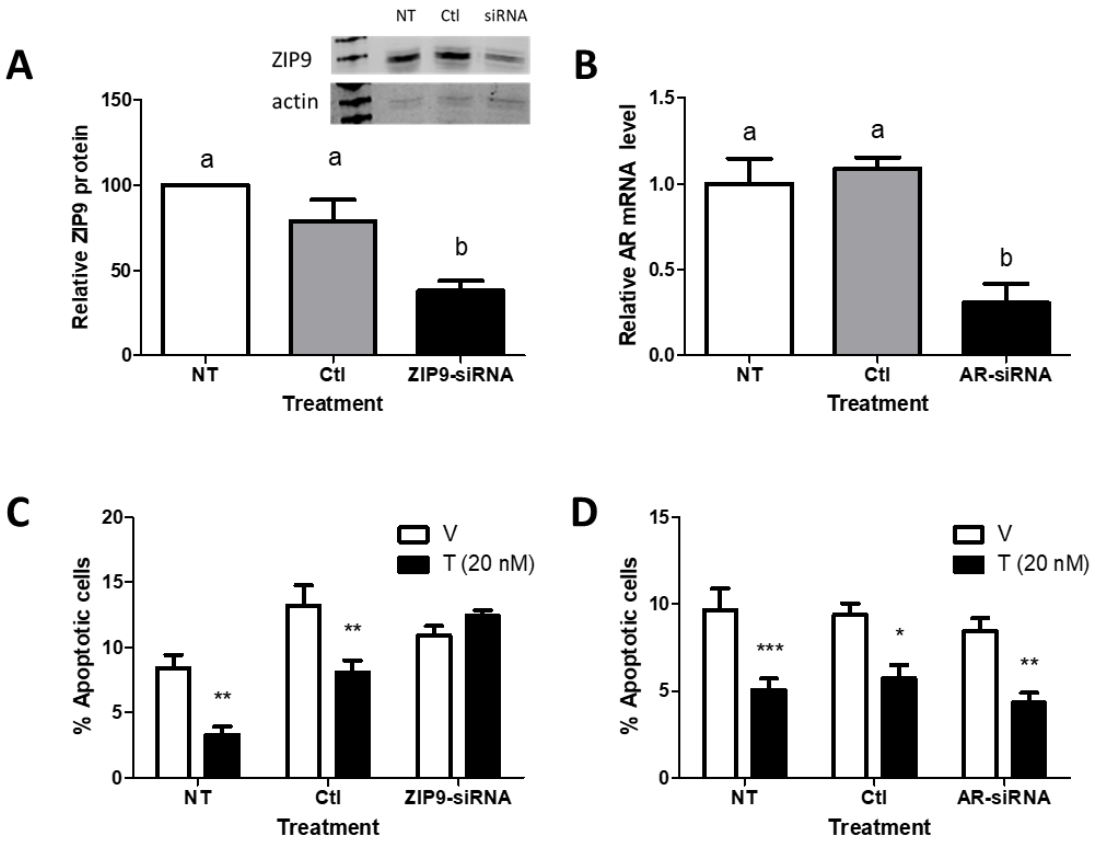

Figure 3.3: Effect of ZIP9- and AR-targeting siRNA on the testosterone-induced anti-apoptotic response of early stage G/T cells. A-B, ZIP9 protein (A) and AR mRNA (B) expression after transfection with targeting and non-targeting siRNA. C-D, Effect of siRNA targeting ZIP9 (C) or AR (D) on the testosterone-induced anti-apoptotic response. All data represents means ± SEM, n=3 (A-B) n=6 (C-D). Significance was determined by one- (A, B) or two-way (C, D) ANOVA followed by Bonferroni multiple comparison post-test. Different letters indicate significant differences between the treatment groups in the one-way ANOVA post hoc test at $p < 0.05$. Level of significance between vehicle and testosterone treatments as determined by the two-way ANOVA post hoc are indicated as *, $p<0.05$; **, $p<0.01$; ***, $p<0.001$. In experiment (C) but not (D), significant interactive effects of the steroid treatment (V & T) and the transfection treatments on G/T cell apoptosis was detected by the two-way ANOVA, which was predicted because ZIP9-targeting siRNA blocked the testosterone-induced responses, while AR-targeting siRNA did not. Experiments were repeated with three fish and each treatment conducted in duplicate with similar results obtained for each. NT, no transfection; Ctl, non-targeting siRNA control; siRNA, small interfering RNA.

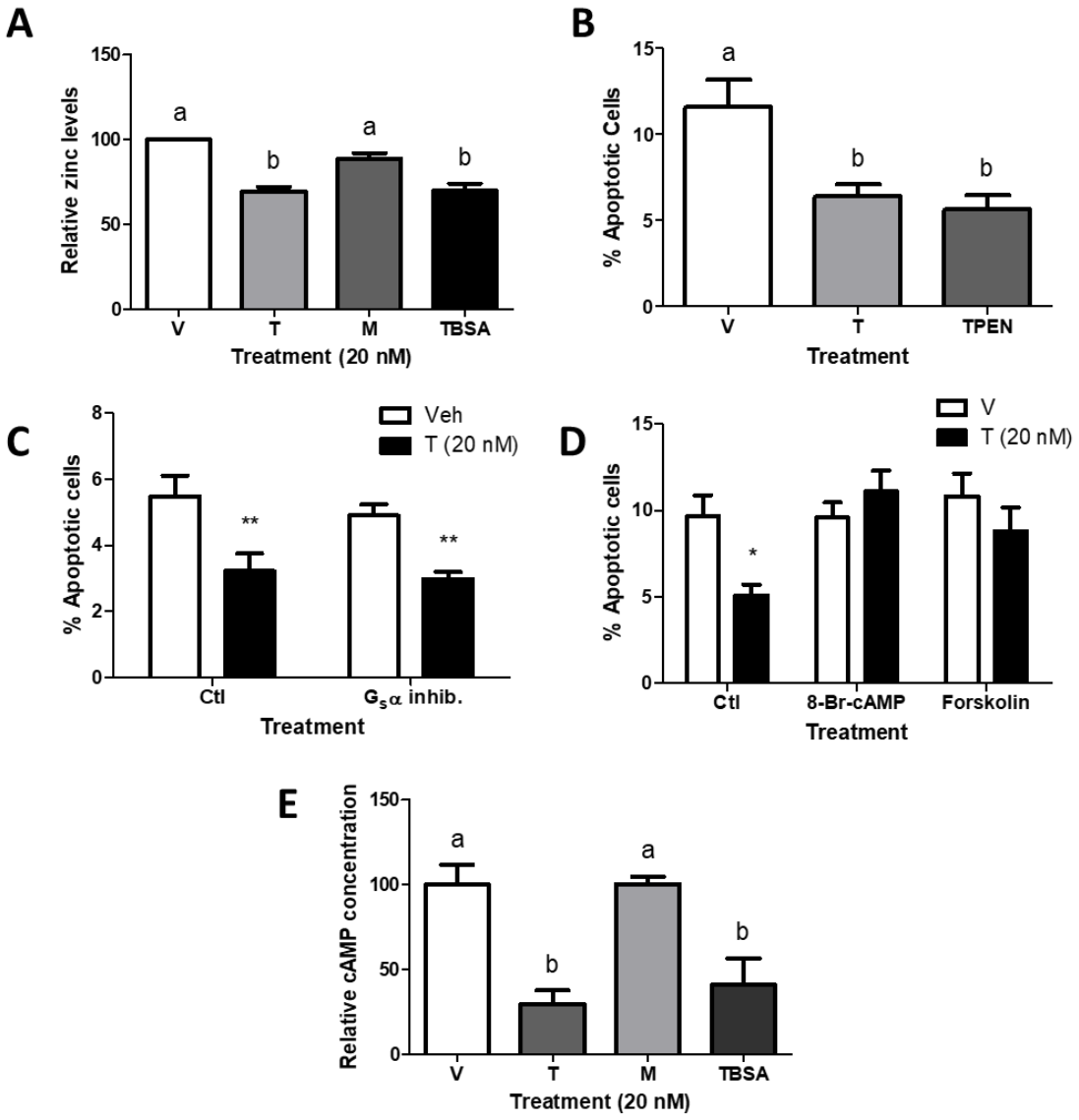

Figure 3.4: Effects of testosterone on components of the ZIP9-mediated apoptotic signaling pathway in early stage G/T cells.

Figure 3.4 (continued): Effects of testosterone on components of the ZIP9-mediated apoptotic signaling pathway in early stage G/T cells. A, Effect of various androgens on intracellular free zinc levels. B, Effect of the zinc chelator TPEN on G/T cell apoptosis. C, Effect of $G_s\alpha$ inhibitor NF449 on the anti-apoptotic effect of testosterone. D, Effects of 8-Br-cAMP and forskolin on the anti-apoptotic response to testosterone. E, Relative cAMP concentrations in early stage G/T cells treated with various androgens for 10 min. All data represents means ± SEM, n=4 (A), n=6 (B, C, D), n=9 (E). Significance was determined by one- (A, B, E) or two-way (C-D) ANOVA with Bonferroni multiple comparison post-test. Different letters indicate significant differences between the treatment groups in the one-way ANOVA post hoc test at $p < 0.05$. Level of significance between vehicle and testosterone treatments as determined by the two-way ANOVA post hoc are indicated as *, $p<0.05$; **, $p<0.01$. In experiment (D), significant interactive effects of testosterone treatment in the presence of the pharmacological agents on G/T cell survival was detected by the two-way ANOVA, which was predicted because 8-Br-cAMP and forskolin effectively blocked the testosterone-mediated response. In experiment (C), no interaction was found between testosterone treatment and the presence of the $G_s\alpha$ inhibitor. Intracellular zinc was assessed in 4 fish, experiments (B-E) were repeated with 3 fish and each treatment conducted in duplicate or triplicate with similar results obtained for each. M, mibolerone; TBSA, testosterone-BSA; TPEN, N,N,N',N'-tetrakis(2-pyridylmethyl)-1,2-ethylenediamine; $G_s\alpha$ inhib., NF449; 8-Br-cAMP, 8-bromoadenosine 3′,5′-cyclic monophosphate.

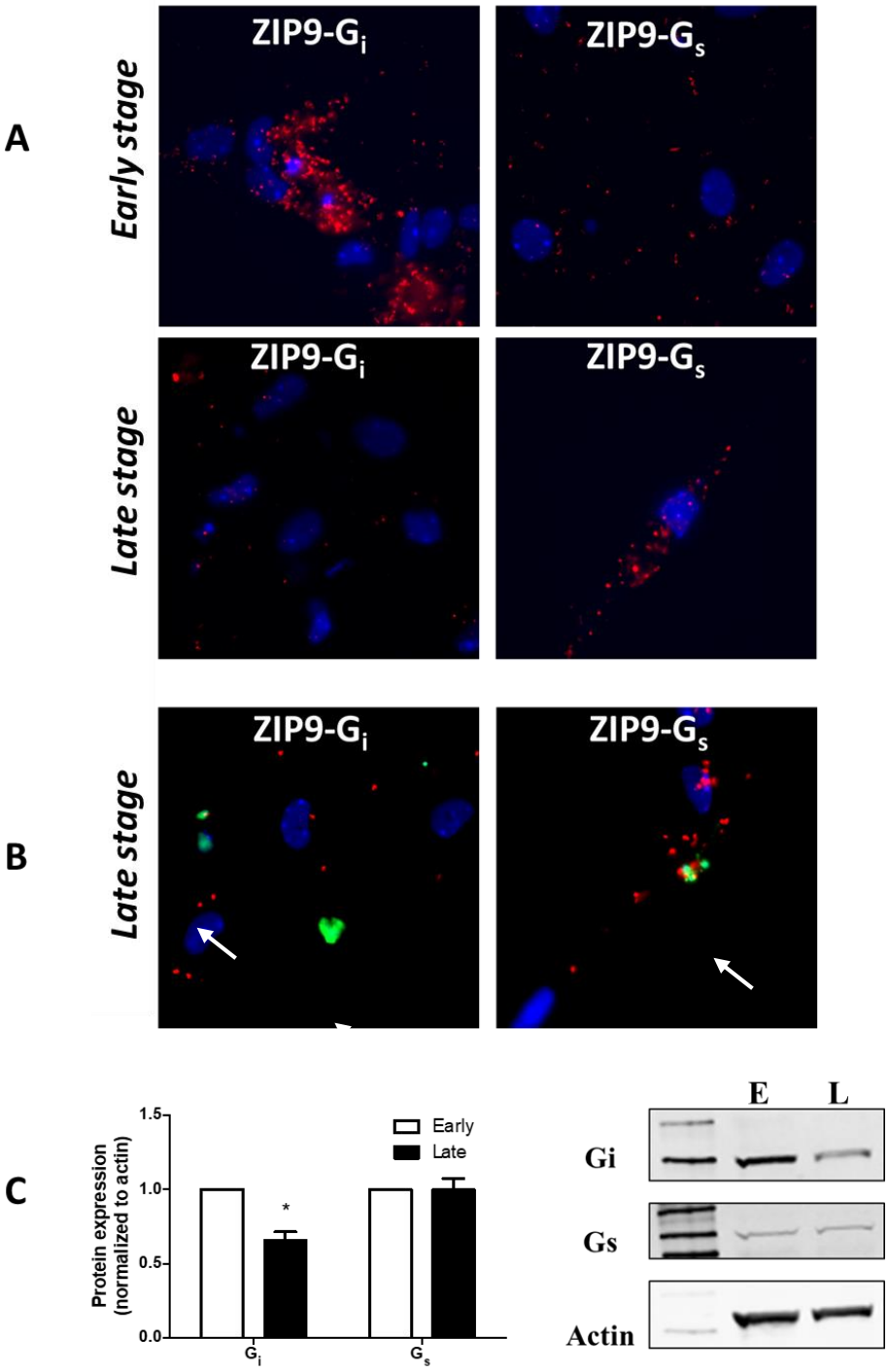

Figure 3.5: Interaction of ZIP9 with G_i and G_s in G/T cells from early and late stage follicles.

Figure 3.5 (continued): Interaction of ZIP9 with G_i and G_s in G/T cells from early and late stage follicles. A. Representative images of ZIP9-G_i and ZIP9-G_s interactions in G/T cells from early and late stage follicles as indicated by red signal in the in situ proximity ligation assay. B, Representative images of co-localization of testosterone-induced apoptotic nuclei (green, indicated by white arrows) with ZIP9-G protein interactions in late stage G/T cells. C, Relative expression of G_i and G_s in early and late stage G/T cells. Data represents means ± SEM, n=3 (A, B), n=5 (C). Significance was determined by Student's t-test. *, $p<0.05$. Experiments were repeated with cells from 3-5 fish with similar results obtained for each. E, early stage; L, late stage.

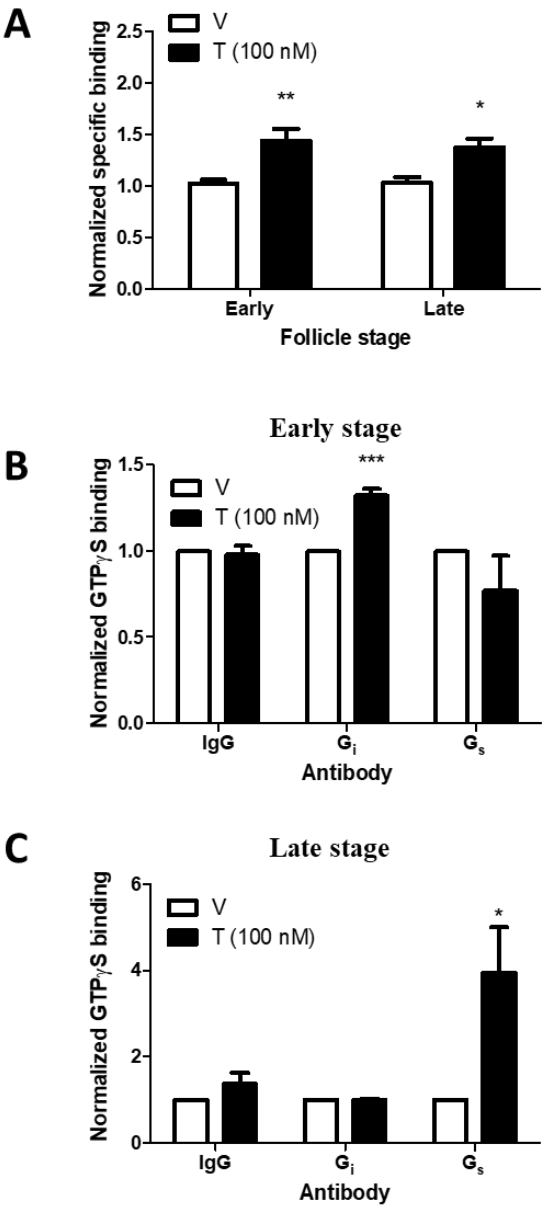

Figure 3.6: Testosterone activation of G proteins in G/T cells from early and late stage follicles. A, Effect of 20 min testosterone treatment on specific [35S]GTPγS binding to plasma membranes of G/T cells from early and late stage follicles. B-C, Immunoprecipitation of testosterone-induced [35S]GTPγS binding to early stage (B) or late stage (C) G/T cell membranes with specific G_i and G_s antibodies or rabbit IgG control. All data represents means ± SEM, n=12-15 (A), n=3 (B, C). Significance was determined by Student's t-test. *, $p<0.05$; **, $p<0.01$; ***, $p<0.001$. Experiments were repeated with 3-4 fish and with similar results obtained for each.

SUPPLEMENTAL DATA

Primer	Forward	Reverse
ZIP9	CTGGCTGTCATCATCCCTGA	ATGAAGACGAAGCCCAGCAC
Bax	TGTCGACTCGTCATCAAAGC	GCCAAAGTGGGAACGAATAC
P53	CAGGGTGGAGGGCAGCCAGA	GGGTCTGCGGTTCATGCCCC
18S	AGAAACGGCTACCACATCCA	TCCCGAGATCCAACTACGAG

Table 3.1: Sequence of primers (5'-3') used for qPCR experiments (Chapter 3).

Chapter 4: Evidence that ZIP9 regulates both G/T cell apoptosis and oocyte activation in the zebrafish ovary

ABSTRACT

The novel membrane androgen receptor ZIP9 mediates androgen-induced apoptosis in Atlantic croaker ovarian granulosa and theca (G/T) cells, however, its role in the ovarian physiology of other teleosts is unknown. In this study, the role of ZIP9 in the zebrafish ovary was investigated using primary G/T cell culture and global ZIP9 knockout models. Zebrafish ovaries highly expression ZIP9 mRNA and possess a testosterone-specific binding site on membrane fractions. Testosterone induces an apoptotic response in zebrafish G/T cells that is blocked with ZIP9-targeting siRNA. Testosterone treatment also increases caspase 3 activity, expression of pro-apoptotic member p53 and Bax mRNA, and a rapid rise in free intracellular zinc. The similarity of the ZIP9-mediated apoptotic pathways in zebrafish and croaker G/T cells suggest this response may be conserved in teleosts. Global ZIP9 knockout using a CRISPR-Cas9 system resulted in reduced female fecundity, with significantly fewer spawned eggs and lower fertilization rates compared to wild-type controls. In addition, ZIP9 knockout females produced eggs that did not undergo chorion elevation, which normally occurs during egg activation. Eggs displaying the non-activated phenotype showed very low fertilization rates and larvae with high levels of pericardial/yolk sac edema and reduced growth compared to larvae hatched from wild-type or normal phenotype ZIP9 knockout eggs. In conclusion, the severe impairment of reproductive capacity and the associated non-activated egg phenotype observed in ZIP9 knockouts suggest that in addition to the role of ZIP9 in mediating apoptosis *in vitro*, the receptor may also play a role in egg activation *in vivo*.

INTRODUCTION

Recently, a putative membrane androgen receptor cloned in Atlantic croaker ovaries was found to be homologous with zinc transporter protein ZIP9, the lone member of the SLC39A subfamily I (25). In the croaker ovary, ZIP9 mediates both testosterone-induced apoptosis and survival of granulosa and theca (G/T) cell co-culture by activating G proteins, which results in rapid signaling events and downstream regulation of pro-apoptotic member mRNA expression and caspase 3 activity (117). Interestingly, androgen activation of ZIP9 also results in regulation of intracellular free zinc levels in croaker G/T cells indicating that the zinc transport functions of ZIP9 are androgen-sensitive, which is unique to this zinc transporter (25). Furthermore, ZIP9 has recently been found to mediate apoptosis in human cancer cell lines (26), tight junction formation in murine Sertoli cells (118), and migration of human glioblastoma cell lines (119). While these initial studies demonstrate several sites of action and functions of ZIP9, we currently have a limited understanding of the functions of this novel membrane androgen receptor and zinc transporter in animal physiology.

In croaker ovaries, ZIP9 protein expression varies throughout the reproductive season with expression being undetectable in regressed ovaries (gonado-somatic index ~0), and dramatically increased in recrudescent and reproductively mature ovaries (25). Furthermore, ovarian ZIP9 protein expression can be regulated by reproductive hormones *ex vivo* (25). Thus, the changes observed in the expression of the receptor *in vivo* throughout the reproductive season and the ability for hormones to mediate expression *ex vivo* suggest a role for ZIP9 in croaker ovarian physiology. Androgens are known to regulate a number of physiological processes in the ovary, many of which have been attributed to activation of the nuclear androgen receptor (AR) in both murine and zebrafish knockout models. Murine and zebrafish AR knockouts show subfertility with premature

ovarian failure (69,135), decreased expression of aromatase (*cyp19a1*) mRNA expression in the ovary (70,135), and decreased litter sizes or fewer ovulated oocytes, in murine (68–70) and zebrafish models (136), respectively. However, many androgen-mediated actions have not been directly attributed to the AR through the use of knockout models. Additionally, the limited work on the role of ZIP9 actions in the ovary and the novelty of its identification as a membrane androgen receptor, indicate a need for further evaluation of mechanisms of androgen action in the ovary to determine the relative importance of the AR and ZIP9 in androgen regulation of ovarian physiology.

Zinc signaling has also recently been shown to have a role in ovarian physiology. In mammals, zinc has been found to mediate events in periovulatory oocytes and those undergoing maturation and activation. Zinc is the most prominent transitional metal detected in late stage oocytes and is actively accumulated during maturation and the resumption of meiosis (germinal vesicle breakdown (GVBD) to metaphase II (MII) arrest) (137). Furthermore, a zinc "spark", or rapid release of zinc to the extracellular space, has been shown to accompany the fertilization-induced wave of free intracellular Ca^{++} in mammalian eggs (138). In murine periovulatory oocytes, zinc has also been found to be involved in meiotic arrest, and zinc chelation and dietary deficiency induce resumption of meiosis but with abnormal spindle configurations resulting in the inability to reach metaphase II (139). An increase in oocyte zinc content has also been observed in the transition of zebrafish oocytes from previtellogenic to late vitellogenic stages (140), and the zebrafish ovary expresses the widest variety of zinc transporters compared to various non-reproductive tissues (141). However, the role of zinc signaling in ovarian and oocyte physiology in fish has not been extensively investigated to date.

While the role of ZIP9 in ovarian granulosa/theca cells has been extensively studied in Atlantic croaker, it is unknown if ZIP9 mediates androgen actions in G/T cells of other

teleosts. The current study looks to further the understanding of ZIP9 in teleost ovarian physiology by investigating the role of the receptor in the ovary of zebrafish. First, using a primary zebrafish G/T cell culture model, we confirmed that ZIP9 meditates testosterone-induced apoptosis in zebrafish G/T cells similar to that observed in croaker G/T cells. Next, a global ZIP9 knockout model was developed using a CRISPR-Cas9 system in order to examine the role of ZIP9 in female reproduction. Effects on reproduction were determined by comparing fecundity, larval health and growth, and ovarian morphology between *ZIP9* wild-type and mutant fish.

MATERIALS AND METHODS

Chemicals and materials

Chemicals were purchased from Sigma-Aldrich (St. Louis, MO) unless otherwise stated. Testosterone and 4-estren-7α, 17α-dimethyl-17β-ol-3-one (Mibolerone) were purchased from Steraloids (Newport, RI). [1,2,6,7-^{3}H]Testosterone ([^{3}H]T) (100 Ci/mmol) was purchased from American Radiolabeled Chemicals (St. Louise, MO). Bovine serum albumin-conjugated testosterone (TBSA) was dialyzed to remove free testosterone by incubation with 5 mg/ml charcoal and 0.5 mg/ml dextran at 55°C under gentle rotation for 30 min followed by removal of the charcoal by two centrifugation cycles at 4600 x g for 20 min each.

Zebrafish husbandry

Wild-type zebrafish (*Danio rerio*) were obtained from Segrest Farms (Gibsonton, FL, USA) and maintained in a 14 hr light:10 hour dark cycle at 28.5°C at the University of Texas Marine Science Institute in Port Aransas, TX. Adult fish were fed 1-2 times a day a mixed diet of commercial flakes, pellets, and live brine shrimp. Larvae (5-10 dpf) were fed boiled egg yolk, and juvenile fish were fed live brine shrimp, twice daily. For tissue

collection, fish were deeply anesthetized by immersion in a bath containing 20 mg/L MS-222 and humanely euthanized by rapid decapitation in accordance with procedures approved by the University of Texas Animal Care and Use Committee.

Primary granulosa/theca cell culture

Ovarian tissue from 7-15 reproductively mature females with high GSI's (12-20%, high proportion of mid and late stage follicles) was pooled, and G/T cell isolation was performed following a modified protocol previously described for Atlantic croaker (*Micropogonias undulatus)* G/T cell isolation (96). Briefly, ovarian tissue was placed into Ca/Mg-free buffer (138 mM NaCl, 8.6 mM KCl, 1.62 mM Na_2HPO_4, 5 mM D-glucose, 15.8 mM HEPES, 1 mM EDTA, 100 mg/L streptomycin, 60 mg/L penicillin, pH 7.4), repeatedly pipetted to separate ovarian follicles, and enzymatically digested with 0.1% collagenase for 1 hr at room temperature. After digestion, G/T cells were sheared from the follicles by repeated pipetting, then the supernatant was passed through a 70 µm filter and centrifuged at 500 x g for 10 min. The cell pellet was resuspended in M199 media (Earle's salts with L-glutamine; Gibco, Waltham, MA), layered onto a 4.5% Percoll pad, and subsequently centrifuged at 2800 x g for 20 min. The G/T cell layer between the Percoll pad and media was removed, and the G/T cells were washed once with media to remove the Percoll. G/T cells were plated and grown in MI99 media containing 10% charcoal-stripped FBS in a 5% CO_2 humidified incubation chamber at 28°C. All culture media contained the aromatase and p450 side chain cleavage inhibitor DL-Aminoglutethimide (100 µM) (Alfa Aesar, Ward Hill, MA). For siRNA and expression plasmid transfections, zebrafish G/T cells were transfected with a mixture of siRNA primers targeting the 5' untranslated region of ZIP9 mRNA sequence (Dharmacon, Lafayette, CO), control siRNA primers (Dharmacon), a zebrafish-ZIP9 open reading frame (ORF) expression plasmid (Genscript, Piscataway, NJ), or both the ZIP9-targeting siRNA and expression plasmid.

Transfection was performed upon initial plating, and media was changed after 16 hr. All treatments were performed 72 hours after transfection.

mRNA isolation and qualitative real-time PCR analysis

Total mRNA was isolated using Tri-reagent (Sigma-Aldrich) following the manufacturer's protocol. For examining the effects of testosterone on the expression of pro-apoptotic genes, G/T cells were starved for 16-24 hrs followed by treatment with testosterone (50nM) or ethanol vehicle for 24 hr prior to mRNA isolation. Qualitative real-time PCR (qPCR) primers were designed against the mRNA sequences of *ZIP9*, *bax*, and *p53* (Table 4.1). qPCR was performed using Verso 1-step RT-qPCR SYBR Green Low ROX kit (Thermo Scientific, Waltham, MA), with 50 ng of mRNA per 15 µL reaction, following the manufacturer's protocol. The qPCR program was as follows, 50°C for 15 min, 95°C for 15 min, and 40 cycles of 95°C for 15 s, 55°C for 30 s, 72°C for 30 s. Amplification was followed by the melting curve program, 95°C for 15 s, 60°C for 15 s and a gradual increase to 95°C over 20 min. Samples were run in duplicate and expression was normalized to the housekeeping gene 18S.

Membrane protein preparation

All steps were carried out at 4°C. Ovarian tissue was homogenized in ice-cold HAED buffer (25 mM HEPES, 10 mM NaCl, 1 mM EDTA, 1 mM DTT, pH 7.6) containing protease inhibitor (1µl/ml), followed by centrifugation at 1000 x g for 7 min to pellet the nuclear fraction. The supernatant was removed and centrifuged at 20000 x g for 20 min to pellet the membrane protein fraction. For Western blot analyses the membrane protein pellet was resuspended in HAED, 5X reducing sample buffer (Thermo Fisher Scientific, Waltham, MA) was added, samples were boiled for 8 min, and stored at -80°C until analysis. For the androgen receptor binding assay, the membrane protein pellet was resuspended in HAED buffer with protease inhibitor.

Membrane androgen receptor binding assay

The ability of non-labeled testosterone and other steroid competitors to displace [^{3}H]T binding to the membrane fractions of ovarian follicles in three-point (T) and single-point (P4, E2, Mibolerone) competitive binding assays was assessed using methods described previously (74). Membrane protein (0.3-0.7 mg/ml final) was added to 5 nM (final) [^{3}H]T in the presence of vehicle, 0.01-1 µM unlabeled testosterone, or various steroid hormones (100 nM). Nonspecific binding was determined in the presence of 1000x unlabeled testosterone (5 µM) and subtracted from total binding to determine specific [^{3}H]T binding. Reactions were conducted in triplicate, and the results are displayed as displacement of specific [^{3}H]T binding.

Apoptosis analyses

Zebrafish G/T cells grown on round glass coverslips were serum-starved for 16-24 hr prior to the addition of testosterone treatment for 24 hours. All treatments were performed in duplicate or triplicate. For Hoechst staining, after treatment, the cells were fixed in 4% paraformaldehyde for 20 min at room temperature, stained with 1µg/ml Hoechst 33342 for 3 min, rinsed with PBS, and mounted face down on microscope slides. Apoptotic nuclei were identified based on the morphology of chromatin under fluorescent microscopy, and % apoptotic cells was determined by examination of 400 cells from each slide. For TUNEL staining, cells were fixed and stained following the manufacturer's protocol (*In Situ* Cell Death Detection Kit; Roche, Indianapolis, IN). Apoptosis was assessed as fluorescent staining of the nuclei, and % apoptotic cells was determined by examination of 600-1200 cells total from a minimum of 4 frames of view (10x) for each coverslip.

Caspase 3 activity assay

Zebrafish G/T cells grown in 6-well plates were serum starved for 16-24 hours, followed by testosterone treatment (50 nM) for 24 hr, harvested, and caspase 3 activity was determined using a Caspase Glo 3/7 Assay kit (Promega, Madison, WI) according to the manufacturer's protocol. Briefly, after treatment, cells were scraped and added in a 1:1 volume to Caspase-Glo reagent in a white-walled 96-well microplate. The luminescence of each sample was immediately analyzed by plate reader (CLARIOstar; BMG Labtech, Cary, NC) and subsequent readings were taken every 3 min until values began to drop. The highest luminescence value obtained for each sample was used and expressed relative to control values. Each treatment was conducted in triplicate, and the experiment was repeated three times.

Intracellular free zinc assay

G/T cells were grown in 96-well plates for 3-4 days. Cells were serum starved for 30 min followed by testosterone (50 nM) treatment for 30 min. Cells were fixed with 4% paraformaldehyde for 25 min at 4°C, stained with 10 μM zinquin ethyl esther (Enzo Life Sciences, Inc., Farmingdale, NY) for 30 min, washed with PBS, and immediately analyzed with a fluorescence plate reader (excitation 368 nm, emission 490 nm). Results are expressed as the relative intensity of the zinc signal compared to control. Each treatment was replicated in 8 wells/experiment, with the treatment average being used to calculate statistical differences between experiments.

Western blot analysis

Electrophoresis was performed on whole cell lysate or plasma membrane protein samples loaded on a 10% SDS-PAGE gel. Protein samples were transferred to a nitrocellulose membrane, blocked with 5% nonfat milk for 1 hr, and incubated with primary antibodies for ZIP9 1:2000 (custom polyclonal (26)) or actin 1:2000 (Thermo Scientific) overnight at 4°C. After incubation, membranes were washed 3 times with PBS

(NaCl 137 mM, KCl, 2.7 mM, Na_2HPO_4 10mM, KH_2PO_4 1.8 mM) followed by incubation with secondary antibodies (1:15000) for 1 hr at room temperature. Protein bands were visualized using Odyssey infrared imaging system (LI-COR, Lincoln, NE).

Design of ZIP9-targeted CRISPR-Cas9 system and gRNA preparation

Targets for ZIP9 mutagenesis were determined using CRISPOR (http://crispor.tefor.net/). The target sequence GAAGGAGTGGTGAGACCCAG in exon 3 was selected for its high specificity and efficiency scores. Synthesis of guide RNA (gRNA) was performed using the methods described in the supplemental protocol for Gagnon et al. 2014 (142). Briefly, an oligonucleotide containing a T7 promoter sequence, the target sequence, and a complementary region, was annealed to an oligonucleotide encoding the reverse-complement sequence of the tracrRNA tail, and the single-stranded DNA overhangs filled by the addition of Phusion high-fidelity PCR master mix (Thermo Scientific) using the thermocycler program 98°C for 2 min, 50°C for 10 min, and 72°C for 10 min. The product was directly used for generation of gRNA using a MAXIscript Kit (Ambion, Foster City, CA). The gRNA was DNase treated, purified by ethanol precipitation, verified for correct length on an agarose gel, and stored at -80°C until use. A stop codon cassette containing a stop codon in every reading frame with arms on either side homologous to the CRISPR-Cas9 system cut site on exon 3 was designed (adapted from (142)) and purchased as oligonucleotides from Invitrogen (Carlsbad, CA). Oligonucleotides used in gRNA generation and the stop codon cassette design are listed in Table 4.2.

Establishment of zebrafish ZIP9 mutant strain

To generate global ZIP9 mutants, an injection mixture containing 0.5 µl 1X Cas9 NLS (New England Biolabs, Ipswich, MA), 0.3 µl gRNA (1 µg/µl), 0.3 µl stop codon cassette oligonucleotide (3 µM), 0.25 µl phenol red, and 1.32 µl nuclease-free water was

incubated for 5 min at room temp and then stored on ice until use in embryo microinjection. Fertilized eggs were collected within 10 minutes of natural spawning of wild-type (WT) fish, and 2 nl of injection mixture was injected into the one-cell stage embryo using a micromanipulator (Narishige, Amityville, NY) and microinjector (Tritech Research, Inc., Los Angeles, CA). At 4-days post fertilization (dpf), fish underwent fin clipping as previously described (143) and the HotSHOT method (144) was used to isolate genomic DNA. Isolated DNA was used in PCR to screen for the presence of the stop codon cassette, and a heteroduplex mobility assay (HMA) (protocol adapted from (145)) was used for mutation detection. Primers used for screening and representative images of mutation screening assays can be found in Table 4.3 and Supplemental Figure 4.1, respectively.

To generate a germline mutation line, a male founder (F0) heterozygous for the knock-in of the stop codon cassette in exon 3 was raised to adulthood and mated with WT females to obtain F1 offspring. Heterozygous F1 fish were crossed to obtain sibling F2 ZIP9 homozygous wild-type (*ZIP9* $^{+/+}$), homozygous mutant (*ZIP9* $^{-/-}$), and heterozygous fish (*ZIP9* $^{+/-}$). Sibling F2 fish were used for the fecundity analysis, while F3 homozygous offspring were used for oocyte, embryo, and ovarian histology studies.

Fecundity analyses

Four-month-old F2 *ZIP9* $^{+/+}$ and *ZIP9* $^{-/-}$ fish were used for fecundity measures. *ZIP9* $^{+/+}$ and *ZIP9* $^{-/-}$ fish were mated with breeding-confirmed WT fish. Females were acclimated to the breeding tank overnight, and the male was added at in the morning within 15 min of light on. Fish were left undisturbed for 2 hours and then removed from the tanks, and verification of spawning and egg analyses were performed. All measures were determined from 5 males/5 female *ZIP9* $^{+/+}$, and 5 male/4 female *ZIP9* $^{-/-}$, which were each spawned twice with a 4-day rest between events. Spawning incidence was determined as the percentage of spawning in two independent events for each individual ((number of

times spawned/2) x 100) (n=4-5). The number of fertilized and unfertilized eggs was determined by visualization under a dissecting microscope. Eggs were considered unfertilized if they were opaque, but it should be noted that at 2 hrs post spawning, unfertilized eggs and those that failed to divide properly are indistinguishable. Percentage fertilization for each fish was determined as fertilized eggs/total eggs spawned x 100, and reported for each spawning event (n=8-10). Chorion diameter was measured from images taken with a dissecting microscope, and the number of eggs with regular and small chorion diameters were counted and presented as a percentage of the total eggs released in a spawning event (n=8-10).

Embryo and larval assessments

The growth of fish through the embryo and larval stages was assessed on F3 *ZIP9* $^{+/+}$ and *ZIP9* $^{-/-}$ fish. Embryos from regular and small diameter chorions were separated before hatching so that the growth and incidence of edema could be assessed for the two phenotypes separately. All length measurements were assessed by orientating unanesthetized (3-10dpf) or anesthetized (10+ dpf) fish eye-over-eye in 3% methyl cellulose (Sigma-Aldrich) followed by imaging with a dissecting microscope. A minimum of 7 *ZIP9* $^{+/+}$ and *ZIP9* $^{-/-}$ (regular chorions) fish from two separate spawning events were assessed at each time point (n=15+). *ZIP9* $^{-/-}$ fish from small chorions were harder to obtain due to high mortality, so limited growth measures were performed and an n<15 was obtained for a number of time points. Yolk sac depletion was determined by measuring the area (mm^2) of the yolk sac of ten 3 dpf fish from 2 separate spawning events using ImageJ software (n=20). The incidence of pericardial and yolk sac edema was determined by visualization under a dissecting microscope. Embryos from 4-5 spawning events were separated by phenotype (regular and small chorions for mutant fish) and assessed at 6 dpf

for incidence of edema ((number of fish showing edema/total number of fish) x 100) (n=4-5).

Morphological and histological analyses

Morphological and histological analyses were performed on ~3 month old, breeding-confirmed, F3 WT and mutant females. Fish were euthanized using MS-222, after which body length, total mass, and ovarian mass were measured. The gonado-somatic index (GSI) was calculated as ovarian mass/total mass x 100. Ovarian tissue was fixed in 4% paraformaldehyde for ~24 hrs. Dehydration, embedding, deparaffinization, sectioning, and hematoxylin and eosin staining for histological analysis was performed by Pacific Pathology, Inc. (San Diego, CA). Ovarian follicle stage identification using the histological preparations was performed by referencing prior works (146,147).

Statistical Analysis

All *in vitro* experiments using G/T cells were repeated a minimum of 3 times. Fecundity analyses were performed on 4-5 fish of each sex/strain. Embryo growth was determined at each time point from a minimum of 15 fish total, from 2 separate spawning events. Statistical significance was determined by Student's *t*-test or one- or two-way ANOVA with a post hoc Bonferroni multiple comparison test. All data is expressed as the mean ± SEM using GraphPad Prism 5 software (GraphPad Software, San Diego, CA).

RESULTS

ZIP9 mRNA tissue distribution and androgen binding to zebrafish ovarian plasma membranes

ZIP9 mRNA was expressed in all tissues examined with expression in the ovary being significantly higher than all other tissues (Figure 4.1A). When gonadal tissues were excluded from the analysis, no significance in the expression of ZIP9 in heart, gill, liver

and brain tissues was observed (Figure 4.1B). [^{3}H]T binding to the plasma membrane fraction of ovarian fragments was displaceable by unlabeled testosterone in a dose-dependent manner over the range of 0.01 to 1 μM, but no displacement was observed by incubation with 0.1 μM progesterone (P4), estradiol (E2), or the AR agonist mibolerone (Figure 4.1C). This indicates there is an androgen binding site on the membrane that is specific to testosterone and not mediated by the AR.

Effects of testosterone on known members of the ZIP9-mediated apoptotic pathway

To examine the effects of testosterone on signaling and apoptotic members that are known to be regulated by ZIP9 in other models (25,26,117), apoptosis, caspase 3 activity, mRNA expression of pro-apoptotic members, and intracellular free zinc levels were examined in testosterone-treated zebrafish G/T cells. Treatment with 100 nM testosterone and bovine serum albumin-conjugated testosterone (TBSA) significantly increased the incidence of G/T cell apoptosis compared to control, while 100 nM mibolerone had no significant effect (Figure 4.2A). Testosterone treatment (50 nM) also resulted in a rise in relative caspase 3 activity and the mRNA expression of pro-apoptotic members Bax and p53 (Figure 4.2B,C). Furthermore, testosterone treatment (50 nM) led to a rapid rise (30 min) in intracellular free zinc compared to vehicle control (Figure 4.2D).

Role of ZIP9 in testosterone-induced apoptosis

To determine the role of ZIP9 in the mediation of testosterone-induced apoptosis, G/T cells were transfected with siRNA targeting ZIP9 and a ZIP9 expression plasmid. Transfection with siRNA targeting ZIP9, but not control siRNA, resulted in a loss of the testosterone-induced apoptotic response (Figure 4.3A). Furthermore, the loss of the apoptotic response was restored when G/T cells were co-transfected with a ZIP9 ORF expression plasmid. Western blot analysis of ZIP9 protein expression confirmed that ZIP9

protein was significantly decreased in ZIP9-targeting siRNA transfected cells, but restored in cells co-transfected with the expression plasmid (Figure 4.3B).

Establishment of *ZIP9* knockout mutant zebrafish strain

Embryos obtained after microinjection of the CRISPR-Cas9 system were fin-clipped at 4 dpf and screening was performed to calculate the rate of mutation. 34% of the fish were found to carry the stop codon cassette. Heteroduplex mobility assays found that 71% of fish had a mutation in exon 3. This indicates that the CRISPR-Cas9 system had a relatively high efficiency in producing double strand break-induced mutations, but the knock-in of the stop codon cassette was less efficient. In addition, all fish possessing the stop codon cassette were found to be genetically mosaic at exon 3. Therefore, a male fish possessing a single copy of the insert was selected to be the founder (F0) for development of a *ZIP9* $^{-/-}$ strain homozygous for knock-in of the stop codon cassette in exon 3. The F0 was outcrossed with WT females to obtain F1 offspring. FI heterozygous carriers of the stop codon cassette were crossed to produce F2 offspring consisting of WT (*ZIP9* $^{+/+}$), homozygous mutants (*ZIP9* $^{-/-}$) and fish heterozygous at ZIP9 (*ZIP9* $^{+/-}$). The presence and absence of the stop codon cassette in exon 3 of F2 *ZIP9* $^{-/-}$ and *ZIP9* $^{+/+}$ fish was confirmed by Sanger sequencing. The mutant line had a 64 nucleotide insert, consisting of the stop codon cassette (35 bp), and additional nucleotides introduced on both sides of the cassette (Figure 4.4A). 3 stop codons in each possible reading frame are present in the cassette, but a stop codon (TAA) encoded in nucleotides 3-5 of the insert is predicted to be in frame. The proposed protein sequence resulting from this mutation is presented in Figure 4.4B, with the WT protein containing 309 amino acids, and the mutant protein truncated at amino acid 95.

Effect of ZIP9 mutation on fecundity

Measures of fecundity examined in *ZIP9* $^{+/+}$ and *ZIP9* $^{-/-}$ fish included incidence of spawning, number of oocytes released, and fertilization rates. Female and male *ZIP9* $^{-/-}$ fish showed no decrease in spawning incidence compared to sibling WT controls (Figure 4.5A). The number of oocytes spawned by females during mating events was significantly lower in *ZIP9* $^{-/-}$ fish (106.7 ± 26.90) compared to *ZIP9* $^{+/+}$ siblings (277.3 ± 21.38) (Figure 4.5B). In addition, the percentage of fertilized eggs was significantly lower for eggs spawned by *ZIP9* $^{-/-}$ (35.48% ± 9.611) than those by *ZIP9* $^{+/+}$ fish (96.77% ± 2.926) (Figure 4.5C). However, there was no significant difference in fertilization rate of eggs produced by WT females that were mated with *ZIP9* $^{-/-}$ (97.50% ± 1.256) males or *ZIP9* $^{+/+}$ (91.79% ± 4.701) (Figure 4.5D).

Effect of ZIP9 mutation on egg phenotype

Inspection of eggs produced by *ZIP9* $^{-/-}$ and *ZIP9* $^{+/+}$ females found many *ZIP9* $^{-/-}$ eggs showed a different phenotype to that seen in eggs from WT fish (Figure 4.6A). Measurement of chorion diameters of eggs produced by *ZIP9* $^{+/+}$ and *ZIP9* $^{-/-}$ females indicated that mutant females produce two distinct phenotypes, those with chorions of similar diameter to eggs produced by *ZIP9* $^{+/+}$ fish (regular egg diameter (RD); 1.203 ± 0.007 mm, and 1.182 ± 0.007 mm, respectively), and those that are significantly smaller in diameter (small egg diameter (SD); 0.8100 ± 0.006 mm) (Figure 4.6B). All *ZIP9* $^{+/+}$ females used for analysis only spawned RD eggs (Figure 4.6C). However, *ZIP9* $^{-/-}$ females showed a high level of variance between the number of RD and SD eggs produced between fish, with two fish producing only SD eggs, and two fish producing both phenotypes (Figure 4.6D). When the percentage of RD eggs for all *ZIP9* $^{-/-}$ and *ZIP9* $^{+/+}$ females are combined, the percentage of RD eggs produced by *ZIP9* $^{-/-}$ females (34.80% ± 15.77) is significantly lower than that for *ZIP9* $^{+/+}$ siblings (100% ± 0.00) (Figure 4.6E). There was no significant difference in the relative percentages of RD (34.80 ± 15.77) and SD (65.20 ± 15.77) eggs

spawned by *ZIP9* $^{-/-}$ females (Figure 4.6F). SD *ZIP9* $^{-/-}$ eggs exhibited significantly lower fertilization rates (21.04% ± 6.783) compared to RD *ZIP9* $^{-/-}$ eggs (67.40% ± 9.197) (Figure 4.6G).

Effect of ZIP9 mutation on larval edema and growth

Edema incidence and growth measures were performed on F3 *ZIP9* $^{+/+}$ and *ZIP9* $^{-/-}$ fish, with *ZIP9* $^{-/-}$ larvae hatched RD and SD eggs examined independently. At 6 dpf, fish from SD *ZIP9* $^{-/-}$ eggs showed a significantly higher incidence of edema (40.08% ± 9.582) compared to those hatched from *ZIP9* $^{+/+}$ (11.40% ± 4.030) or RD *ZIP9* $^{-/-}$ eggs (15.36% ± 5.833) (Figure 4.7A,B). Using the average number of eggs spawned (*ZIP9* $^{+/+}$, 277.3; *ZIP9* $^{-/-}$, 106.7) fertilization rate (*ZIP9* $^{+/+}$, 96.8%; *ZIP9* $^{-/-}$, 35.5%), and incidence of edema (*ZIP9* $^{+/+}$, 11.40%; *ZIP9* $^{-/-}$, 27.72% (avg of SD and RD)), a graph showing the number of surviving larva after day 6 from a representative spawn for each genotype was compiled in Figure 4.7C. While WT females produce an average spawn of 277 eggs with 91.3% (253) of larvae surviving at day 6, *ZIP9* $^{-/-}$ females produce an average of 107 eggs per spawning event, and only 30.8% (33) of larvae would survive past day 6 on average. In the larval growth analyses, larvae from SD *ZIP9* $^{-/-}$ eggs had a significantly larger yolk sac at 3 dpf compared to those from *ZIP9* $^{+/+}$ and RD *ZIP9* $^{-/-}$ eggs (Figure 4.8A). No significant difference in yolk area was observed between the different genotypes/phenotypes at 0 dpf (data not shown), so the larger yolk sac present in 3 dpf larvae from SD *ZIP9* $^{-/-}$ eggs may be due to inefficient yolk absorption. Analysis of larval growth under starvation conditions from 3-10 dpf, indicated that *ZIP9* $^{-/-}$ fish from SD eggs were significantly shorter in length compared to *ZIP9* $^{+/+}$ fish at every time point (Figure 4.8B). SD egg *ZIP9* $^{-/-}$ larvae were also significantly shorter than *ZIP9* $^{-/-}$ fish from RD eggs at every time point except 9 dpf, which was the only time that *ZIP9* $^{-/-}$ fish from RD eggs were significantly smaller than *ZIP9* $^{+/+}$ fish. In fish fed endogenously after 6 dpf, *ZIP9* $^{-/-}$ fish from SD eggs were

significantly smaller than larvae from RD *ZIP9* $^{-/-}$ and *ZIP9* $^{+/+}$ eggs at 15 and 25 dpf, while *ZIP9* $^{-/-}$ larvae from RD eggs showed no difference from *ZIP9* $^{+/+}$ fish at every time point (Figure 4.8C). Representative images of a *ZIP9* $^{+/+}$ and a *ZIP9* $^{-/-}$ SD fish 15 dpf is presented in Figure 4.8D.

Comparison of ovarian morphology of *ZIP9* $^{+/+}$ and *ZIP9* $^{-/-}$ fish

ZIP9 $^{+/+}$ and ZIP9 $^{-/-}$ fish of similar length (ZIP9 $^{+/+}$, 3.360 ± 0.06205 cm; ZIP9 $^{-/-}$, 3.190 ± 0.08124 cm), weight (ZIP9 $^{+/+}$, 0.4460 ± 0.02182 g; ZIP9 $^{-/-}$, 0.3560 ± 0.04874 g), and GSI (ZIP9 $^{+/+}$, 16.02 ± 1.285%; ZIP9 $^{-/-}$, 12.56 ± 2.518%) were selected for comparison of ovarian morphology. *ZIP9* $^{-/-}$ fish ovaries had a significantly smaller proportion of perinuclear stage and a significantly higher proportion of cortical alveolus stage oocytes compared to ZIP9 $^{+/+}$ fish (Figure 4.9A). However, no significant differences were observed in the proportions of oocytes at later stages of development between genotypes. Representative histological images of follicles from ovaries of each genotype are shown in Figures 4.9B.

DISCUSSION

Here we present evidence that testosterone mediates an apoptotic response in zebrafish G/T cells harvested from mature ovaries and that it is mediated by ZIP9. The apoptotic response in zebrafish involves rapid increases in intracellular zinc as well increased caspase 3 activity and mRNA expression of pro-apoptotic members, identical to that seen in the ZIP9-mediated apoptosis of croaker G/T cells (25,117). The finding that ZIP9 has the same function in two distantly-related teleost species belonging to the two largest superorders, Acanthopterygii (croaker) and Ostariophysi (zebrafish), suggests ZIP9 mediation of ovarian G/T cell apoptosis is likely a shared response in teleosts. We further investigated the role of ZIP9 in ovarian physiology by developing a global ZIP9 knockout

model by utilizing a CRISPR-Cas9 system. *ZIP9* $^{-/-}$ females showed significant reductions in fecundity, with decreased numbers of oocytes spawned and a reduction in oocyte quality as evident by reduced fertilization capacity and abnormal larval development. However, no abnormalities between *ZIP9* $^{-/-}$ and *ZIP9* $^{+/+}$ ovarian morphology were apparent by histological examination. Overall, this study indicates while ZIP9 plays a role in apoptosis of ovarian follicle cells *in vitro*, the receptor likely also has other functions in the teleosts ovary, potentially in the maturation and/or activation responses of oocytes.

This study demonstrates that the ZIP9-mediated apoptotic response exhibited by G/T cells *in vitro* is shared by Atlantic croaker, zebrafish, and potentially all teleosts. ZIP9 is 85% homologous between zebrafish and croaker, and while croaker ZIP9 is predicted to have 7 transmembrane (TM) domains, zebrafish and human ZIP9 are predicted to have 8 TM domains (25). It is unknown if this difference in ZIP9 structure results in differences in androgen-induced signaling mediated by the receptor. ZIP9 mediates androgen-induced apoptosis by coupling to a G_s in croaker G/T cells but mediates a very similar response in human cancer cell lines through activation of a G_i. Further examination of Gα-subunit signaling events and ZIP9-G protein coupling will be essential in determining if the apoptotic response observed in zebrafish G/T cells is mediated through ZIP9 coupling to a G_i or G_s. An additional complexity of ZIP9 signaling has been observed in the croaker G/T cells model, in which ZIP9 alternatively couples to G_s and G_i to mediate opposite physiological responses depending on the developmental stage from which the G/T cells are derived. ZIP9-G_s coupling dominates in late stage croaker ovarian follicles and mediates the androgen-induced apoptotic response. When croaker G/T cells from all stage follicles are pooled, androgen-induced apoptosis is the primary response observed. Zebrafish are daily spawners that maintain an asynchronous store of follicles in the ovary, similar to that seen in croaker during their reproductive season (128). Therefore, there is a

potential that if dual signaling events are mediated by ZIP9 activation in zebrafish G/T cells, one pathway may dominate due to the mixed population of follicles from which the G/T pool is derived. Further investigation of dual coupling of ZIP9 to multiple G proteins in the zebrafish G/T cell model would help test this possibility.

This study is the first to utilize a ZIP9 global knockout to investigate the role of the receptor in reproduction. *ZIP9* $^{-/-}$ males show no abnormal reproductive phenotype based on spawning incidence and fertilization rate. However, *ZIP9* $^{-/-}$ females show significant reductions in fecundity compared to WT siblings, with fewer eggs spawned, lower fertilization rates, and high incidences of edema in surviving larvae. Of interest, the reduction in fecundity of mutant females does not appear to be due to oogenesis, as apparent from the similar proportions of vitellogenic follicles produced in WT and mutant female ovaries. Therefore, the differences in egg phenotype, fertilization rates, and health of mutant larvae, likely arise during the process of oocyte maturation or activation. Oocyte maturation occurs when the germinal vesicle breaks down and meiosis proceeds to metaphase II where it remains arrested until fertilization (148). In zebrafish, egg activation occurs upon exposure to the external spawning media and involves a wave of free intracellular Ca^{++} (149,150) inducing cortical granule exocytosis, which results in the separation of the chorion from the vitelline (plasma) membrane to create a perivitelline space (149,151). The increase in free Ca^{++} also allows programmed development to proceed. Interestingly in zebrafish, since activation is not dependent on fertilization, the developmental program will ensue within ~30s of activation with or without fertilization. However unfertilized eggs will only divide several times before cleavage failure (149). If sperm is present and the egg undergoes fertilization, meiosis is completed, and the egg develops normally (149,150). Of interest, androgens and zinc have been found play a role

in oocyte maturation and activation, respectively, in a variety of models (44,45,137,138,152–155).

Androgens have been shown to stimulate oocyte maturation in *Xenopus* (44,45), murine (156) and porcine models (153). In *Xenopus*, progestins are also potent promoters of oocyte maturation (44,157,158) and are widely accepted as the primary maturation-inducing steroid (MIS) in amphibians, as they are in teleosts (97,159). The regulation of maturation of mammalian oocytes is less clear, as steroids have not been shown to be obligatory to the induction of LH-mediated oocyte maturation (160). Additionally, high doses of androgens are required to induce maturation of murine and porcine oocytes, which suggests these responses may not be physiologically relevant (161). As previously mentioned, the role of progestins in the mediation of teleost oocyte maturation has been extensively established and is well accepted (97,159,162). This along with little support that androgens are fundamental in oocyte maturation in other models suggests that the abnormal phenotype of eggs produced by *ZIP9* $^{-/-}$ females may be due to disruption in an alternative process, such as egg activation.

In zebrafish, oocyte activation is essential to complete meiosis and begin embryonic development. The most identifying feature of egg activation is the rapid rise in free intracellular Ca^{++} which has been observed in all vertebrate (*Xenopus* (163); teleosts (149,164); mammals (165,166)) and invertebrate (*Drosophila* (167); *C. elagans* (168)) models examined to date. In addition to Ca^{++}, a role for zinc in egg activation has recently been proposed in mammals (137,138,154,155). The mammalian oocyte undergoes dramatic zinc accumulation between GVBD and metaphase II (MII), with progression to MII being halted if zinc is chelated (137). This zinc accumulation ensures meiotic arrest at MII until the egg is activated at fertilization. In mice, non-human primates and humans, a rapid zinc “spark”, or release from the egg, immediately follows the fertilization-induced

free Ca^{++} wave (138,154). Furthermore, mammalian eggs arrested in MII undergo parthenogenetic cell cycle resumption when zinc is chelated (138,155), indicating that the Ca^{++} wave may not be essential for meiosis resumption, but a reduction of intracellular zinc is. An elevation of intracellular zinc using pharmacological agents after the resumption of meiosis II will once again arrest the egg at metaphase, inhibiting cell cycle progression and embryo development (138). Overall, these studies indicate that in the mammalian eggs, zinc regulation is important to both maturation and activation processes, with increases in egg zinc content being associated with maturation (resumption of meiosis to MII), and a decreased intracellular zinc resulting in meiosis II resumption, completion of meiosis, and subsequent embryo development. Free zinc signaling has not been well examined in teleost oocytes to date, however zinc levels in the oocyte increase over the course of development (140) similar to as seen in mammalian oocytes (137). Thus, it remains unclear if the role of zinc in oocyte maturation/activation is unique to mammals, or shared in vertebrates or all animal phyla as the Ca^{++} activation wave is.

The phenotype of the *ZIP9* $^{-/-}$ eggs with small chorion diameter is remarkably similar to that observed by Mei et al. 2009 (169) in zebrafish with a mutated heterogeneous nuclear ribonucleoprotein I (hnRNP I). hnRNP I mutants showed normal oogenesis but were defective in the IP_3-mediated rise in Ca^{++} associated with egg activation, which resulted in cortical granule exocytosis failure. This produced a phenotype of decreased chorion elevation, resulting in an egg with a smaller chorion diameter. These eggs showed varying amounts of cytoplasmic segregation to the animal pole and cleavage defects, ultimately resulting in high mortality (169). Interestingly, there was high variability between individual clutches produced by mutant females, with variable proportions of activated and non-activated eggs (between 27-94% egg showed defective activation) (169). The non-activation phenotype was rescuable with injection of Ca^{++} or IP_3 into the embryo,

suggesting that hnRNP I acts upstream of IP_3 activation. The similarities in the phenotype of the smaller diameter chorion eggs, and the variability in the extremity of abnormality between individual eggs, clutches, and spawning females observed in *ZIP9* $^{-/-}$ and hnRNP I mutants suggest that both proteins are likely involved in the signaling pathway that mediates egg activation in zebrafish. However, further verification of this is required to determine the role of ZIP9 and where it lies on this pathway. It is also important to note, that neither ZIP9 or hnRNP I mutation results in full failure of oocyte activation, suggesting that there may be additional means of compensation for oocyte activation in the zebrafish model. Further examination of the roles of ZIP9 and zinc signaling in zebrafish oocyte maturation and activation *in vitro* using WT and ZIP9 mutant fish will potentially clarify the SD chorion phenotype observed in *ZIP9* $^{-/-}$ fish.

While this examination of *ZIP9* $^{-/-}$ zebrafish has provided evidence for a role of ZIP9 in female reproduction, a role for ZIP9 in androgen-induced apoptosis *in vivo* was not apparent. Apoptosis is generally confined to atretic and postovulatory follicles in the fish ovary (82–84), with atresia typically occurring under stress and postovulatory follicle breakdown occurring after a spawning event. In the current study, atretic and postovulatory follicles were absent in the histological preparations of *ZIP9* $^{+/+}$ and *ZIP9* $^{-/-}$ fish ovaries, which was expected since the fish had not recently spawned (>3 days) or undergone environmental stress. It would be of interest to examine the ovaries of *ZIP9* $^{+/+}$ and *ZIP9* $^{-/-}$ fish after spawning or induction of stress to identify potential differences in apoptotic responses between the strains.

It should be emphasized that induction of both apoptosis and zinc transport can be mediated by numerous proteins, and therefore, compensation of ZIP9-mediated events in a global knockout model would not be surprising. Compensation of physiological functions of proteins involved in reproduction is well documented in teleost knockout models. For

example knockout of GnRH, kisspeptin 1 and 2 (reviewed in (170)), and the LH receptor (171) show no abnormal reproductive phenotypes in zebrafish. Apoptosis is essential for the maintenance of homeostasis in all tissues, with numerous endocrine, autocrine and paracrine factors being able to influence apoptosis and survival of cells in a tissue at any given time (172,173). Furthermore, there are 19 members of the ZnT (Slc30A) and ZIP (Slc39A) families of zinc transporters in zebrafish (141), many of which are highly expressed in the zebrafish ovary. Therefore, while it is of interest to continue the examination of *ZIP9* knockout model phenotypes to infer physiological roles of the receptor, there is the potential that some ZIP9-mediated functions will not result in abnormal phenotypes due to compensation by other physiological processes. Additional investigation of the ZIP9 global knockout phenotypes, as well as its use in in vitro experimentation, will be essential in understanding ZIP9's role in the zebrafish ovary.

In summary, the present study demonstrates that ZIP9 mediates androgen-induced apoptosis in croaker and zebrafish G/T cells, and that this response is likely conserved in teleosts. Investigation of the role of ZIP9 in the zebrafish ovary using a global knockout model demonstrated that *ZIP9* $^{-/-}$ females showed a severe reduction in fecundity compared to WT fish. This reduced fecundity is primarily driven by a non-activated oocyte phenotype, with a large proportion of spawned eggs showing lack of chorion elevation, low fertilization rates, and high incidences of edema in fish that do develop from the eggs. This suggests a role of ZIP9 in zebrafish oocyte maturation and/or activation, however further work looking into the mechanism driving this phenotype is required. Additionally, examination of apoptotic events in the ovary *in vivo* as well as using the global knockout model to examine loss of ZIP9's apoptotic function in *ZIP9* $^{-/-}$ G/T cells *in vitro* will provide further insight into the role of ZIP9 in ovarian apoptosis. Overall, the work presented in

this study strongly suggests an important role for ZIP9 in teleost ovarian physiology and highlights the need for future research on this receptor in animal reproductive physiology.

FIGURES

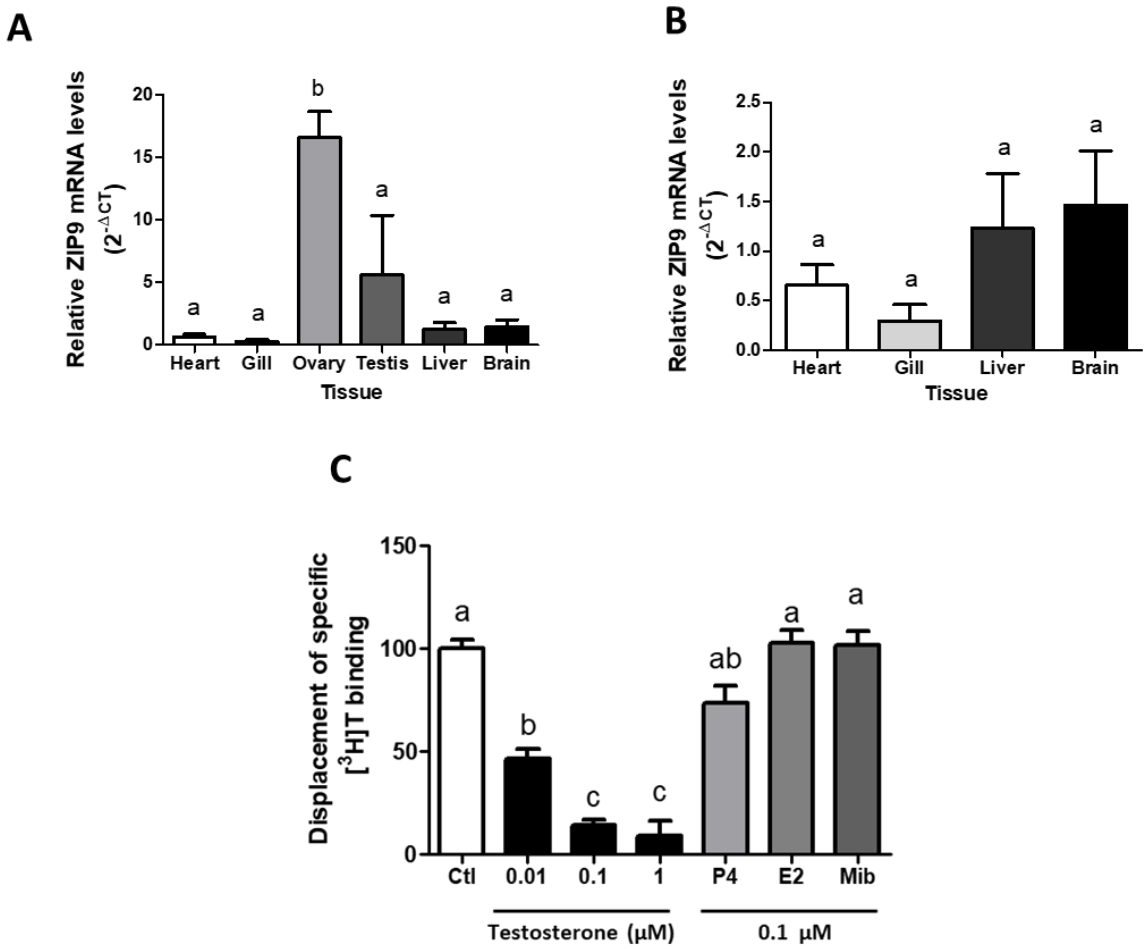

Figure 4.1: Tissue distribution of ZIP9 mRNA expression and androgen binding to ovarian plasma membranes. A, Relative ZIP9 mRNA levels in various zebrafish tissues. B, relative ZIP9 mRNA levels in non-reproductive tissues. C, Displacement of membrane-bound [3H]T by unlabeled testosterone and various steroid hormones. All data represents means ± SEM, n=3-6 (A,B), n=9 (C). Significance was determined by one-way ANOVA with Bonferroni multiple comparison post-test. Different letters indicate significant differences between the treatment groups in the post hoc test at $p < 0.05$. ZIP9 mRNA expression was determined in tissue samples from 3 females and 3 males, with sexes combined for analysis of non-reproductive tissues. For binding experiments, each treatment was conducted in triplicate with similar results obtained for each, and the experiment was repeated 3 times. Ctl, total binding; P4, progesterone; E2, estradiol; Mib, mibolerone.

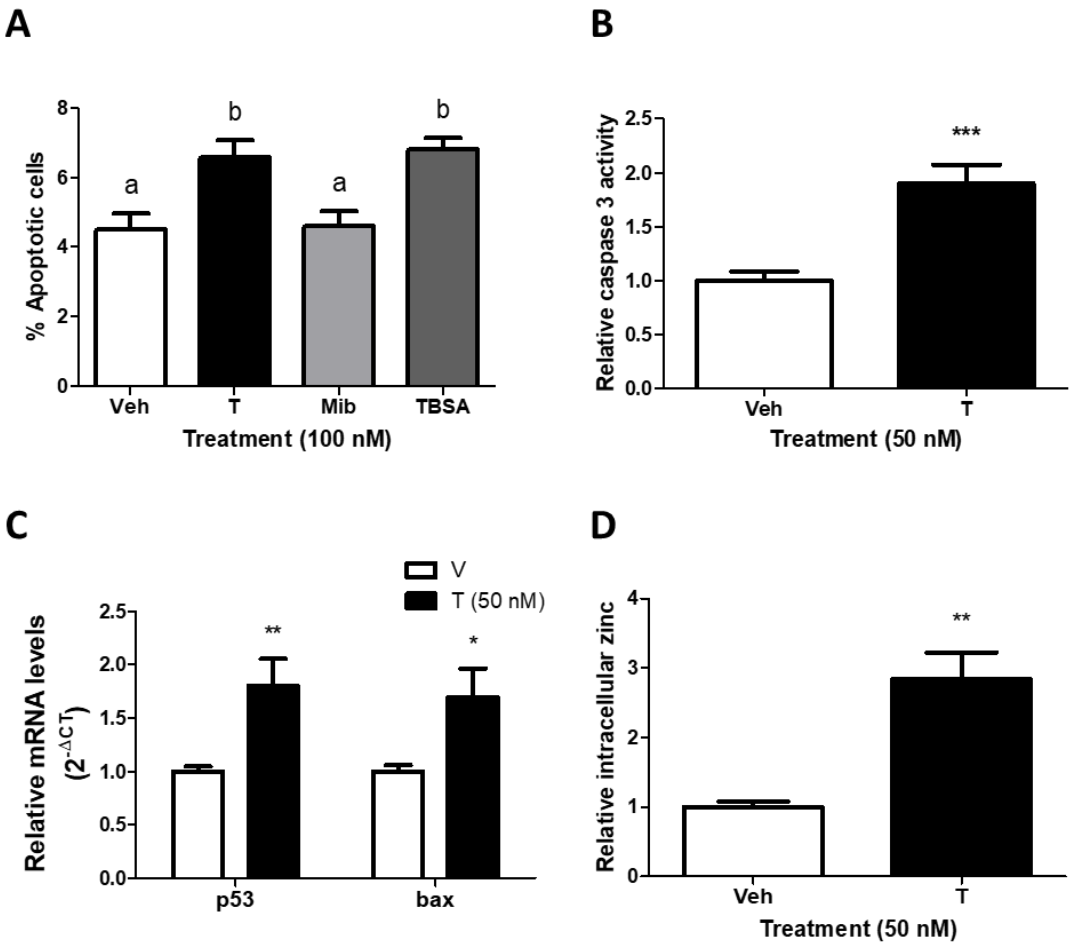

Figure 4.2: Effect of testosterone on apoptosis, caspase 3 activity, pro-apoptotic member mRNA expression and intracellular free zinc. A, Effects of various androgen treatments on % apoptotic nuclei as determined by Hoechst staining. B, Effect of testosterone on caspase 3 activity. C, Expression of p53 and bax mRNA after 24 hr testosterone treatment of G/T cells. D, Effect of testosterone on intracellular free zinc levels. All data represents means ± SEM, n=8-9 (A-C), n=3 (D). Significance was determined by Student's t-test (B-D; *, $p<0.05$, **, $p<0.01$, ***, $p<0.001$) or one-way ANOVA with Bonferroni multiple comparison post-test (A). Different letters indicate significant differences between the treatment groups in the post hoc test at $p < 0.05$. Incidence of apoptosis (A) and caspase 3 activity (B) experiments were repeated with 3 pools of G/T cells and each treatment conducted in duplicate or triplicate with similar results obtained for each. Pro-apoptotic member mRNA expression analysis (C) was repeated with 4 pools of G/T cells and each treatment conducted in duplicate. Intracellular zinc was assessed in 3 pools of G/T cells. Veh, ethanol vehicle; T, testosterone; Mib, mibolerone; TBSA, bovine serum albumin-conjugated testosterone.

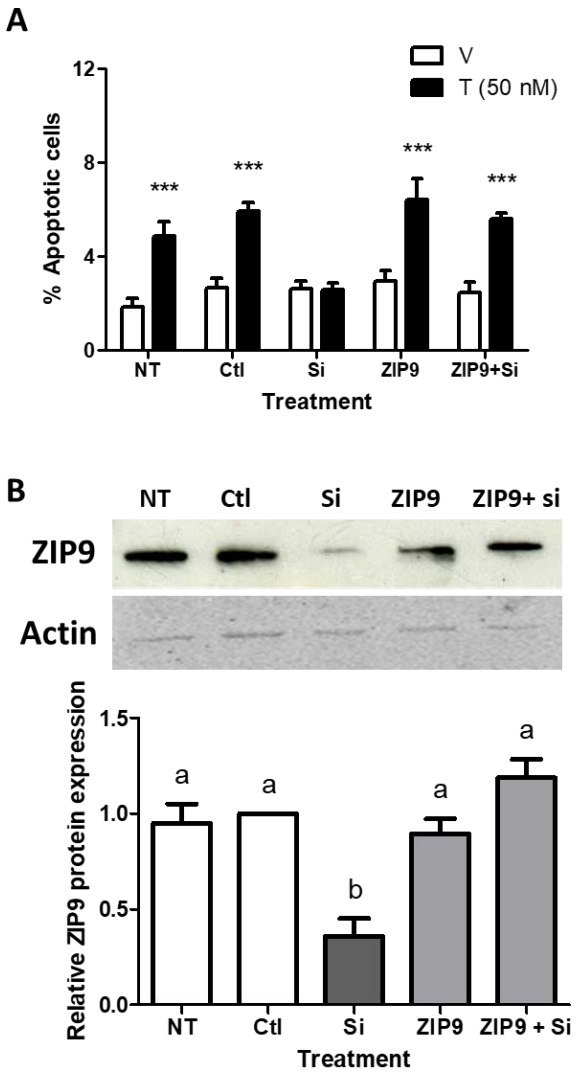

Figure 4.3: Role of ZIP9 in testosterone-induced apoptosis as determined by TUNEL staining. A-B, Effect of transfection of siRNA targeting-ZIP9 and ZIP9 ORF expression plasmid on testosterone-induced apoptosis (A) and ZIP9 protein expression (B). All data represents means ± SEM, n=6 (A), n=3 (B). Significance was determined by one- (B) or two-way (A) ANOVA followed by Bonferroni multiple comparison post-test. Different letters indicate significant differences between the treatment groups in the one-way ANOVA post hoc test at $p < 0.05$. Level of significance between vehicle and testosterone treatments as determined by the two-way ANOVA post hoc are indicated as ***, $p<0.001$. In experiment (A) significant interactive effects of the steroid treatment (V & T) and the transfection treatments on G/T cell apoptosis was detected by the two-way ANOVA, which was predicted because ZIP9-targeting siRNA blocked the testosterone-induced responses, while effects of transfection with control siRNA and the expression plasmid did not. Experiments were repeated with three fish and each treatment conducted in duplicate with similar results obtained for each. NT, no transfection; Ctl, non-targeting siRNA control; Si, small interfering RNA, ZIP9, ZIP9 ORF expression plasmid.

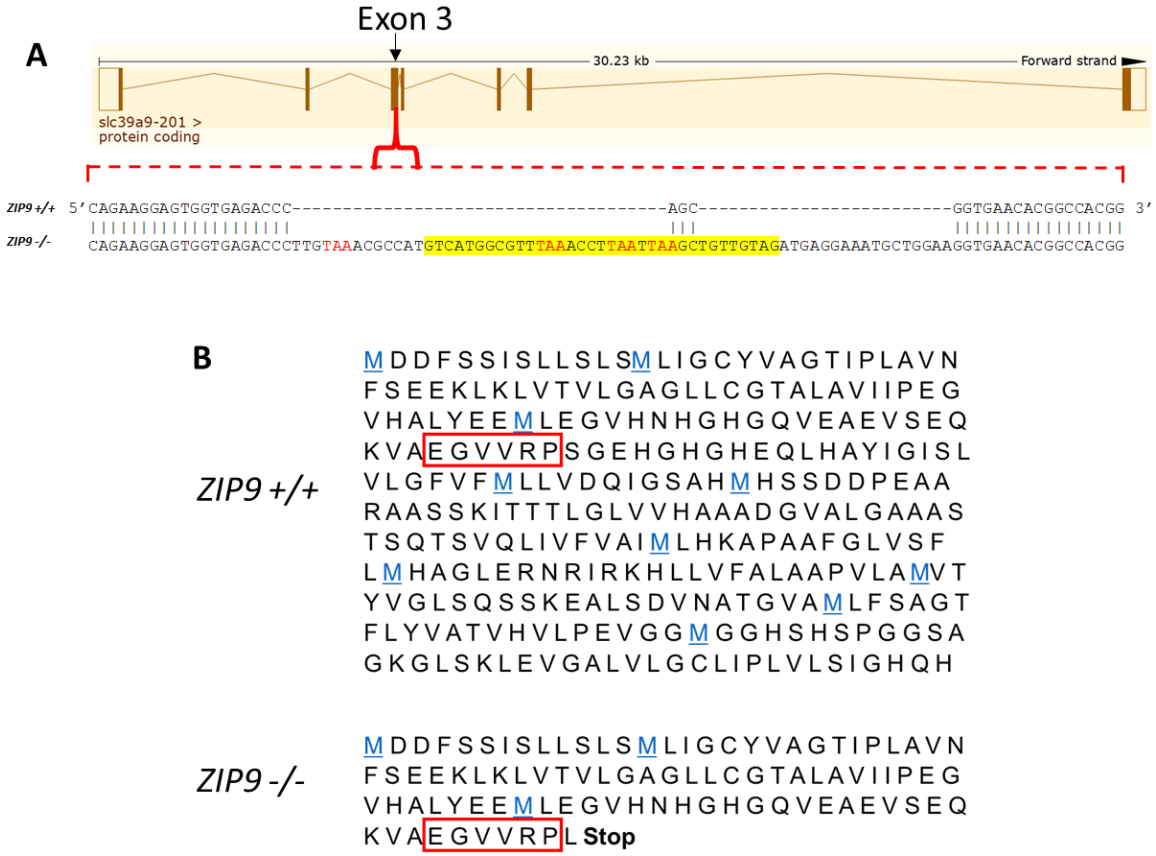

Figure 4.4: Disruption of ZIP9 exon 3 by a CRISPR-Cas9 system. A, Schematic representation of genomic ZIP9, and the comparison of mutant (*ZIP9* $^{-/-}$) and wild-type (*ZIP9* $^{+/+}$) exon 3 nucleotide sequence. B, Comparison of predicted mutant and wild-type ZIP9 protein sequence. Highlighted nucleotide sequence indicated the stop codon cassette, red-text nucleotides indicate stop codons, red boxed-amino acids are adjacent to the site of early truncation in the mutant ZIP9.

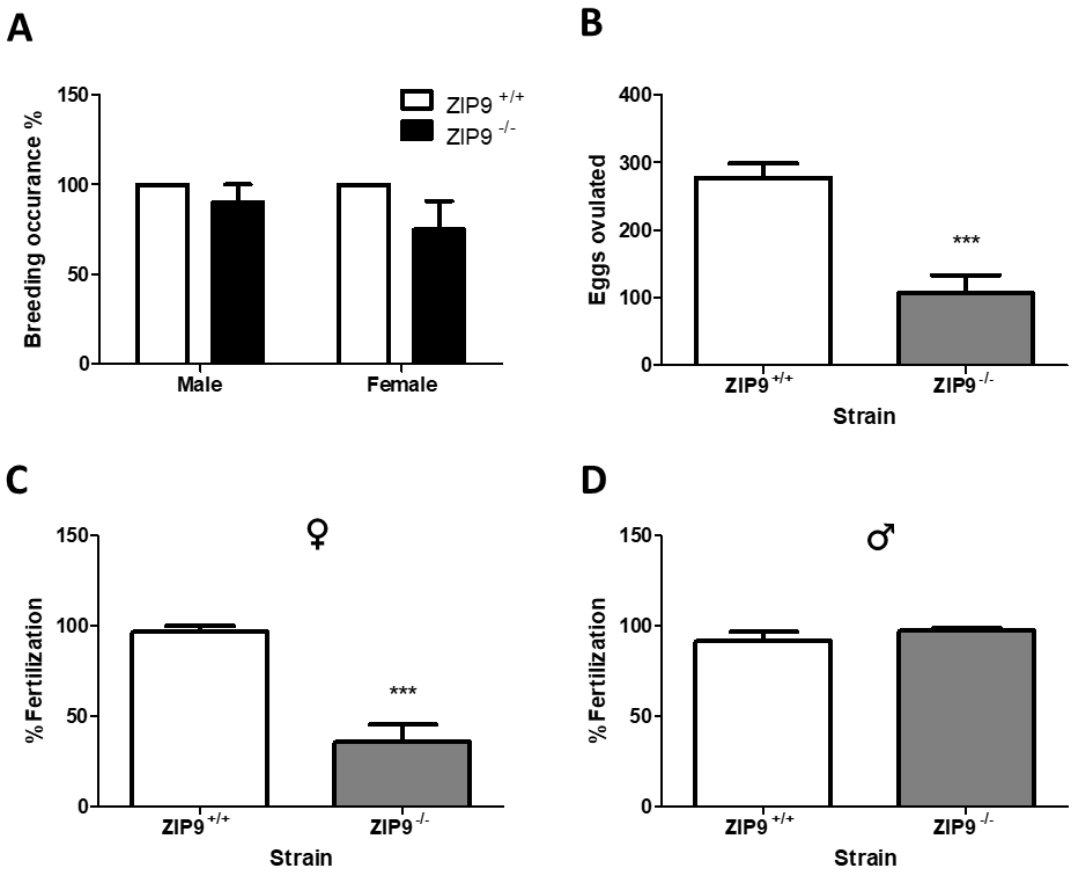

Figure 4.5: Measures of fecundity in ZIP9 mutant and wild-type zebrafish. A, Breeding occurrence in male and female *ZIP9* $^{-/-}$ and *ZIP9* $^{+/+}$ fish mated with breeding-confirmed wild-type fish of opposite sex. B, Number of eggs ovulated by *ZIP9* $^{-/-}$ and *ZIP9* $^{+/+}$ in single breeding events. C, Percent of eggs ovulated by *ZIP9* $^{-/-}$ and *ZIP9* $^{+/+}$ females that underwent successful fertilization when mated with wild-type males. D, Percent of eggs ovulated by wild-type females that underwent successful fertilization when mated with *ZIP9* $^{-/-}$ and *ZIP9* $^{+/+}$ males. All data represents means ± SEM, n=4-5 (A), n=9-10 (B-D). Significance was determined by Student's t-test (***, $p \leq 0.0001$). Experiments were repeated with 5 male and 5 female *ZIP9* $^{+/+}$ fish, and 5 male and 4 female *ZIP9* $^{-/-}$ fish, that were each spawned on 2 separate occasions.

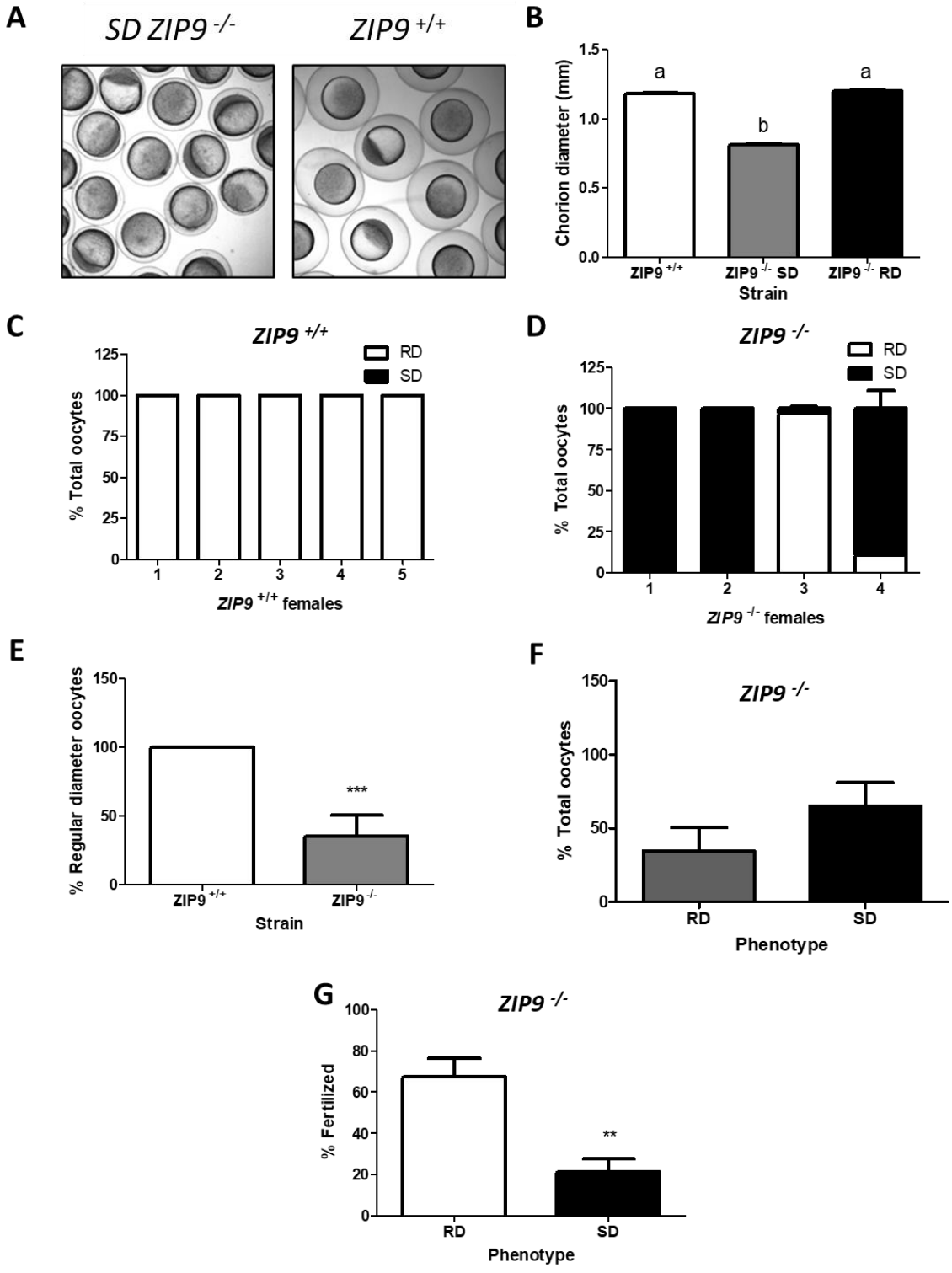

Figure 4.6: Analysis of egg phenotypes produced by *ZIP9* $^{-/-}$ and *ZIP9* $^{+/+}$ fish.

Figure 4.6 (continued): Analysis of egg phenotypes produced by *ZIP9* $^{-/-}$ and *ZIP9* $^{+/+}$ fish. A, A representative image of small diameter egg phenotype and regular egg phenotype. B, Chorion diameter of eggs spawned by *ZIP9* $^{-/-}$ and *ZIP9* $^{+/+}$ females. C, Relative proportion of regular and small diameter eggs spawned by individual *ZIP9* $^{+/+}$ females. D, Relative proportion of regular and small diameter eggs spawned by individual *ZIP9* $^{-/-}$ females. E, Percentage of regular diameter eggs spawned by *ZIP9* $^{-/-}$ and *ZIP9* $^{+/+}$ females. F, Proportion of regular diameter and small diameter eggs spawned by *ZIP9* $^{-/-}$ females. G, Percent of small diameter and large diameter eggs spawned by *ZIP9* $^{-/-}$ females that underwent successful fertilization. All data represents means ± SEM, n=50 (B), n=2 (C, D), n=9-10 (E, F), n=4-8 (G). Significance was determined by Student's t-test (**, $p<0.01$, ***, $p<0.001$) or by one-way ANOVA with Bonferroni multiple comparison post-test. Different letters indicate significant differences between the treatment groups in the *post hoc* test at $p < 0.05$. Chorion diameter analyses were performed by measuring 25 eggs from 2 spawning events. Percentages of regular and small diameter eggs (C, D) was determined from 2 spawning events for each individual spawning events. Experiments (E-G) were repeated with 5 female *ZIP9* $^{+/+}$ fish, and 4 female *ZIP9* $^{-/-}$ fish, that were each spawned on 2 separate occasions. SD, small diameter egg; RD, regular diameter egg.

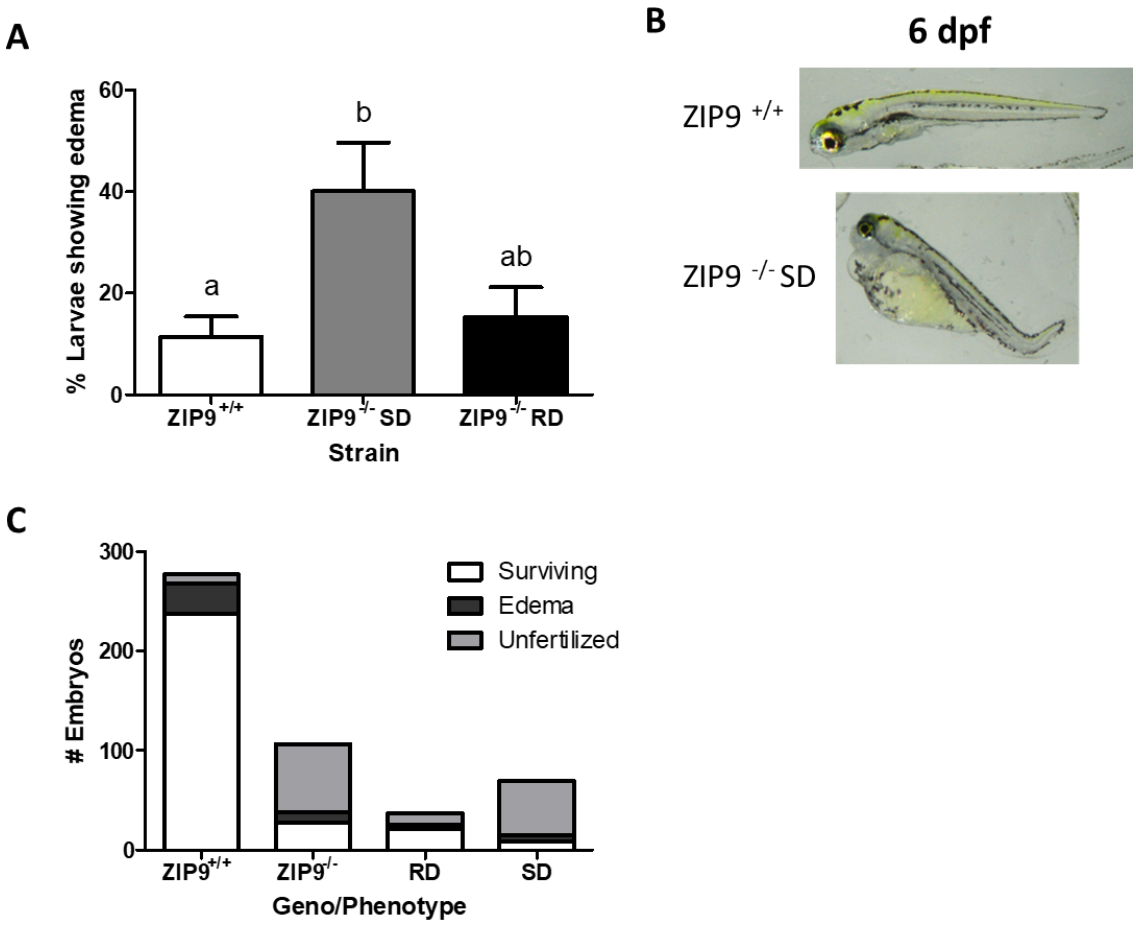

Figure 4.7: Analysis of ZIP9 $^{-/-}$ and ZIP9 $^{+/+}$ larvae health. A, Incidence of pericardial and yolk sac edema in 6 dpf *ZIP9* $^{-/-}$ and *ZIP9* $^{+/+}$ larvae. B, Representative image of 6 dpf larvae showing regular development (ZIP9 $^{+/+}$) and pericardial/yolk sac edema (ZIP9 $^{-/-}$ SD). C, Ideal representation of surviving fish of each genotype from an average spawning event. All data represents means ± SEM, n=4-5. Significance was determined by one-way ANOVA with Bonferroni multiple comparison post-test. Different letters indicate significant differences between the treatment groups in the *post hoc* test at $p < 0.05$ (A). Edema incidence was determined on larvae spawned from 4-5 separate events for each genotype/phenotype. Averages previously reported for # eggs spawned, fertilized, and larval incidence of edema were used to construct a graph showing surviving fish at 6 dpf for each genotype. SD, small diameter egg; RD, regular diameter egg.

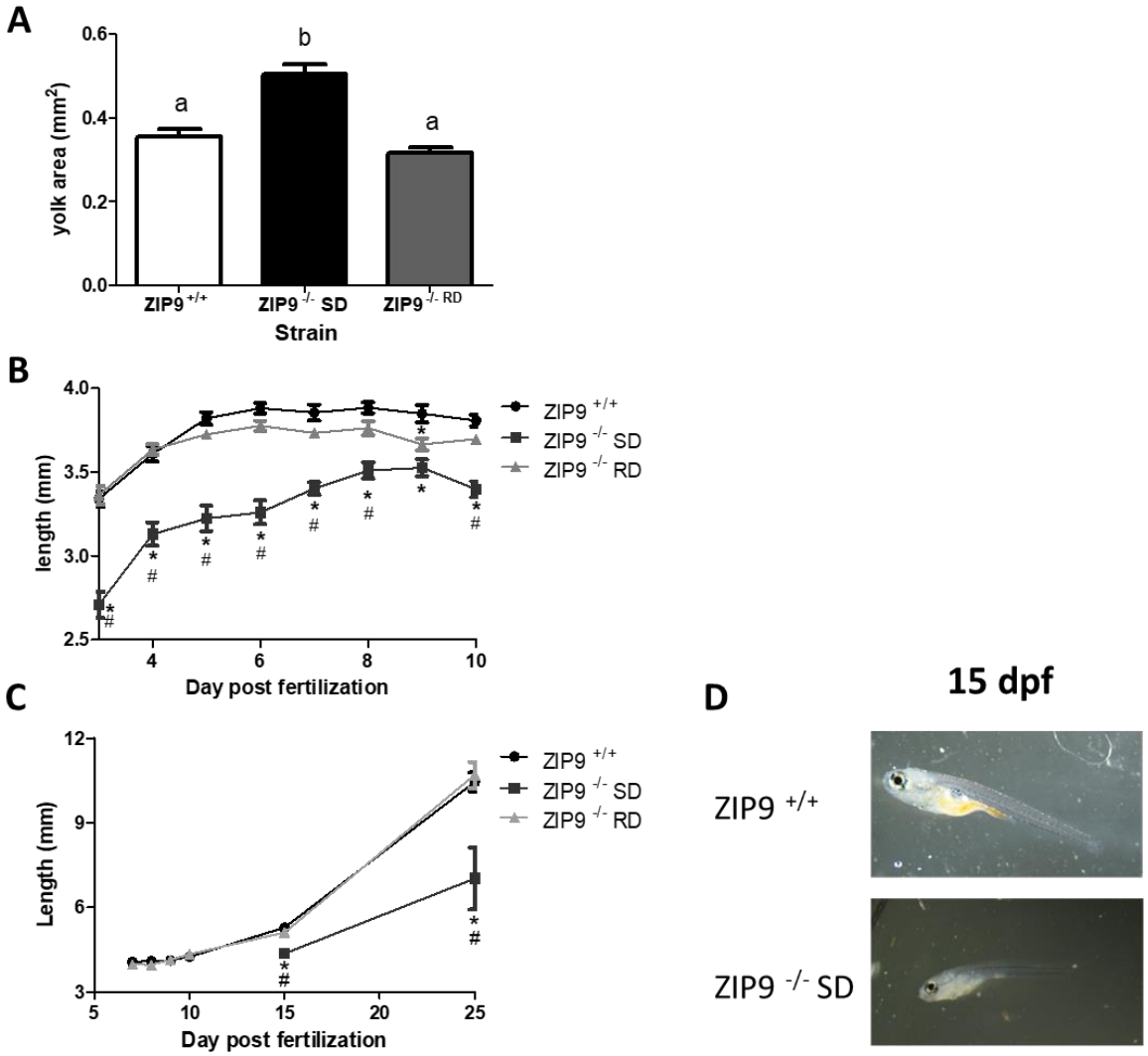

Figure 4.8: Analysis of ZIP9 $^{-/-}$ and ZIP9 $^{+/+}$ larvae growth. A, Yolk sac area of 3 dpf *ZIP9* $^{-/-}$ and *ZIP9* $^{+/+}$ larvae. B, Length of *ZIP9* $^{-/-}$ and *ZIP9* $^{+/+}$ larvae under starvation conditions between 3-10 dpf. C, Length of *ZIP9* $^{-/-}$ and *ZIP9* $^{+/+}$ larvae fed endogenously after 6 dpf. D, Representative image of 15 dpf *ZIP9* $^{+/+}$ and *ZIP9* $^{-/-}$ SD larvae. All data represents means ± SEM, n=20 (A), n=15-22 (B) For (C), n=20 (6-10 dpf); n= 40-55(15, 25 dpf *ZIP9* $^{+/+}$ & *ZIP9* $^{-/-}$ RD); n=37 (15 dpf *ZIP9* $^{-/-}$ SD); n=8 (25 dpf *ZIP9* $^{-/-}$ SD). Significance was determined by one-way ANOVA with Bonferroni multiple comparison post-test. Different letters indicate significant differences between the treatment groups in the *post hoc* test at $p < 0.05$ (A). For growth analysis, * indicates significance difference from WT, while # indicated significant difference from *ZIP9* $^{-/-}$ RD. Growth analyses were performed on approximately 10 fish from 2 separate spawning events for time point and each genotype/phenotype (specific n values listed above). SD, small diameter egg; RD, regular diameter egg.

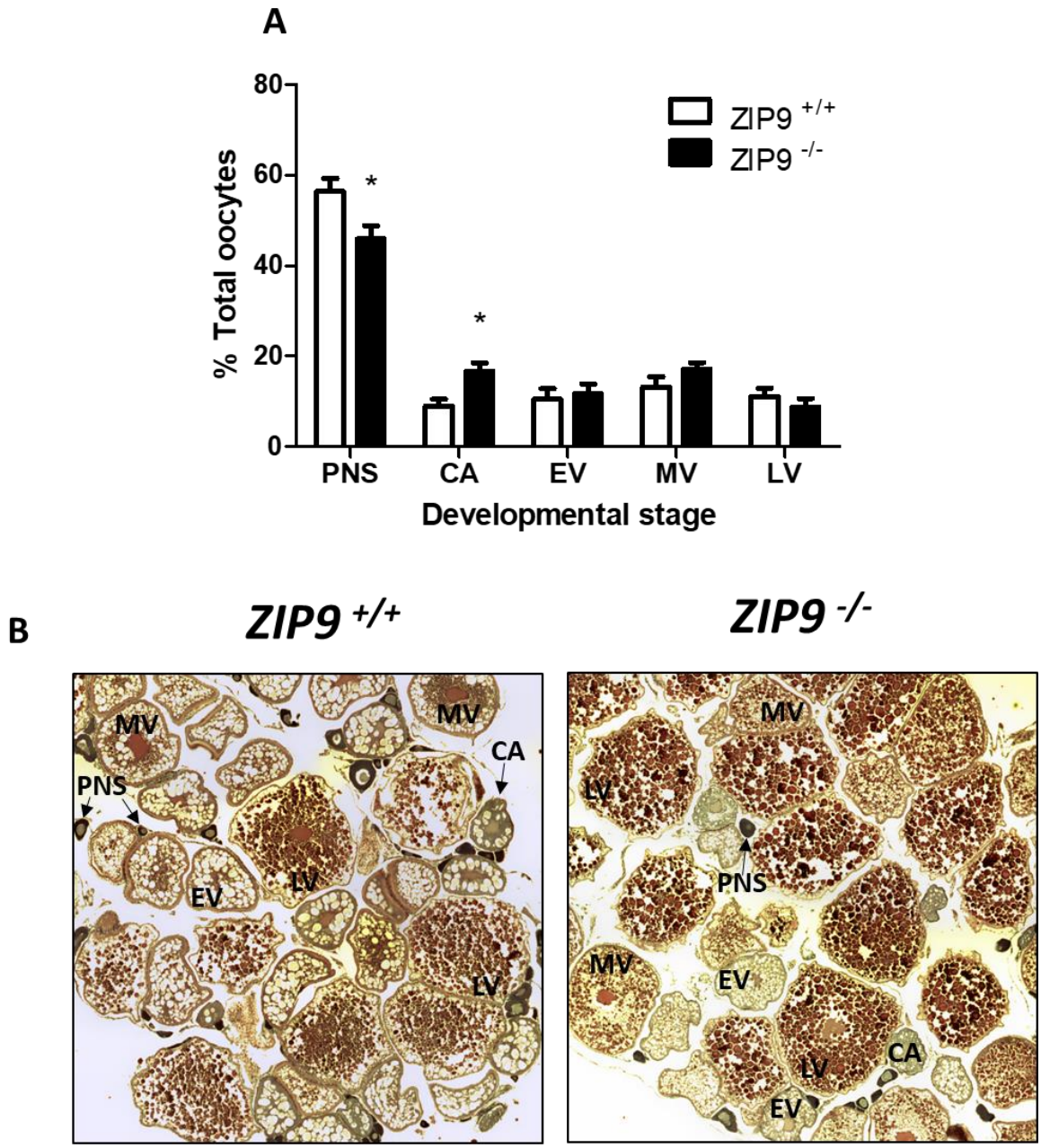

Figure 4.9: Ovarian morphology of ZIP9 -/- and ZIP9 +/+ fish. A, The relative proportion of ovarian follicles at different stages of development in *ZIP9* $^{-/-}$ and *ZIP9* $^{+/+}$ ovaries. B, Representative images of histological ovarian preparation from *ZIP9* $^{-/-}$ and *ZIP9* $^{+/+}$ fish. All data represents means ± SEM, n=5. Significance was determined by Student's t-test (*, $p<0.05$). The analysis was performed with 5 *ZIP9* $^{-/-}$ and *ZIP9* $^{+/+}$ females. PNS, perinuclear stage; CA, cortical alveoli stage; EV, early vitellogenic stage; MV, mid vitellogenic stage; LV, late vitellogenic stage.

SUPPLEMENTAL DATA

Primer	Forward	Reverse
ZIP9	AGCAGCTCCACGCTTACATT	CATGGACGACCAATCCGACT
Bax	GATACGGGCAGTGGCAATGA	ACTCCGGGTCACTTCAGCAT
P53	CACAGGGGTCATTTGGGGAA	CGCCAGTGCTGGTAAAACAC
18S	AGAAACGGCTACCACATCCA	TCCCGAGATCCAACTACGAG

Table 4.1: Sequence of primers (5'-3') used for qPCR experiments (Chapter 4).

Primer	(5'-3')
Exon 3 specific	TAATACGACTCACTATAGAAGGAGTGGTGAGACCCAGGTTTTAGA GCTAGAAATAGCAAG
tracrRNA tail	AAAAGCACCGACTCGGTGCCACTTTTTCAAGTTGATAACGGACTA GCCTTATTTTAACTTGCTATTTCTAGCTCTAAAAC
Exon 3 specific stop codon cassette	GCAGAAGGAGTGGTGAGACCGTCATGGCGTTTAAACCTTAATTAA GCTGTTGTAGCAGCGGTGAACACGGCCACG

Table 4.2: Oligonucleotide sequences used in gRNA generation and stop codon cassette. Exon 3 specific- blue, T7 promoter; red, target sequence of gRNA; orange, complementary region. tracrRNA tail- orange, complementary region. Exon 3 specific stop codon cassette- red, stop codon cassette.

Primer	Forward	Reverse
HMA	ATGCATTGTGCTGCTAGTTGTT	CCAGAGAAATCCCAATGTAAGC
Stop cassette specific	GGTGAGACCGTCATGGCGTTTA	CGCAGTGTGAGCCAATCCAAATA
Homo/heterozygous screening	ATGCATTGTGCTGCTAGTTGTT	CGCAGTGTGAGCCAATCCAAATA

Table 4.3: Primers used in mutation screening assays.

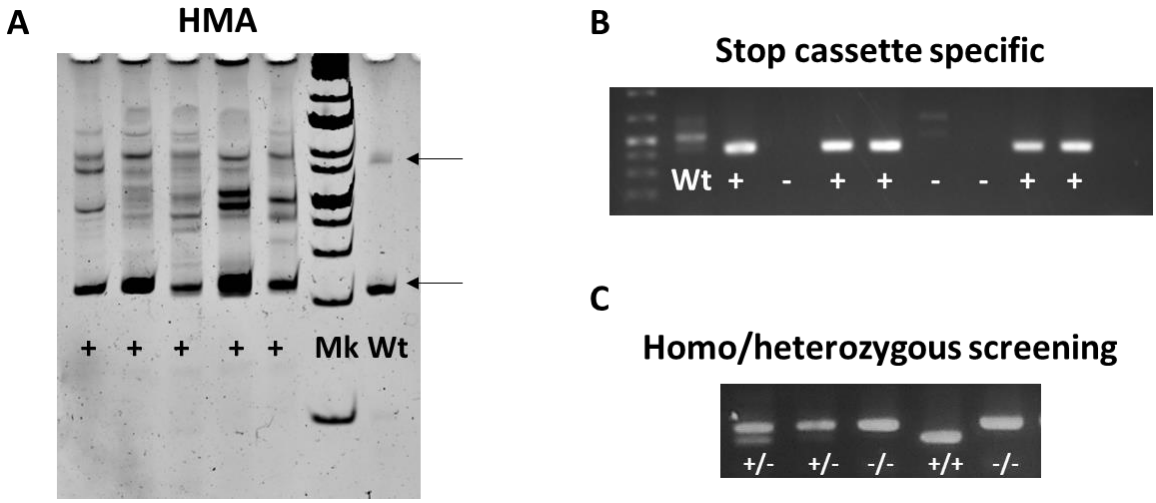

Figure 4.10: Representative images of screening used for detection of mutations and stop codon insertion. A, Representative HMA screening, additional bands (+) from what is observed in WT (non-injected fish) indicate a CRISPR-Cas9-induced mutation in exon 3. B, Stop cassette screening, bands indicate the fish is positive (+) for insert of the stop codon cassette. C, Screening for homo/heterozygous ZIP9 fish. The 64 bp insertion can be detected by running on an agarose gel. Fish denoted by ZIP9 genotype, +/-, possesses both WT and stop codon insert; -/-, homozygous for stop codon insert; +/+, homozygous WT.

Chapter 5: Summary and Conclusions

The results of the present study demonstrate that ZIP9 mediates androgen-induced apoptosis of both Atlantic croaker and zebrafish G/T cells *in vitro*. Both of these apoptotic responses involve a rapid rise in intracellular free zinc, upregulation of pro-apoptotic member mRNA, and increased caspase 3 activity. Thus, these downstream physiological responses mediated by ZIP9 may be conserved in all teleosts. However, while the apoptotic response in croaker G/T cells was found to involve activation of a stimulatory G protein and MAPK activity, rapid signaling events initiated by ZIP9 in zebrafish G/T cells are unknown. Further investigation of G protein coupling and kinase signaling members would provide insight into how similar ZIP9-mediated apoptotic signaling is between croaker and zebrafish G/T cell models.

This work also demonstrates that androgens act to promote both apoptosis and survival in croaker G/T cells through activation of ZIP9. These differential responses to androgens can be attributed to the follicle stage from which the G/T cells are harvested, with testosterone treatment decreasing apoptosis in early stage follicle G/T cells, and inducing apoptosis of late stage follicle G/T cells. ZIP9 mediates these differential physiological responses by coupling to and activating different G proteins depending on the G/T cell stage. The apoptotic response exhibited by late stage follicle G/T cells involves ZIP9-G_s coupling, which was previously observed by Berg et al., 2014 in G/T cells from fish at the peak of reproduction. ZIP9 couples to a G_i in early stage G/T cells and involves opposite trends in many of the responses characterized in the apoptotic response. Thus, G_i signaling is likely inhibitory to apoptosis, while G_s signaling promotes apoptosis in the croaker G/T cell model. The zinc transporter function of ZIP9 also appears to play a role in both pro- and anti-apoptotic responses, with a rise in intracellular free zinc being required for induction of apoptosis (25), while the anti-apoptotic response coincides with

a testosterone-induced reduction in intracellular free zinc. This ZIP9-G protein coupling switch that occurs in croaker G/T cells would allow ovarian follicles to respond to the same stimuli in a follicle stage-dependent manner, and thus, undergo physiological processes independently of one another. In the ovary, testosterone may help protect follicles during primary and early secondary growth, but act as an apoptotic factor in follicles at the final stages of development, potentially to aid in follicle rupture or breakdown of cells remaining after ovulation. However, the role of ZIP9 in these processes has not been verified to date. Additionally, it should be noted that the mechanism that drives the switching in ZIP9-G protein coupling remains unknown. Further investigation of this switch in the croaker G/T model may give valuable insight into potential properties of ZIP9 in other models such as human cancer cells in which ZIP9 is highly expressed and promotes apoptosis (26). It also remains unknown if differential ZIP9-G protein coupling occurs in zebrafish G/T cells.

This study is the first to examine a global ZIP9 knockout model. Development of a ZIP9 knockout strain of zebrafish allowed for a broad examination of reproductive phenotypes that are associated with the mutant genotype. While ZIP9 knockout males showed no reduction in the ability to fertilize eggs, female knockouts had a significant reduction in fecundity compared to wild-type fish. Eggs spawned by ZIP9 knockouts consisted of a high proportion that displayed an abnormal phenotype characteristic of failure to activate. Eggs with this abnormal phenotype showed severe reductions in fertilization and produced larvae that showed a significantly higher incidence of edema and reduced growth compared to wild-type larvae and those hatched from normal phenotype ZIP9 knockout eggs. Of interest, while egg activation involves a wave of free Ca^{++} in all animals, zinc has recently been shown to also play an essential role in mammalian egg activation (137,138,155). Therefore, it is of interest to further investigate the role of zinc in teleost egg activation and examine the role of ZIP9 in zinc regulation of oocytes.

Finally, while the current study examined broad reproductive measures using ZIP9 knockout and wild-type models, there are additional studies that should be performed using the mutant model to further investigate ZIP9's role in the ovary. The current study has highlighted multiple roles of ZIP9 in teleost G/T cells *in vitro*, but the apoptotic (and potentially anti-apoptotic) actions of ZIP9 were not verified in the global knockout zebrafish model. Use of the mutant fish in *in vitro* experimentation will be essential in verifying the apoptotic effect observed in wild-type G/T cells. Furthermore, apoptotic events can be examined *in vivo* by inducing atresia through environmental stressors or examination of postovulatory breakdown after controlled spawning events. *In vitro* examination of egg maturation and activation in both mutant and wild-type eggs will also verify if ZIP9 is involved in these processes. In addition, generation of a conditional or inducible ZIP9 knockout model would aid in the examination of the role of the receptor in ovarian physiology without the potential influence of ZIP9 knockout effects on other tissues in the hypothalamus-pituitary-gonad axis. Thus, the use of both wild-type and ZIP9 knockout models will be essential in understanding the physiological roles of the receptor in the teleost ovary. In conclusion, this dissertation confirms the hypothesis that ZIP9 plays an important role in the teleost ovary, however, additional studies are required to make mechanistic links between the *in vitro* and *in vivo* data acquired.

References

1. **Elmore S.** Apoptosis: a review of programmed cell death. *Toxicol. Pathol.* 2007;35(4):495–516.
2. **Wensveen FM, Alves NL, Derks IAM, Reedquist KA, Eldering E.** Apoptosis induced by overall metabolic stress converges on the Bcl-2 family proteins Noxa and Mcl-1. *Apoptosis* 2011;16(7):708–721.
3. **Chandra J, Samali A, Orrenius S.** Triggering and modulation of apoptosis by oxidative stress. 2000;29(3/4):323–333.
4. **Norbury CJ, Zhivotovsky B.** DNA damage-induced apoptosis. *Oncogene* 2004;23(16):2797–2808.
5. **Milleron RS, Bratton SB.** "Heated" debates in apoptosis. *Cell. Mol. Life Sci.* 2007;64(18):2329–2333.
6. **Yadav S, Shi Y, Wang F, Wang H.** Arsenite induces apoptosis in human mesenchymal stem cells by altering Bcl-2 family proteins and by activating intrinsic pathway. *Toxicol. Appl. Pharmacol.* 2010;244(3):263–272.
7. **Tilly JL.** Molecular and genetic basis of normal and toxicant-induced apoptosis in female germ cells. *Toxicol. Lett.* 1998;102–103:497–501.
8. **Canman CE, Gilmer TM, Coutts SB, Kastan MB.** Growth factor modulation of p53-mediated growth arrest versus apoptosis. *Genes Dev.* 1995;9(5):600–611.
9. **Reddy KB.** Epidermal growth factor induced apoptosis. *Apoptosis* 1996;1(1):33–39.
10. **Logue SE, Martin SJ.** Caspase activation cascades in apoptosis. *Biochem. Soc. Trans.* 2008;36(Pt 1):1–9.
11. **Cory S, Adams JM.** The BCL2 family: Regulators of the cellular life-or-death switch. *Nat. Rev. Cancer* 2002;2(9):647–656.
12. **Slee EA, Adrain C, Martin SJ.** Executioner caspase-3, -6, and -7 perform distinct, non-redundant roles during the demolition phase of apoptosis. *J. Biol. Chem.* 2001;276(10):7320–7326.
13. **Evans-Storms R, Cidlowski J.** Regulation of apoptosis by steroid hormones. *J. Steroid Biochem. Mol. Biol.* 1995;53(1–6):1–8.
14. **Amsterdam A, Dantes A, Hosokawa K, Schere-Levy CP, Kotsuji F, Aharoni D.** Steroid regulation during apoptosis of ovarian follicular cells. *Steroids* 1998;63(5–6):314–318.
15. **Kurita T, Wang YZ, Donjacour AA, Zhao C, Lydon JP, O'Malley BW, Isaacs JT, Dahiya R, Cunha GR.** Paracrine regulation of apoptosis by steroid hormones in the male and female reproductive system. *Cell Death Differ* 2001;8(2):192–200.
16. **Falkenstein E, Tillmann HC, Christ M, Feuring M, Wehling M.** Multiple actions of steroid hormones--a focus on rapid, nongenomic effects. *Pharmacol. Rev.* 2000;52(4):513–556.
17. **Thomas P.** Rapid steroid hormone actions initiated at the cell surface and the receptors that mediate them with an emphasis on recent progress in fish models. *Gen. Comp. Endocrinol.* 2012;175(3):367–83.
18. **Benten WPM, Guo Z, Krücken J, Wunderlich F.** Rapid effects of androgens in

macrophages. *Steroids* 2004;69(8–9):585–590.
19. **Chaban V V, Lakhter AJ, Micevych P.** A membrane estrogen receptor mediates intracellular calcium release in astrocytes. *Endocrinology.* 2004;145(8):3788–3795.
20. **Sun Y-H, Gao X, Tang Y-J, Xu C-L, Wang L-H.** Androgens induce increases in intracellular calcium via a G protein-coupled receptor in LNCaP prostate cancer cells. *J. Androl.* 2006;27(5):671–678.
21. **Filardo EJ, Quinn JA, Frackelton AR, Bland KI.** Estrogen action via the G protein-coupled receptor, GPR30: stimulation of adenylyl cyclase and cAMP-mediated attenuation of the epidermal growth factor receptor-to-MAPK signaling axis. *Mol. Endocrinol.* 2002;16(1):70–84.
22. **Thomas P, Pang Y, Filardo EJ, Dong J.** Identity of an Estrogen Membrane Receptor Coupled to a G Protein in Human Breast Cancer Cells. *Endocrinology.* 2005;146(2):624–632.
23. **Tubbs C, Thomas P.** Progestin signaling through an olfactory G protein and membrane progestin receptor-alpha in Atlantic croaker sperm: potential role in induction of sperm hypermotility. *Endocrinology.* 2009;150(1):473–484.
24. **Dressing GE, Pang Y, Dong J, Thomas P.** Progestin signaling through mPRα in Atlantic croaker granulosa/theca cell cocultures and its involvement in progestin inhibition of apoptosis. *Endocrinology.* 2010;151(12):5916–5926.
25. **Berg AH, Rice CD, Rahman MS, Dong J, Thomas P.** Identification and characterization of membrane androgen receptors in the ZIP9 zinc transporter subfamily: I. discovery in female Atlantic croaker and evidence ZIP9 mediates testosterone-induced apoptosis of ovarian follicle cells. *Endocrinology.* 2014;155(11):4237–4249.
26. **Thomas P, Pang Y, Dong J, Berg AH.** Identification and characterization of membrane androgen receptors in the ZIP9 zinc transporter subfamily: II. role of human ZIP9 in testosterone-induced prostate and breast cancer cell apoptosis. *Endocrinology.* 2014;155(11):4250–4265.
27. **Gatson JW, Kaur P, Singh M.** Dihydrotestosterone differentially modulates the mitogen-activated protein kinase and the phosphoinositide 3-kinase/Akt pathways through the nuclear and novel membrane androgen receptor in C6 cells. *Endocrinology.* 2006;147(4):2028–2034.
28. **Papadopoulou N, Charalampopoulos I, Anagnostopoulou V, Konstantinidis G, Föller M, Gravanis A, Alevizopoulos K, Lang F, Stournaras C.** Membrane androgen receptor activation triggers down-regulation of PI-3K/Akt/NF-kappaB activity and induces apoptotic responses via Bad, FasL and caspase-3 in DU145 prostate cancer cells. *Mol. Cancer* 2008;7(88).
29. **Gu S, Papadopoulou N, Nasir O, Föller M, Alevizopoulos K, Lang F, Stournaras C.** Activation of membrane androgen receptors in colon cancer inhibits the prosurvival signals Akt/bad in vitro and in vivo and blocks migration via vinculin/actin signaling. *Mol. Med.* 2011;17(1–2):48–58.
30. **Estrada M, Espinosa A, Müller M, Jaimovich E.** Testosterone stimulates

intracellular calcium release and mitogen-activated protein kinases via a G protein-coupled receptor in skeletal muscle cells. *Endocrinology.* 2003;144(8):3586–3597.
31. **Tan W, Thomas P.** Involvement of epidermal growth factor receptors and mitogen-activated protein kinase in progestin-induction of sperm hypermotility in Atlantic croaker through membrane progestin receptor-alpha. *Mol Cell Endocrinol* 2015;414:194–201.
32. **Zhu Y, Rice CD, Pang Y, Pace M, Thomas P.** Cloning, expression, and characterization of a membrane progestin receptor and evidence it is an intermediary in meiotic maturation of fish oocytes. *Proc. Natl. Acad. Sci.* 2003;100(5):2231–2236.
33. **Thomas P, Pang Y, Filardo EJ, Dong J.** Identity of an Estrogen Membrane Receptor Coupled to a G Protein in Human Breast Cancer Cells. 2005;146(2):624–632.
34. **Revankar CM, Cimino DF, Sklar LA, Arterburn JB, Prossnitz ER.** A transmembrane intracellular estrogen receptor mediates rapid cell signaling. *Science (80-.).* 2005;307(5715):1625–1630.
35. **Yamada Y.** Effects of testosterone on unit activity in rat hypothalamus and septum. *Brain Res.* 1979;172:165–168.
36. **Christian HC, Rolls N, Morris JF.** Nongenomic Actions of Testosterone on a Subset of Lactotrophs in the Male Rat Pituitary. *Endocrinology.* 2000;141(9):3111–3119.
37. **Gatson JW, Singh M.** Activation of a membrane-associated androgen receptor promotes cell death in primary cortical astrocytes. *Endocrinology.* 2007;148(5):2458–2464.
38. **Gorczynska E, Handelsman D.** Androgens rapidly increase the cytosolic calcium concentration in Sertoli cells. *Endocrinology.* 1995;136:2052–2059.
39. **Lyng FM, Jones GR, Rommerts FF.** Rapid androgen actions on calcium signaling in rat sertoli cells and two human prostatic cell lines: similar biphasic responses between 1 picomolar and 100 nanomolar concentrations. *Biol. Reprod.* 2000;63(3):736–747.
40. **Fix C, Jordan C, Cano P, Walker WH.** Testosterone activates mitogen-activated protein kinase and the cAMP response element binding protein transcription factor in Sertoli cells. *Proc. Natl. Acad. Sci. U. S. A.* 2004;101(30):10919–10924.
41. **Machelon V, Nomé F, Tesarik J.** Nongenomic effects of androstenedione on human granulosa luteinizing cells. *J. Clin. Endocrinol. Metab.* 1998;83(1):263–269.
42. **Benten WPM, Lieberherr M, Sekeris CE, Wunderlich F.** Testosterone induces Ca2+ influx via non-genomic surface receptors in activated T cells. *FEBS Lett.* 1997;407(2):211–214.
43. **Benten WP, Lieberherr M, Giese G, Wrehlke C, Stamm O, Sekeris CE, Mossmann H, Wunderlich F.** Functional testosterone receptors in plasma membranes of T cells. *FASEB J.* 1999;13(1):123–133.
44. **Lutz LB, Cole LM, Gupta MK, Kwist KW, Auchus RJ, Hammes SR.** Evidence

that androgens are the primary steroids produced by Xenopus laevis ovaries and may signal through the classical androgen receptor to promote oocyte maturation. *Proc. Natl. Acad. Sci. U. S. A.* 2001;98(24):13728–13733.

45. **Lutz LB, Jamnongjit M, Yang W-H, Jahani D, Gill A, Hammes SR.** Selective modulation of genomic and nongenomic androgen responses by androgen receptor ligands. *Mol. Endocrinol.* 2003;17(6):1106–1116.
46. **Gill A, Jamnongjit M, Hammes SR.** Androgens promote maturation and signaling in mouse oocytes independent of transcription: a release of inhibition model for mammalian oocyte meiosis. *Mol. Endocrinol.* 2004;18(1):97–104.
47. **Atif M. Nakhla, Khan MS, Rosner W.** Biologically Active Steroids Activate Receptor-Bound Human Sex Hormone-Binding Globulin to Cause LNCaP Cells to Accumulate Adenosine 3',5'-Monophosphate. *J. Clin. Endocrinol. Metab.* 1990;71(2):398–404.
48. **Steinsapir J, Socci R, Reinach P.** Effects of androgen on intracellular calcium of LNCaP cells. *Biochem. Biophys. Res. Commun.* 1991;179(1):90–96.
49. **Kampa M, Papakonstanti E a, Hatzoglou A, Stathopoulos EN, Stournaras C, Castanas E.** The human prostate cancer cell line LNCaP bears functional membrane testosterone receptors that increase PSA secretion and modify actin cytoskeleton. *FASEB J.* 2002;16(11):1429–1431.
50. **Hatzoglou A, Kampa M, Kogia C, Charalampopoulos I, Theodoropoulos P a, Anezinis P, Dambaki C, Papakonstanti E a, Stathopoulos EN, Stournaras C, Gravanis A, Castanas E.** Membrane androgen receptor activation induces apoptotic regression of human prostate cancer cells in vitro and in vivo. *J. Clin. Endocrinol. Metab.* 2005;90(2):893–903.
51. **Papadopoulou N, Charalampopoulos I, Alevizopoulos K, Gravanis A, Stournaras C.** Rho/ROCK/actin signaling regulates membrane androgen receptor induced apoptosis in prostate cancer cells. *Exp. Cell Res.* 2008;314(17):3162–3174.
52. **Gu S, Papadopoulou N, Gehring E-M, Nasir O, Dimas K, Bhavsar SK, Föller M, Alevizopoulos K, Lang F, Stournaras C.** Functional membrane androgen receptors in colon tumors trigger pro-apoptotic responses in vitro and reduce drastically tumor incidence in vivo. *Mol. Cancer* 2009;8(114).
53. **Kampa M, Nifli A-P, Charalampopoulos I, Alexaki V-I, Theodoropoulos PA, Stathopoulos EN, Gravanis A, Castanas E.** Opposing effects of estradiol- and testosterone-membrane binding sites on T47D breast cancer cell apoptosis. *Exp. Cell Res.* 2005;307(1):41–51.
54. **Wang H, Andoh K, Hagiwara H, Xiaowei L, Kikuchi N, Abe Y, Yamada K, Fatima R, Mizunuma H.** Effect of adrenal and ovarian androgens on type 4 follicles unresponsive to FSH in immature mice. *Endocrinology.* 2001;142(11):4930–4936.
55. **Vendola K, Zhou J, Adesanya O, Weil S, Bondy C.** Androgens stimulate early stages of follicular growth in the primate ovary. *J. Clin. Invest.* 1998;101(12):2622–2629.

56. **Murray A, Gosden R, Allison V, Spears N.** Effect of androgens on the development of mouse follicles growing in vitro. *J. Reprod. Fertil.* 1998;113:27–33.
57. **Forsgren KL, Young G.** Stage-specific effects of androgens and estradiol-17beta on the development of late primary and early secondary ovarian follicles of coho salmon (Oncorhynchus kisutch) in vitro. *Biol. Reprod.* 2012;87(3):1–14.
58. **Hickey TE, Marrocco DL, Gilchrist RB, Norman RJ, Armstrong DT.** Interactions Between Androgen and Growth Factors in Granulosa Cell Subtypes of Porcine Antral Follicles. *Biol. Reprod.* 2004;71(1):45–52.
59. **Yang MY, Fortune JE.** Testosterone Stimulates the Primary to Secondary Follicle Transition in Bovine Follicles In Vitro. *Biol. Reprod.* 2006;75:924–932.
60. **Hillier SG, Ross GT.** Effects of exogenous testosterone on ovarian weight, follicular morphology and intraovarian progesterone concentration in estrogen-primed hypophysectomized immature female rats. *Biol. Reprod.* 1979;20:261–268.
61. **Billig H, Furuta I, Hsuehs JW.** Estrogens inhibit and androgens enhance ovarian granulosa cell apoptosis. *Endocrinology.* 1993;133(5):2204–2212.
62. **Bagnell CA, Mills TM, Costoff A, Mahesh VB.** A model for the study of androgen effects on follicle atresia and ovulation. *Biol. Reprod.* 1982;27:903–914.
63. **Azzolin G, Saiduddin S.** Effect of androgens on the ovarian morphology of the hypophysectimized rat. *Proc. Soc. Exp. Biol. Med.* 983;172:70–73.
64. **Duda M, Durlej M, Knet M, Knapczyk-Stwora K, Tabarowski Z, Slomczynska M.** Does 2-hydroxyflutamide inhibit apoptosis in porcine granulosa cells? - An in vitro study. *J. Reprod. Dev.* 2012;58(4):438–444.
65. **Knet M, Tabarowski Z, Slomczynska M, Duda M.** The effects of the environmental antiandrogen vinclozolin on the induction of granulosa cell apoptosis during follicular atresia in pigs. *Theriogenology* 2014;81(9):1239–1247.
66. **Lyon M, Glenister P.** Evidence from Tfm/0 that androgen is inessential for reproduction in female mice. *Nature* 1974;247:366–367.
67. **Yeh S, Tsai M-Y, Xu Q, Mu X-M, Lardy H, Huang K, Lin H, Yeh S, Altuwaijri S, Zhou X, Xing L, Boyce BF, Hung M, Zhang S, Gan L, Chang C, Hung M-C.** Generation and characterization of androgen receptor knockout (ARKO) mice: an in vivo model for the study of androgen functions in selective tissues. *Proc. Natl. Acad. Sci. U. S. A.* 2002;99(21):13498–13503.
68. **Hu Y, Wang P, Yeh S, Wang R, Xie C, Xu Q, Zhou X, Chao H, Tsai M, Chang C.** Subfertility and defective folliculogenesis in female mice lacking androgen receptor. *Proc. Natl. Acad. Sci. U. S. A.* 2004;101(31):11209–11214.
69. **Shiina H, Matsumoto T, Sato T, Igarashi K, Miyamoto J, Takemasa S, Sakari M, Takada I, Nakamura T, Metzger D, Chambon P, Kanno J, Yoshikawa H, Kato S.** Premature ovarian failure in androgen receptor-deficient mice. *Proc. Natl. Acad. Sci. U. S. A.* 2006;103(1):224–229.
70. **Walters KA, Allan CM, Jimenez M, Lim PR, Davey RA, Zajac JD, Illingworth P, Handelsman DJ.** Female mice haploinsufficient for an inactivated androgen receptor (AR) exhibit age-dependent defects that resemble the AR null

phenotype of dysfunctional late follicle development, ovulation, and fertility. *Endocrinology.* 2007;148(8):3674–3684.
71. **Sen A, Hammes SR.** Granulosa cell-specific androgen receptors are critical regulators of ovarian development and function. *Mol. Endocrinol.* 2010;24(7):1393–1403.
72. **Walters KA, Middleton LJ, Joseph SR, Hazra R, Jimenez M, Simanainen U, Allan CM, Handelsman DJ.** Targeted loss of androgen receptor signaling in murine granulosa cells of preantral and antral follicles causes female subfertility. *Biol. Reprod.* 2012;87(6):151, 1–11.
73. **Sen A, Prizant H, Light A, Biswas A, Hayes E, Lee H-J, Barad D, Gleicher N, Hammes SR.** Androgens regulate ovarian follicular development by increasing follicle stimulating hormone receptor and microRNA-125b expression. *Proc. Natl. Acad. Sci. U. S. A.* 2014;111(8):3008–3013.
74. **Braun AM, Thomas P.** Biochemical characterization of a membrane androgen receptor in the ovary of the atlantic croaker (Micropogonias undulatus). *Biol. Reprod.* 2004;71(1):146–55.
75. **Zhang C.** Testosterone acts at the cell surface to induce granulosa/theca cell death via an apoptotic pathway in Atlantic croaker (Micropogonias undulatus). *Master's thesis* 2011.
76. **Pradeep PK, Li X, Peegel H.** Proliferation by Decreasing the Cyclin D2 mRNA Expression and Cell Cycle Arrest at G1 Phase. 2008;143(8):2930–2935.
77. **Matsumoto T, Shiina H, Kawano H, Sato T, Kato S.** Androgen receptor functions in male and female physiology. *J. Steroid Biochem. Mol. Biol.* 2008;109(3–5):236–241.
78. **Prizant H, Gleicher N, Sen A.** Androgen actions in the ovary: balance is key. *J. Endocrinol.* 2014;222(3):R141–R151.
79. **Braun AM, Thomas P.** Androgens inhibit estradiol-17beta synthesis in Atlantic croaker (Micropogonias undulatus) ovaries by a nongenomic mechanism initiated at the cell surface. *Biol. Reprod.* 2003;69(5):1642–1650.
80. **Sperry TS, Thomas P.** Characterization of two nuclear androgen receptors in Atlantic croaker: comparison of their biochemical properties and binding specificities. *Endocrinology.* 1999;140(4):1602–11.
81. **Tilly JL.** Apoptosis and ovarian function. *Rev. Reprod.* 1996;1(3):162–172.
82. **Santos HB, Rizzo E, Bazzoli N, Sato Y, Moro L.** Ovarian regression and apoptosis in the South American teleost Leporinus taeniatus Lütken (Characiformes, Anostomidae) from the São Francisco Basin. *J. Fish Biol.* 2005;67:1446–1459.
83. **Morais RDVS, Thomé RG, Lemos FS, Bazzoli N, Rizzo E.** Autophagy and apoptosis interplay during follicular atresia in fish ovary: A morphological and immunocytochemical study. *Cell Tissue Res.* 2012;347:467–478.
84. **Drummond CD, Bazzoli N, Rizzo E, Sato Y.** Postovulatory follicle: a model for experimental studies of programmed cell death or apoptosis in teleosts. *J. Exp. Zool.* 2000;287(2):176–182.

85. **Wood A, Van Der Kraak G.** Apoptosis and ovarian function: novel perspectives from the teleosts. *Biol. Reprod.* 2001;64(1):264–271.
86. **Coleman JE.** Zinc proteins: enzymes, storage proteins, transcription factors, and replication proteins. *Annu. Rev. Biochem.* 1992;61:897–946.
87. **Beyersmann D, Haase H.** Functions of zinc in signaling, proliferation and differentiation of mammalian cells. *BioMetals* 2001;14(3–4):331–341.
88. **Zhang Y, Wang H, Li J, Jimenez DA, Levitan ES, Aizenman E, Rosenberg PA.** Peroxynitrite-Induced Neuronal Apoptosis Is Mediated by Intracellular Zinc Release and 12-Lipoxygenase Activation. 2004;24(47):10616–10627.
89. **Feng P, Li T, Guan Z, Franklin RB, Costello LC.** The involvement of Bax in zinc-induced mitochondrial apoptogenesis in malignant prostate cells. *Mol. Cancer* 2008;7(25). doi:10.1186/1476-4598-7-25.
90. **Martin S, Mazdai G, Strain J, Cotter T, Hannigan B.** Programmed cell death (apoptosis) in lymphoid and myeloid cell lines during zinc deficiency. *Clin. Exp. Immunol.* 1990;83:338–343.
91. **Ahn YH, Kim YH, Hong SH, Koh JY.** Depletion of intracellular zinc induces protein synthesis-dependent neuronal apoptosis in mouse cortical culture. *Exp. Neurol.* 1998;154(154):47–56.
92. **Hashemi M, Ghavami S, Eshraghi M, Booy EP, Los M.** Cytotoxic effects of intra and extracellular zinc chelation on human breast cancer cells. *Eur. J. Pharmacol.* 2007;557(1):9–19.
93. **Zalewski PD, Forbes IJ, Seamark RF, Borlinghaus R, Betts WH, Lincoln SF, Ward a. D.** Flux of intracellular labile zinc during apoptosis (gene-directed cell death) revealed by a specific chemical probe, Zinquin. *Chem. Biol.* 1994;1(3):153–161.
94. **Lee JY, Hwang JJ, Park MH, Koh JY.** Cytosolic labile zinc: A marker for apoptosis in the developing rat brain. *Eur. J. Neurosci.* 2006;23(2):435–442.
95. **Fukada T, Kambe T.** Molecular and genetic features of zinc transporters in physiology and pathogenesis. *Metallomics* 2011;3(7):662–674.
96. **Benninghoff AD, Thomas P.** Gonadotropin regulation of testosterone production by primary cultured theca and granulosa cells of Atlantic croaker: I. Novel role of CaMKs and interactions between calcium- and adenylyl cyclase-dependent pathways. *Gen. Comp. Endocrinol.* 2006;147(3):276–287.
97. **Trant JM, Thomas P.** Structure-activity relationships of steroids in inducing germinal vesicle breakdown of Atlantic croaker oocytes in vitro. *Gen. Comp. Endocrinol.* 1988;71(2):307–317.
98. **Daaka Y, Luttrell LM, Lefkowitz RJ.** Switching of the coupling of the beta2-adrenergic receptor to different G proteins by protein kinase A. *Nature* 1997;390(6):88–91.
99. **Shihan M, Chan K-H, Konrad L, Scheiner-Bobis G.** Non-classical testosterone signaling in spermatogenic GC-2 cells is mediated through ZIP9 interacting with Gnα11. *Cell. Signal.* 2015;27(10):2077–2086.
100. **Clapham DE, Neer EJ.** New roles for G-protein beta gamma-dimers in

transmembrane signalling. *Nature* 1993;365(6445):403–406.
101. **Crespo P, Cachero TG, Xu N, Gutkind JS.** Dual Effect of Beta-Adrenergic Receptors on Mitogen-activated Protein Kinase. *J. Biol. Chem.* 1995;270(42):25259–25265.
102. **Goldsmith ZG, Dhanasekaran DN.** G Protein regulation of MAPK networks. *Oncogene* 2007;26(22):3122–3142.
103. **Aharoni D, Dantes A, Oren M, Amsterdam A.** cAMP-mediated signals as determinants for apoptosis in primary granulosa cells. *Exp. Cell Res.* 1995;218:271–282.
104. **Zwain IH, Amato P.** cAMP-induced apoptosis in granulosa cells is associated with up-regulation of P53 and bax and down-regulation of clusterin. *Endocr. Res.* 2001;27(1&2):233–249.
105. **Breckwoldt M, Selvaraj N, Aharoni D, Barash A, Segal I, Insler V, Amsterdam A.** Expression of Ad4-BP/cytochrome P450 side chain cleavage enzyme and induction of cell death in long-term cultures of human granulosa cells. *Mol. Hum. Reprod.* 1996;2(6):391–400.
106. **Hosokawa K, Aharoni D, Dantes A, Shaulian E, Schere-levy C, Atzmon R, Kotsuji F, Oren M, Vlodavsky I, Amsterdam A.** Modulation of Mdm2 expression and p53-induced apoptosis in immortalized human ovarian granulosa cells. *Endocrinology.* 1998;139(11):4688–4700.
107. **Velasco L, Sánchez M, Rubín JM, Hidalgo A, Bordallo C, Cantabrana B.** Intracellular cAMP increases during the positive inotropism induced by androgens in isolated left atrium of rat. *Eur. J. Pharmacol.* 2002;438(1–2):45–52.
108. **Bagchi G, Wu J, French J, Kim J, Moniri NH, Daaka Y.** Androgens transduce the G alpha s-mediated activation of protein kinase A in prostate cells. *Cancer Res.* 2008;68(9):3225–3231.
109. **Amsterdam A, Keren-Tal I, Aharoni D.** Cross-talk between cAMP and p53-generated signals in induction of differentiation and apoptosis in steroidogenic granulosa cells. *Steroids* 1996;61(4):252–256.
110. **Kambe T, Yamaguchi-Iwai Y, Sasaki R, Nagao M.** Overview of mammalian zinc transporters. *Cell. Mol. Life Sci.* 2004;61(1):49–68.
111. **Maret W.** Zinc in Cellular Regulation: The Nature and Significance of "Zinc Signals." *Int. J. Mol. Sci.* 2017;18(11):2285.
112. **Matsuura W, Yamazaki T, Yamaguchi-Iwai Y, Masuda S, Nagao M, Andrews GK, Kambe T.** SLC39A9 (ZIP9) regulates zinc homeostasis in the secretory pathway: characterization of the ZIP subfamily I protein in vertebrate cells. *Biosci. Biotechnol. Biochem.* 2009;73(5):1142–1148.
113. **Dhanasekaran DN, Reddy EP.** JNK signaling in apoptosis. *Oncogene* 2008;27(48):6245–6251.
114. **Lim JJ, Han CY, Lee DR, Tsang BK.** Ring finger protein 6 mediates androgen-induced granulosa cell proliferation and follicle growth via modulation of androgen receptor signaling. *Endocrinology.* 2017;158(4):993–1004.
115. **Lokman PM, George KAN, Divers SL, Algie M, Young G.** 11-Ketotestosterone

and IGF-I increse the size of previttelogenic oocytes from shortfinned eel, Anguilla australis, in vitro. *Reproduction* 2007;133(5):955–967.
116. **Kortner TM, Rocha E, Arukwe A.** Previtellogenic oocyte growth and transcriptional changes of steroidogenic enzyme genes in immature female Atlantic cod (Gadus morhua L.) after exposure to the androgens 11-ketotestosterone and testosterone. *Comp. Biochem. Physiol. - A Mol. Integr. Physiol.* 2009;152(3):304–313.
117. **Converse A, Zhang C, Thomas P.** Membrane androgen receptor ZIP9 induces croaker ovarian cell apoptosis via stimulatory G protein alpha subunit and MAP kinase signaling. *Endocrinology.* 2017;158(9):3015–3029.
118. **Bulldan A, Dietze R, Shihan M, Scheiner-Bobis G.** Non-classical testosterone signaling mediated through ZIP9 stimulates claudin expression and tight junction formation in Sertoli cells. *Cell. Signal.* 2016;28(8):1075–1085.
119. **Munnich N, Wernhart S, Hogstrand C, Schlomann U, Nimsky C, Bartsch JW.** Expression of the zinc importer protein ZIP9/SLC39A9 in glioblastoma cells affects phosphorylation states of p53 and GSK-3beta and causes increased cell migration. *BioMetals* 2016;26(6):995–1004.
120. **Thomas P, Pang Y, Dong J.** Membrane androgen receptor characteristics of human ZIP9 (SLC39A) zinc transporter in prostate cancer cells: Androgen-specific activation and involvement of an inhibitory G protein in zinc and MAP kinase signaling. *Mol. Cell. Endocrinol.* 2017;447:23–34.
121. **Thomas P, Pang Y, Filardo EJ, Dong J.** Identity of an estrogen membrane receptor coupled to a G protein in human breast cancer cells. *Endocrinology.* 2005;146(2):624–632.
122. **Pang Y, Dong J, Thomas P.** Estrogen signaling characteristics of Atlantic croaker G protein-coupled receptor 30 (GPR30) and evidence it is involved in maintenance of oocyte meiotic arrest. *Endocrinology.* 2008;149(7):3410–3426.
123. **Filardo EJ, Quinn JA, Bland KI, Frackelton AR.** Estrogen-induced activation of Erk-1 and Erk-2 requires the G protein-coupled receptor homolog, GPR30, and occurs via trans-activation of the epidermal growth factor receptor through release of HB-EGF. *Mol. Endocrinol.* 2000;14(10):1649–1660.
124. **Ding Q, Gros R, Limbird LE, Chorazyczewski J, Feldman RD.** Estradiol-mediated ERK phosphorylation and apoptosis in vascular smooth muscle cells requires GPR 30. 2009:1178–1187.
125. **Dosiou C, Hamilton AE, Pang Y, Overgaard MT, Tulac S, Dong J, Thomas P, Giudice LC.** Expression of membrane progesterone receptors on human T lymphocytes and Jurkat cells and activation of G-proteins by progesterone. *J. Endocrinol.* 2008;196(1):67–77.
126. **Sleiter N, Pang Y, Park C, Horton TH, Dong J, Thomas P, Levine JE.** Progesterone Receptor A (PRA) and PRB -Independent Effects of Progesterone on Gonadotropin-Releasing Hormone Release. 2009;150(8):3833–3844.
127. **Tubbs C, Thomas P.** Progestin signaling through an olfactory G protein and membrane progestin receptor-alpha in Atlantic croaker sperm: potential role in

induction of sperm hypermotility. *Endocrinology.* 2009;150(1):473–484.
128. **Barbieri L, Chittenden Jr. M, Lowerre-Barbieri SK.** Maturity, Spawning, and ovarian cycle of Atlantic croaker, Micropogonias undulatus, in the Chesapeake Bay and adjacent coastal waters. 1994;685(1871):671–685.
129. **Lawler OA, Miggin SM, Kinsella BT.** Protein Kinase A-mediated Phosphorylation of Serine 357 of the Mouse Prostacyclin Receptor Regulates Its Coupling to Gs-, to G i-, and to Gq-coupled Effector Signaling. *J. Biol. Chem.* 2001;276(36):33596–33607.
130. **Luo X, Zeng W, Xu X, Popov S, Davignon I, Wilkie TM, Mumby SM, Muallem S.** Alternate Coupling of Receptors to Gs and Gi in Pancreatic and Submandibular Gland Cells. *Biochemistry* 1999;274(25):17684–17690.
131. **Martin NP, Whalen EJ, Zamah MA, Pierce KL, Lefkowitz RJ.** PKA-mediated phosphorylation of the β1-adrenergic receptor promotes Gs/Gi switching. *Cell. Signal.* 2004;16(12):1397–1403.
132. **Zhu WZ, Zheng M, Koch WJ, Lefkowitz RJ, Kobilka BK, Xiao RP.** Dual modulation of cell survival and cell death by beta(2)-adrenergic signaling in adult mouse cardiac myocytes. *Proc. Natl. Acad. Sci. U. S. A.* 2001;98(4):1607–1612.
133. **Pankhurst NW.** Gonadal steroids: functions and patterns of change. *Fish Reprod.* 2008;(Chapter 3):67–111.
134. **Ondricek K, Thomas P.** Effects of hypoxia exposure on apoptosis and expression of membrane steroid receptors, ZIP9, mPRα and GPER in Atlantic croaker ovaries. *Comp. Biochem. Physiol. -Part A* 2018;224:84–92.
135. **Yu G, Zhang D, Liu W, Wang J, Liu X, Zhou C.** Zebrafish androgen receptor is required for spermatogenesis and maintenance of ovarian function. *Oncotarget* 2018;9(36):24320–24334.
136. **Crowder CM, Lassiter CS, Gorelick DA.** Nuclear Androgen Receptor Regulates Testes Organization and Oocyte Maturation in Zebrafish. *Endocrinology.* 2018;159(2):980–993.
137. **Kim A, Vogt S, O'Halloran T, Woodruff T.** Zinc availability regulates exit from meiosis in maturing mammalian oocytes. *Nat. Chem. Biol.* 2010;6(9):674–681.
138. **Kim AM, Bernhardt ML, Kong BY, Ahn RW, Vogt S, Woodruff TK, O'Halloran T.** Zinc sparks are triggered by fertilization and facilitate cell cycle resumption in mammalian eggs. *ACS Chem. Biol.* 2011;6(7):716–723.
139. **Tian X, Diaz FJ.** Zinc depletion causes multiple defects in ovarian function during the periovulatory period in mice. *Endocrinology.* 2012;153(2):873–886.
140. **Riggio M, Filosa S, Parisi E, Scudeiro R.** Changes in zinc, copper and metallothionein contents during oocyte growth and early development of the teleost Danio rerio (zebrafish). *Comp. Biochem. Physiol. Part C* 2003;135:191–196.
141. **Feeney GP, Zheng D, Kille P, Hogstrand C.** The phylogeny of teleost ZIP and ZnT zinc transporters and their tissue specific expression and response to zinc in zebrafish. *Biochim. Biophys. Acta* 2005;1732(1–3):88–95.
142. **Gagnon JA, Valen E, Thyme SB, Huang P, Ahkmetova L, Pauli A, Montague**

TG, Zimmerman S, Richter C, Schier AF. Efficient mutagenesis by Cas9 protein-mediated oligonucleotide insertion and large-scale assessment of single-guide RNAs. *PLoS One* 2014;9(5):5–12.
143. **Wilkinson RN, Elworthy S, Ingham PW, van Eeden FJM.** A method for high-throughput PCR-based genotyping of larval zebrafish tail biopsies. *Biotechniques* 2013;55(6):314–316.
144. **Meeker ND, Hutchinson SA, Ho L, Trede NS.** Method for isolation of PCR-ready genomic DNA from zebrafish tissues. *Biotechniques* 2007;43(5):610–614.
145. **Ellis JS, Zambon MC.** Combined PCR-heteroduplex mobility assay for detection and differentiation of influenza A viruses from different animal species. *J. Clin. Microbiol.* 2001;39(11):4097–4102.
146. **Koç ND, Aytekin Y, Yüce R.** Ovary maturation stages and histological investigation of ovary of the Zebrafish (Danio rerio). *Brazilian Arch. Biol. Technol.* 2008;51(3):513–522.
147. **Zhang Z, Lau SW, Zhang L, Ge W.** Disruption of zebrafish follicle-stimulating hormone receptor (fshr) but not luteinizing hormone receptor (lhcgr) gene by TALEN leads to failed follicle activation in females followed by sexual reversal to males. *Endocrinology.* 2015;156(10):3747–3762.
148. **Lubzens E, Young G, Bobe J, Cerdà J.** Oogenesis in teleosts: How fish eggs are formed. *Gen. Comp. Endocrinol.* 2010;165(3):367–389.
149. **Lee KW, Webb SE, Miller AL.** A wave of free cytosolic calcium traverses zebrafish eggs on activation. *Dev. Biol.* 1999;214(1):168–180.
150. **Coward K, Bromage NR, Hibbitt O, Parrington J.** Gamete physiology, fertilization and egg activation in teleost fish. *Rev. Fish Biol. Fish.* 2002;12(1):33–58.
151. **Schalkoff ME, Hart NH.** Effects of A23187 upon cortical granule exocytosis in eggs of Brachydanio. *Roux's Arch. Dev. Biol.* 1986;195(1):39–48.
152. **Gill A, Jamnongjit M, Hammes SR.** Androgens Promote Maturation and Signaling in Mouse Oocytes Independent of Transcription: A Release of Inhibition Model for Mammalian Oocyte Meiosis. *Mol. Endocrinol.* 2004;18(1):97–104.
153. **Li M, Ai J-S, Xu B-Z, Xiong B, Yin S, Lin S-L, Hou Y, Chen D-Y, Schatten H, Sun Q-Y.** Testosterone Potentially Triggers Meiotic Resumption by Activation of Intra-Oocyte SRC and MAPK in Porcine Oocytes. *Biol. Reprod.* 2008;79(5):897–905.
154. **Duncan FE, Que EL, Zhang N, Feinberg EC, Halloran TVO, Woodruff TK.** The zinc spark is an inorganic signature of human egg activation. *Sci. Rep.* 2016;6(24737). doi:10.1038/srep24737.
155. **Suzuki T, Yoshida N, Suzuki E, Okuda E, Perry ACF.** Full-term mouse development by abolishing Zn 2 + -dependent metaphase II arrest without Ca 2 + release. *Development* 2010;137:2659–2669.
156. **Gill A, Jamnongjit M, Hammes SR.** Androgens promote maturation and signaling in mouse oocytes independent of transcription: a release of inhibition model for mammalian oocyte meiosis. *Mol. Endocrinol.* 2004;18(1):97–104.

157. **Ferrell JE.** Xenopus oocyte maturation: New lessons from a good egg. *BioEssays* 1999;21(10):833–842.
158. **Bayaa M, Booth RA, Sheng Y, Liu XJ.** The classical progesterone receptor mediates Xenopus oocyte maturation through a nongenomic mechanism. *Proc. Natl. Acad. Sci.* 2000;97(23):12607–12612.
159. **Nagahama Y, Adachi S.** Identification of maturation-inducing steroid in a teleost, the amago salmon (Oncorhynchus rhodurus). *Dev. Biol.* 1985;109(2):428–435.
160. **Motola S, Popliker M, Tsafriri A.** Are steroids obligatory mediators of luteinizing hormone/human chorionic gonadotropin-triggered resumption of meiosis in mammals? *Endocrinology.* 2007;148(9):4458–4465.
161. **Sun QY, Miao YL, Schatten H.** Towards a new understanding on the regulation of mammalian oocyte meiosis resumption. *Cell Cycle* 2009;8(17):2741–2747.
162. **Nagahama Y, Yamashita M.** Regulation of oocyte maturation in fish. *Dev. Growth Differ.* 2008;50:195–219.
163. **Sato K, Fukami Y, Stith BJ.** Signal transduction pathways leading to Ca 2 + release in a vertebrate model system : Lessons from Xenopus eggs. *Semin. cell Dev. Biol. Biol.* 2006;17:285–292.
164. **Gilkey JC, Jaffe LF, Ridgway EB, Reynolds GT.** A free calcium wave traverses the activating egg of medaka, Oryzias latipes. *J. Cell Biol.* 1978;76:448–466.
165. **Homa ST, Swann K.** A cytosolic sperm factor triggers calcium oscillations and membrane hyperpolarizations in human oocytes. *Hum. Reprod.* 1994;9(12):2356–2361.
166. **Cuthbertson KSR, Whittingham D., Cobbold PH.** Free Ca2+ increases in exponential phases during mouse oocyte activation. *Nature* 1981;294:754–757.
167. **Sartain C V, Wolfner MF.** Cell Calcium Calcium and egg activation in Drosophila. *Cell Calcium* 2013;53(1):10–15.
168. **Samuel ADT, Murthy VN, Hengartner MO.** Calcium dynamics during fertilization in C . elegans. *BMC Dev. Biol.* 2001;1(8).
169. **Mei W, Lee KW, Marlow FL, Miller AL, Mullins MC.** hnRNP I is required to generate the Ca2+ signal that causes egg activation in zebrafish. *Development* 2009;136(17):3007–3017.
170. **Trudeau VL.** Facing the Challenges of Neuropeptide Gene Knockouts : Why Do They Not Inhibit Reproduction in Adult Teleost Fish ? *Front. Neurosci.* 2018;12(302):1–8.
171. **Zhang Z, Lau S, Zhang L, Ge W.** Disruption of Zebrafish Follicle-Stimulating Hormone Receptor (fshr) but Not Luteinizing Hormone Receptor (ihcgr) Gene by TALEN Leads to Failed Follicle Activation in Females Followed by Sexual Reversal to Males. *Endocrinology.* 2015;156(10):3747–3762.
172. **Craig J, Orisaka M, Wang H, Orisaka S, Thompson W, Zhu C, Kotsuji F, Tsang BK.** Gonadotropin and intra-ovarian signals regulating follicle development and atresia: the delicate balance between life and death. *Front. Biosci.* 2007;12:3628–3639.
173. **Hussein MR.** Apoptosis in the ovary: Molecular mechanisms. *Hum. Reprod.*

Update 2005;11(2):161–177.